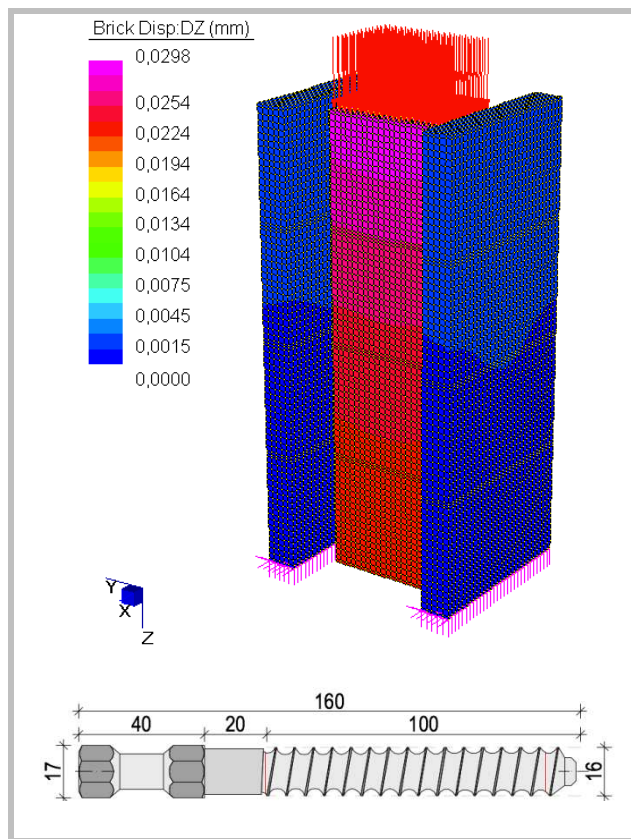


“Load test virtual laboratory dry connectors Al-fer srl”



Ing. Cristian Zenari

Summary

1	INTRODUCTION	3
2	Description of the experimental tests	3
2.1	Introduction	3
2.2	Experimental evidence matrix	3
2.3	Steel connectors and wooden beam LE.AC.1/2/3	4
2.3.1	The al-fer dry connector	4
2.3.2	Geometry of the samples	4
2.3.3	Scheme of the tests	5
2.3.4	Matrix of tests Wood Steel	5
2.4	Experimental response	6
2.4.1	Test report	6
2.4.2	Available data	6
2.4.3	LE.AC.1	7
2.4.4	LE.AC.2	12
2.4.5	LE.AC.3	15
2.4.6	Conclusions	16
3	Stiffness of the connection	17
3.1	Introduction	17
3.2	Reference specimens	17
3.3	Analytical models for the calculation of stiffness and bearing capacity	18
3.3.1	Pin connectors joined to the wood with epoxy resin	18
3.3.2	Dry connectors within calibrated holes	21
3.3.3	Regulations	26
3.3.4	Comparison of the proposed analytical models	31
3.3.5	Linearization of the capacity curve	32
3.3.6	Al-fer bilinear model	34
3.4	Considerations	35
4	Numerical models	36
4.1	Entire specimen	36
4.1.1	Definition of geometry and type of elements	36
4.1.2	Definition of constraint conditions	37
4.1.3	Definition of load conditions	38
4.1.4	Definition of material properties	39
4.1.5	Model resolution	40
4.1.6	Post-processing of the model	40
4.1.7	Free buckling length	48
4.1.8	Conclusions	51
4.2	Composite beams	55
4.2.1	Introduction	55
4.2.2	Composite beam theory	55
4.2.3	FEM application: wood-concrete composite floor or with Al-fer srl connectors	63
	Bibliography	75

1 INTRODUCTION

The study carried out has as its objective the mechanical characterization of a special connector, patented by the company Al-fer srl of Montorio (VR), used for the construction of mixed wood-concrete structures. The results of push-over tests conducted on concrete and wood specimens assembled using Al-fer connectors in digital format are available. This resource has prompted the writer to study the main factors on which this phenomenon depends. We will proceed step by step, first illustrating the available data and then making comparisons with analytical models from legislation, with analogous connection systems and finally with numerical simulations. Therefore, a simplified model for the stiffness of the connection has been proposed, suitable for practical numerical implementations,

2 Description of the experimental tests

2.1 Introduction

In June 2002, an experimental study was conducted at the Department of Construction and Transport of the University of Padua, aimed at evaluating the effectiveness of the mechanical behavior of Al-fer srl dry connectors for the construction of mixed wood-concrete floors. Slip tests (push-out) were carried out in the laboratory on ad hoc samples, these tests allow to identify the characteristic parameters, both of resistance and deformability, for the design of the reinforcement intervention on existing and newly built floors ; in particular, the study was aimed at calibrating the coefficient of specific stiffness (sliding modulus of the connector) on which the value of the coefficient of effectiveness of the connection of the composite composite structure depends.

The tests have provided the load-displacement diagrams and will be presented only after the description of the experimental activity carried out.

2.2 Experimental evidence matrix

The experimental activity included preliminary tests for the physical-mechanical qualification of the base materials (in particular wood, concrete and connectors) and push-out mechanical tests on wooden or concrete floor elements reinforced with concrete slabs made on site. Today, due to unknown reasons, only the mechanical qualification tests of the connector are available; while the data relating to the mechanical characteristics of concrete and wood were estimated for the numerical applications.

The slip tests to evaluate the effectiveness of the connection were performed on three different test configurations, as specified below. In particular, the use of steel and aluminum connectors has been envisaged for the reinforcement of existing wooden floors with concrete slabs, while for the brick-cement type floor, only connection by means of steel connectors with the slab has been envisaged collaborating.

In order to obtain sufficiently significant results, 3 experimental tests were carried out for each combination of connectors/type of existing floor. Therefore, the evidence matrix can be summarized as follows:

LE.AC.1/2/3	(Beam in THE gno.connectors in B.C hello.test number); (Beam in THE
LE.AL.1/2/3	gno.connectors in TO THE aluminum.specimen number); (Beam inc
CA.AC.1/2/3	Armato element.connectors in B.C hi.test number).

Tab. 1: Overall evidence matrix

This work analyzes in detail the series of tests with connectors in**B.C**hi and beam in**THE**gno, as it is nowadays a case of undoubted interest in the building industry. In fact, in recent years there has been a growing interest in mixed wood-concrete structures, both in terms of restoration and new constructions. These interventions, which are possible through the use of special connection devices of which the dry connector Al-fer srl represents an example among the many available on the market.

2.3 Steel connectors and wooden beam LE.AC.1/ 2/3

2.3.1 The al-fer dry connector

The Al-fer srl dry connector is made by suitably shaping a 9SMnPb36 type lead steel bar. Fig. 1 shows the geometry and some cross sections of the same.

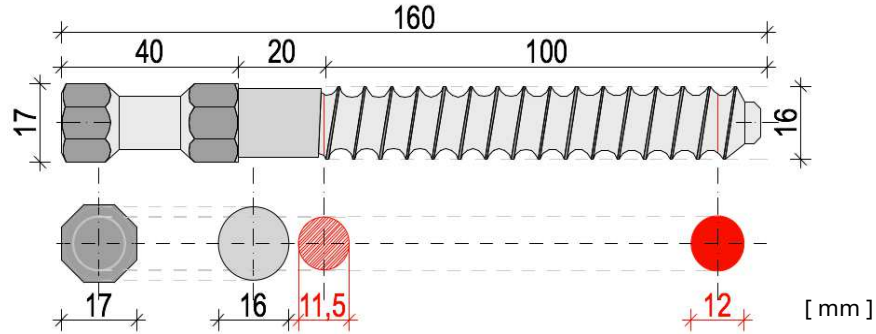


Fig. 1: Geometry of dry connectors Al-fer srl

2.3.2 Geometry of the samples

Representative samples of existing attics in **wood** they were made from a single central wooden beam (14x20 cm and 76 cm long) with two 5 cm thick reinforced concrete slabs on the sides, including electro-welded mesh. The behavior of steel connectors with a useful diameter of 16 mm at a distance of 19 cm was tested. A 2.5 cm thick wooden plank was interposed between the slabs and the beams, continuous above the beam on both sides.

Fig. 2 shows the plan and section of a typical specimen.

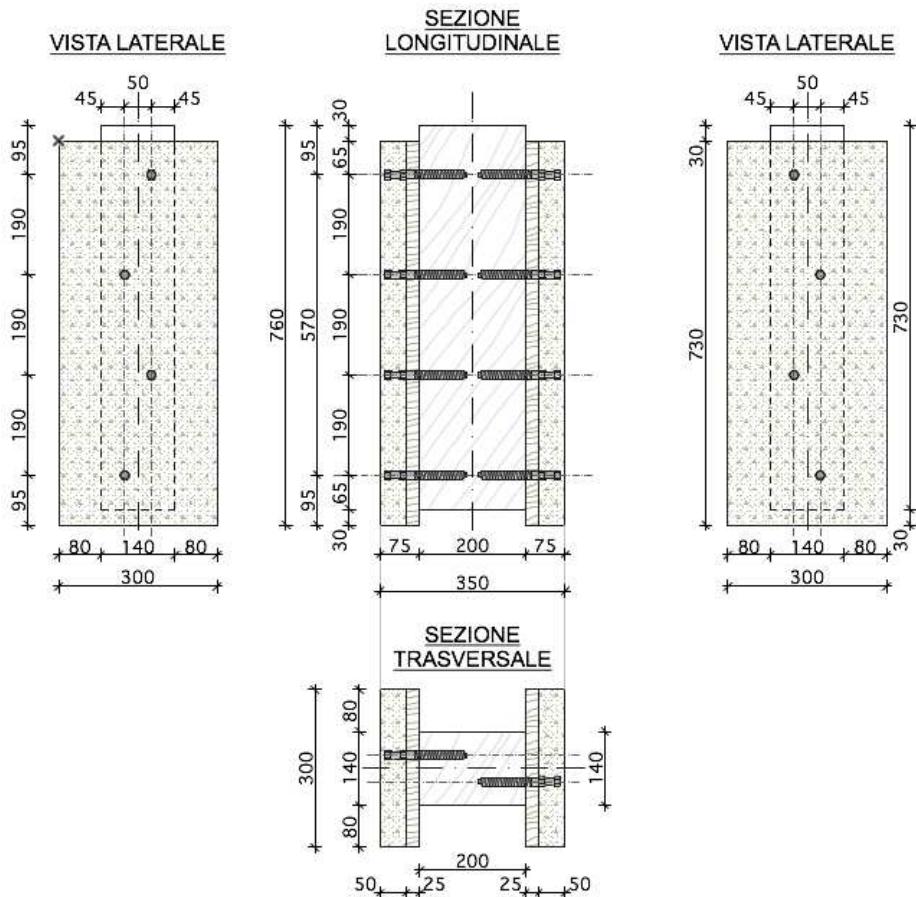


Fig. 2: Geometry of the case specimens of wooden beam and steel connectors

2.3.3 Scheme of the tests

Fig. 3 shows the scheme of the tests; the vertical load was applied through a preliminary settling cycle and subsequent measurement cycles up to failure, which varied according to the tested sample.

The following equipment, available at the Experimental Testing Laboratory on Materials of the Department of Construction and Transport of the University of Padua, was used to carry out the tests:

- N. 1 "Spider 8" acquisition unit;
- N.4 inductive displacement transducers type W;
- N.1 loading portal with 30 t jack;
- N.1 load cell of 10 t.

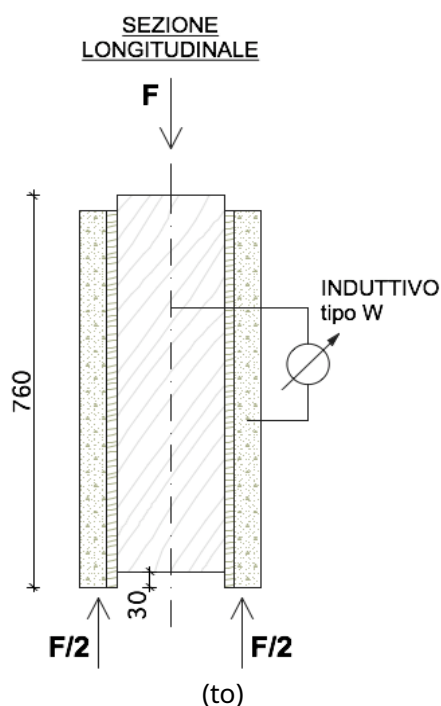


Fig. 3: Push-out test scheme

2.3.4 Matrix of tests Wood Steel

Three specimens of the previously specified geometry were subjected to sliding tests and the load applied to the wooden beam and the displacement immediately of the wood-concrete composite element by means of the dry connector Al-fer srl were measured on each of these .

The evidence matrix for the case in question is shown below.

test no	audition name	test no	experimental test name
1	LE.AC.1	1	01_1_acc
		2	01_2_acc
		3	01_rupture_acc
2	LE.AC.2	4	02_1_acc
3	LE.AC.3	5	03_1_acc

Tab. 2: Case test matrix of wooden beam and steel connectors

2.4 Experimental response

2.4.1 Test report

The test report of the Department of Construction and Transport of the University of Padua, delivered to the manufacturer of the connectors under study at the end of the experimentation carried out in July 2002, is shown below.

RAPPORTO DI PROVA N. 18905

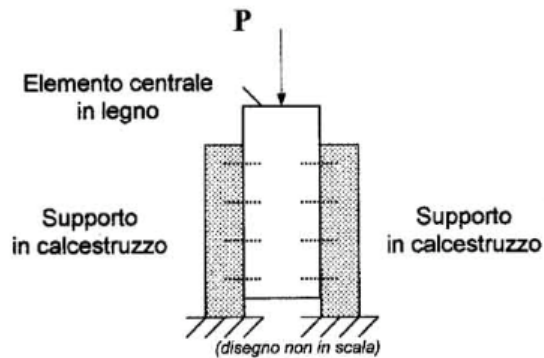
Pag. 1/1

Richiedente: AL.FER s.r.l., via dei Castagni n. 7 – VERONA.

Data della domanda di prova: 03 Luglio 2002.

Materiale: N. 03 campioni di elementi in calcestruzzo armato e legno da costruzione, assemblati mediante connettori in acciaio di produzione del Richiedente.

Prove richieste: prove di scorrimento per taglio come da schema di seguito riportato, secondo modalità non normative e concordate con il Richiedente.



Modalità di prova:

I campioni sono stati sottoposti a compressione in senso longitudinale, con applicazione del carico sulla sommità dell' elemento centrale, seguendo un ciclo composto dalle due seguenti fasi:

- 1^a fase: da scarico a circa 4000 daN e di nuovo scarico, per assestamento del campione,
- 2^a fase: da scarico fino al raggiungimento del carico massimo a rottura.

La prova vuole valutare la resistenza dei connettori, simulando le normali condizioni di utilizzo.

La prova si conclude con l'osservazione del tipo di rottura dei materiali impiegati.

CAMPIONE	CARICO MASSIMO	OSSERVAZIONI
1	18998 daN	In tutti i campioni si sono osservate la simultanea rottura del calcestruzzo e la rilevante deformazione dei connettori metallici con cedimento di alcuni di essi
2	17882 daN	
3	17038 daN	

Fig. 4: *Experimental test report of the University of Padua*

2.4.2 Available data

The behavior of the three samples, of the steel connectors and wooden beam series, subjected to the creep tests is analyzed below. For each test, the data detected by the load and displacement transducers are available, in Excel format, with which it was possible to construct the following types of curves:

- Load – time (F,t);
- Load – displacement (F,u).

From these graphs, the following aspects can be understood:

- Load speed (F/t) expressed in N/sec;
- Loading and unloading phases;
- Stiffness of the wood-concrete-connector system;
- Ultimate value of the load which corresponds to the real or conventional failure of the connection.

2.4.3 LE.AC.1

The first specimen, identified with the name LE.AC.1, was used as a test to calibrate the load cycles of the following 2 specimens, three tests were performed on it. The first load test, identified with the code 01_1_acc, was carried out by applying the force to the wooden beam in a monotonous way up to a value of about 2.000 daN, once this value was reached, the system was unloaded. The second test, identified with the code 01_2_acc, was performed on the same specimen and was carried out using two load intervals:

- a first cycle up to 2.000 daN with subsequent unloading;
- second load cycle from zero up to about 12.000 daN and unloading.

The third test, identified with the code 01_rottura_acc, took place at the end of test 01_2_acc, in these conditions the specimen was unloaded and showed permanent deformations. We proceeded to increase the value of the load from zero until the failure of the connected system was reached. Fig. 5 shows the trend of the load applied to the system as a function of time, for specimen LE.AC.1 and as a function of the three tests performed.

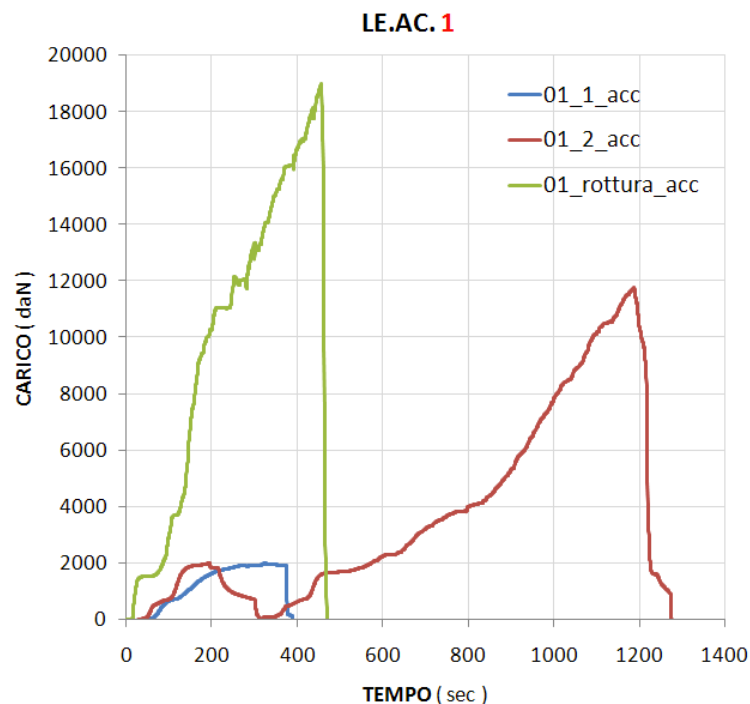


Fig. 5: Load graph - time for specimen LE.AC.1

Once the dynamics with which the experimentation was carried out have been clarified, the nomenclature used to identify the various samples as well as the tests on each of them, it is possible to enter into the merits of the load-displacement curves. These graphs have been obtained by processing the available data and are undoubtedly the most important material, through these curves it is in fact possible to study the stiffness values of the connected system or to understand the responses of the materials subjected to external load.

The transducers were positioned differently depending on the sample tested. More precisely as regards sample LE.AC.1, the transducers detected positive and negative slips. This fact appears to be attributable, since this information is not available, to the evaluation of possible clearances or imperfections of the samples. Although the origin of this choice is not known, it is still possible to draw some engineering considerations in this regard. As shown in Fig. 6, the transducers of sample LE.AC.1 are integral with the wooden beam and measure positive slips if the rod undergoes a shortening while negative slips are recorded in the case of lengthening of the same. The 4 transducers are positioned in pairs on the 2 longitudinal sections of the sample as shown in the figure.

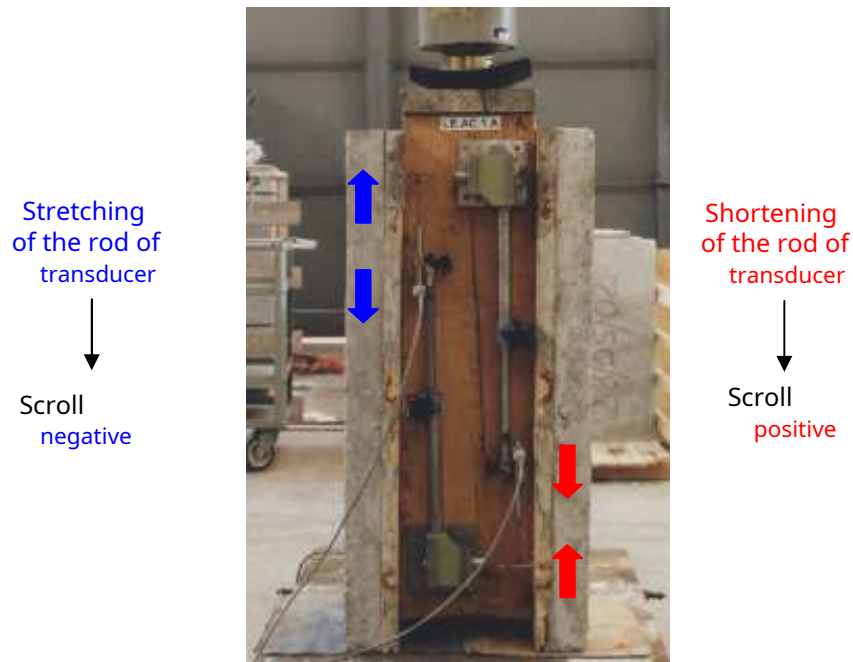


Fig. 6: Positioning of inductive type transducers on the specimen LE.AC.1

As it is reasonable to imagine, the transducers that recorded the greatest slips were those with positive values. As shown in Fig. 6, the transducer on the right detects a shortening between a point at a connector on the wooden beam close to the load cell and a point integral with the end slab. In the vicinity of the hydraulic jack, boundary conditions are expected such as to cause sudden variations in the state of tension and from which a greater range of displacements can be expected. Conversely, points of the wooden beam in correspondence with the lower test bench will be subjected to a lower state of stress and therefore less slip, as proved by the following graphs (left transducer-elongation).

The graphs relating to only the first two tests carried out on sample LE.AC.1 are shown below since the graphs of the breaking test, as already anticipated, are not clear enough to draw an understandable load-displacement diagram but are of undoubted interest the values of the ultimate load recorded at failure.

In the following we will refer to the data detected by the transducers, through the 4 channels dedicated to scrolling, indicating them with the symbol CH, diminutive of the Anglo-Saxon term channel followed by the corresponding number. For more understanding:

- CH1_channel 1_transducer dedicated to the passage of time in seconds;
- CH2_channel 2_transducer dedicated to the load in daN;
- CH3_channel 3_displacement transducer, in mm, on face A of the sample.
- CH4_channel 4_displacement transducer, in mm, on face A of the sample.
- CH5_channel 5_displacement transducer, in mm, on face C of the sample.
- CH6_channel 6_displacement transducer, in mm, on face C of the sample.

A) 01_1_acc

Fig. 7 shows the characteristic diagram F - u detected during the first test conducted on sample LE.AC.1.

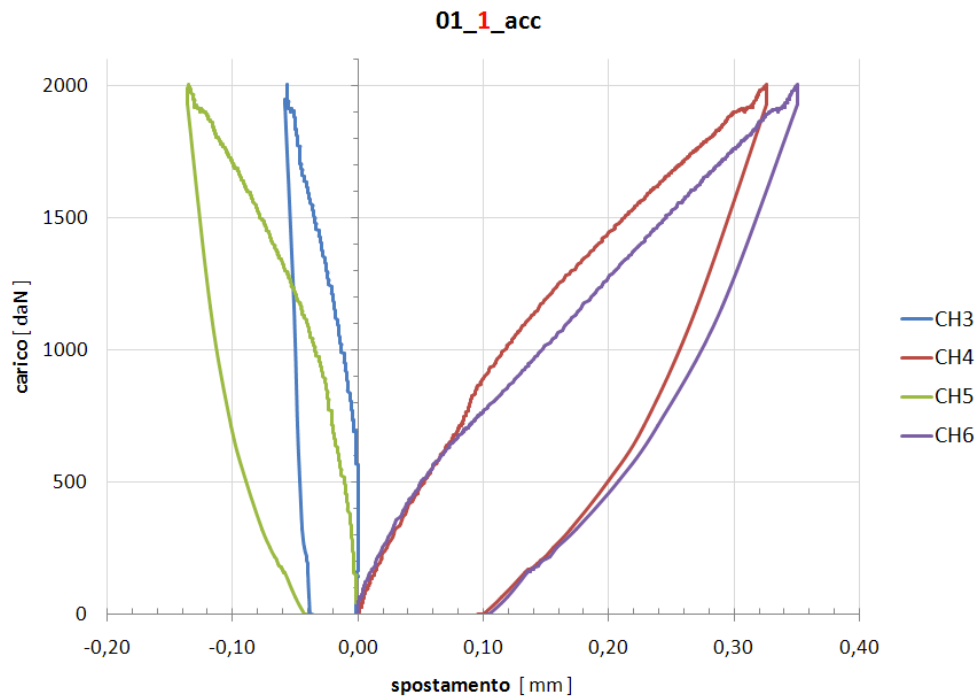


Fig. 7: *Experimental data - Load-slip curve test 01_1_acc sample LE.AC.1*

From the graph it is possible to make some observations:

- 1) The hypothesis of different sliding of points belonging to two different height levels is confirmed, with respect to the longitudinal section of the wooden beam, Fig. 8 (a). The curves with negative slips show a marked stiffness so that channel 3, CH3, begins to record displacements for force values greater than 700 daN;
- 2) The force absorbed by the single connector is proportional to the displacement (or sliding) to which it is subjected, it is reasonable to think that the connector near the lower support should absorb a smaller force than the connector at the head of the specimen where the application of the load, Fig. 8(b);
- 3) A fairly linear behavior is observed with a rather high slope of the curve, in fact you need 2-004 daN to produce a maximum slip of the sample equal to 0.351mm;
- 4) At the end of the test, a permanent deformation of about 1/10 of a millimeter is recorded.

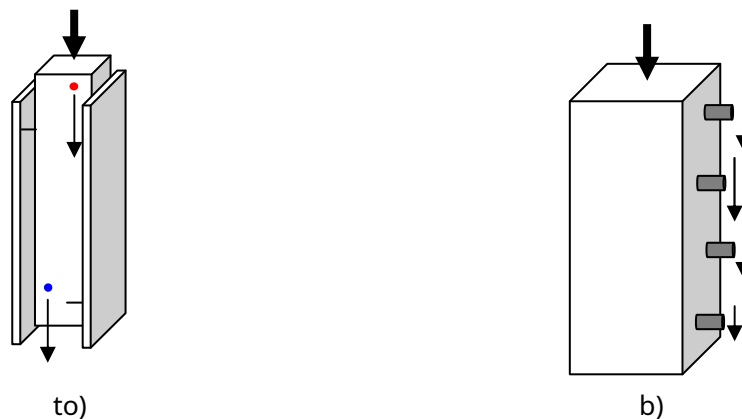


Fig. 8: *Diagram of the load specimen*

B) 01_2_acc

Fig. 9 shows the characteristic diagram F - u detected during the second test conducted on sample LE.AC.1.

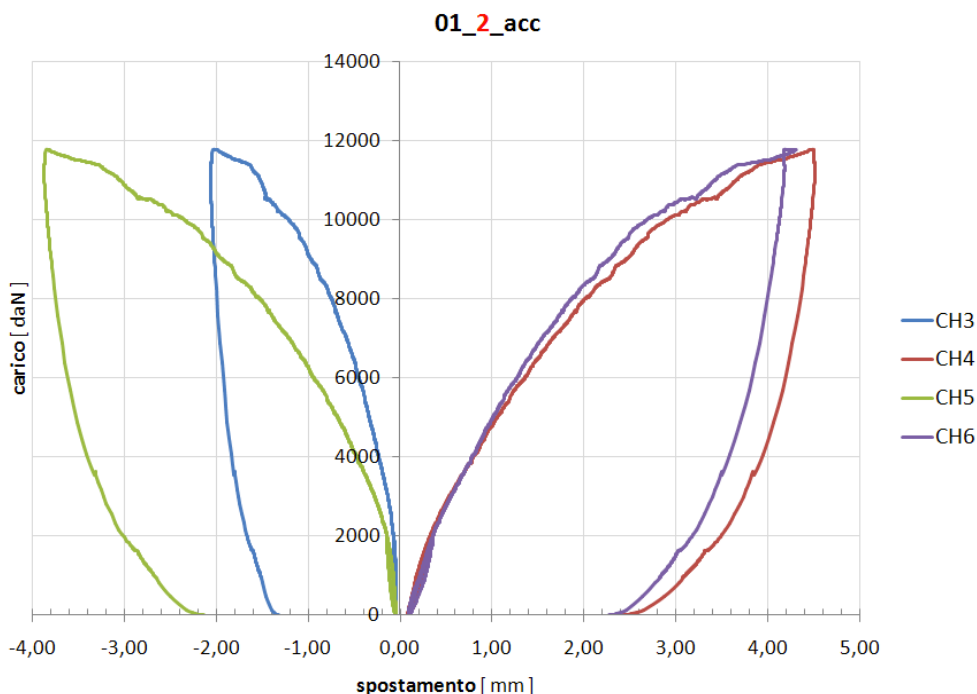


Fig. 9: *Experimental data - Load-slip curve test 01_2_acc sample LE.AC.1*

The first load cycle stopped at about 2.000 daN, we proceeded with the unloading and subsequent reloading up to 12.000 daN. The following considerations can be made:

- 1) The first cycle, by settling the sample, was performed to eliminate any friction caused by the presence of the wooden table. This gap, which is usually present in the consolidation interventions of wooden floors, was specifically inserted in the sample so as to faithfully reproduce the operating conditions to which the connector is usually subjected in practice. In fact, for reasons related to the practicality of laying the connectors, this planking is preferable to be continuous even if its presence modifies the static behavior of the connection. In the following, reference will be made to the studies conducted by professors Giancarlo Turrini and Maurizio Piazza and specifically to three articles, published in the magazine RECUPERARE ANNO 1983, which deal in detail with a static recovery technique for wooden floors. The technique described involves the use of connectors made of a steel rod (of the type with improved adherence for reinforced concrete), inserted into holes previously made in the wooden structure, and connected to the same by means of a semi-fluid epoxy resin-based glue. These connectors, the article explains, may exhibit a certain variety of static behavior in relation to the different ways of performing the intervention. Thus, three different types of behavior are distinguished: they may present a certain variety of static behavior in relation to the different methods of carrying out the intervention. Thus, three different types of behavior are distinguished: they may present a certain variety of static behavior in relation to the different methods of carrying out the intervention. Thus, three different types of behavior are distinguished:
 - cut (concrete slab in direct contact with the wooden beam);
 - in shear and bending (concrete slab connected to the wooden beam and continuous planking);
 - axial (connectors arranged inclined at 45° with respect to the axis of the beam).

The Al-fer dry connector does not use epoxy resins and its behaviour, in analogy with the Turrini system, is close to that of shear and bending connectors.

- 2) Also in this test, up to load values equal to 2000 daN, the behavior of the system is quite linear. Subsequently the curves denote a character of a non-linear type;
- 3) The maximum slip recorded is 4.156 mm for a load value of 11.776 daN.

C) 01_breakage_acc

This test was carried out quickly and the corresponding diagrams are not shown as they are strongly influenced by the failure of some connectors, Fig.10 (a), and by parts of the concrete slab in contact with the planking, Fig.10b). It will only be said, as reported by the report of proof, that the ultimate value of the load applied to the system was 18.898 daN with sliding values of about 25 mm, Fig. 10 (c), a value comparable with the initial deviation between the wooden beam and the test bench equal to 30 mm.

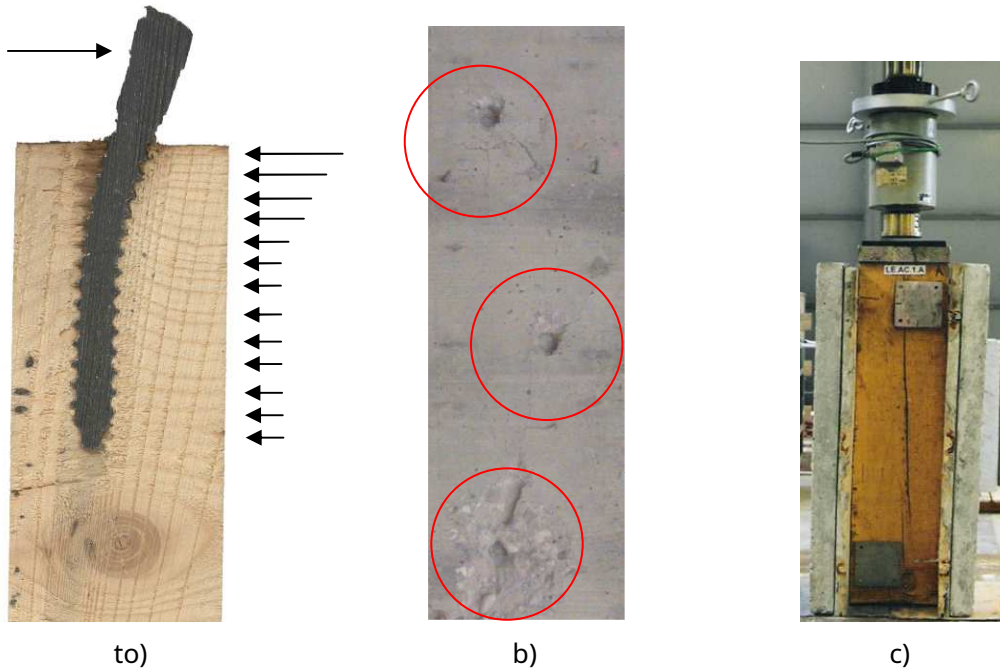


Fig.10: Images at the end of the test on specimen LE.AC.1

Below is a table including the numeric values detected.

LE.AC. 1							
Campione	prova	fase	carico CH2 daN	scorrimento			
				CH3 mm	CH4 mm	CH5 mm	CH6 mm
LE.AC.1	01_01_acc	1° carico	2004	-0,056	0,326	-0,135	0,351
	01_02_acc	1° carico	2004	-0,066	0,331	-0,141	0,361
		2° carico	2002	-0,070	0,333	-0,141	0,363
			4001	-0,229	0,796	-0,465	0,786
	01_rottura_acc	1° carico	11776	-1,990	4,469	-3,825	4,306
			1988	-2,291	-2,235	-4,414	-25,114
			4015	-2,291	-2,234	-4,415	-25,114
11790			-2,293	-2,234	-4,42	-25,115	
18998	-2,293	-2,234	-4,459	-25,115			

Tab.3: Numerical values for characteristic loads and slips on the specimen LE.AC.1

Conclusions on the LE.AC.1 specimen:

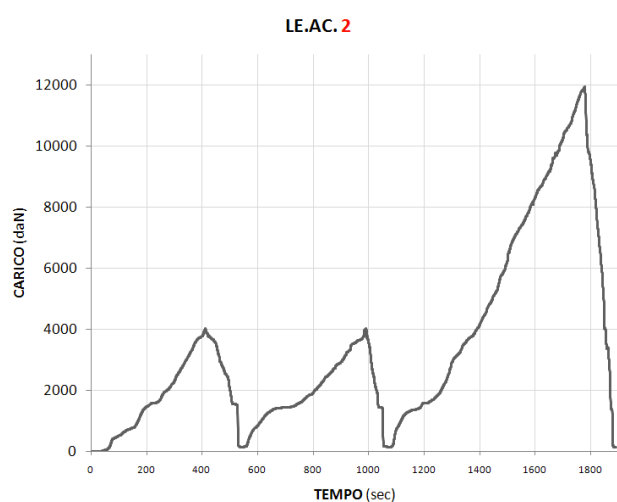
- 1) With this specimen the domain of values, respectively of the load and of the slips, admissible for the connected system under study was tested;
- 2) The first test, with a maximum load value of 2000 daN, approximately 2500 N on each connector, is useful for investigating the instantaneous behavior of the connectors or better for evaluating the service stiffness used for verifications at the operational limit states. Ample space will be given to this theme below;
- 3) The second test, with a maximum load value of 12,000 daN, which corresponds to approximately 15,000 N on each connector, is useful for studying the final behavior of the system where the materials reach significant plasticisations. It will be possible to obtain values of the ultimate stiffness, useful for the purposes of verifications at the ultimate limit state;
- 4) For both the first two tests, the incidence of loading and unloading cycles was evaluated, as it happens in reality. In fact, the floors, regardless of the material with which they are made, can be subject to variations in the configuration of the weights imposed on them during their useful life;

To conclude, during all the tests and in particular from the failure test, thanks also to the effective destruction of parts of the specimen, Fig 10 (b), it was possible to investigate the crucial aspects concerning the phenomenon. With reference to the studies conducted by the authors Turrini and Piazza, the main factors on which the stiffness and strength parameters of the connection via Al-fer srl dry connector depend can be summarized as follows:

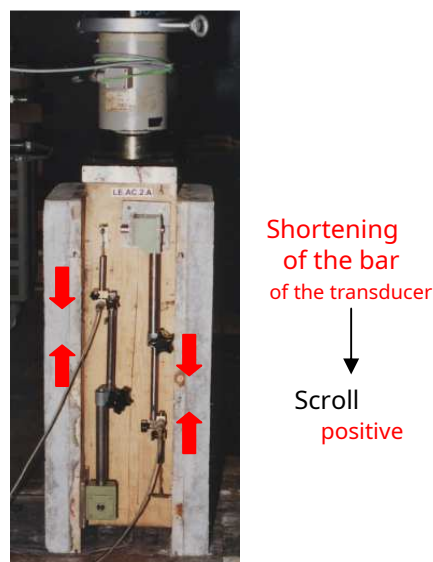
- Diameter, length of insertion in the connected materials and mechanical characteristics of the connector;
- filling of the connected materials (concrete slab and wooden beam);
- presence of a plank (shear and bending behaviour).

2.4.4 LE.AC.2

This sample differs from the first both in the way the test is performed, Fig. 11 (a), and in the different configuration of the transducers, Fig. 11 (b). All 4 of these have been positioned integral with the wooden beam and the measurements are due to the shortening of the rod of each transducer.



t)



b)

Fig. 11: Method and sample test scheme LE.AC.2

As regards the test methods, the load cycles carried out on the only test which concerned this specimen were:

- 1st CYCLE from zero to 4000 daN and unloading;
- 2nd CYCLE from zero to 4000 daN and unloading;
- 3rd CYCLE from zero to 12000 daN and unloading.

From the point of view of the writer, it is a test that wanted to investigate the relationship between the parameters of strength and stiffness of the connection and repeated load-unload cycles, Fig.11 (a). In this regard, it is advisable to introduce the Fu curves which clearly show the behavior of the connection solicited in the manner described above.

By virtue of the particular configuration of the survey equipment, the graphs are all 4 in the positive half-space differently from what happened for sample LE.AC.1 in which 2 channels detected lengthening and the other 2 shortening. Thus, for this second specimen, the shortening was detected with respect to two connectors, one close to the load cell and the other close to the lower bench, for 2 points of each face of the specimen, Fig.11 (b). It is therefore possible to evaluate the sliding of the system in correspondence with the 2 most stressed connectors, at the head of the beam.

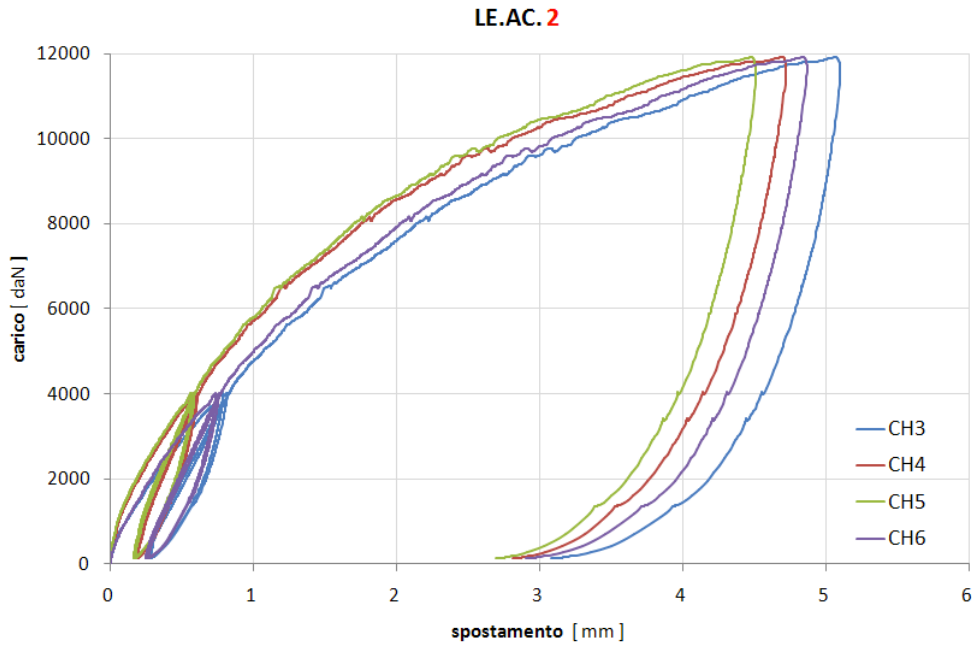


Fig. 12: Load-slip graph of the LE.AC.2 specimen

LE.AC. 2							
Campione	prova	fase	carico CH2 daN	scorrimento			
				CH3 mm	CH4 mm	CH5 mm	CH6 mm
LE.AC.2	02_01_acc	1° carico	1999	0,301	0,199	0,184	0,283
			3992	0,773	0,579	0,559	0,726
		2° carico	1999	0,504	0,344	0,323	0,474
			4000	0,811	0,606	0,581	0,759
		3° carico	1999	0,530	0,363	0,339	0,494
			3992	0,824	0,614	0,586	0,768
		11930	5,075	4,700	4,486	4,846	

Tab. 4: Numerical values for characteristic loads and slips on the specimen LE.AC.2

A first consideration can be made with regard to the curve Fu, Fig. 12, it can be seen that there is a good correspondence between the pair of curves of channels CH4 and CH5 and the pair CH3 and CH6. This fact suggests that the transducers 4/5 belong to one face, and the transducers 3/6 to the second face of the same sample.

It seems legitimate, after an analysis of the first two samples examined (LE.AC.1/2), to frame the connection of the wood-concrete composite system with Al-fer srl dry connectors from the point of view of a non-linear elastic constitutive bond. The stiffness/softness parameters are a function of the stress and/or strain level reached. In the logic of introducing a constitutive bond for the connection it appears evident how the bilinear model, Fig. 13(a), seems well to represent the simplified behavior of the tested samples, Fig.13(b).

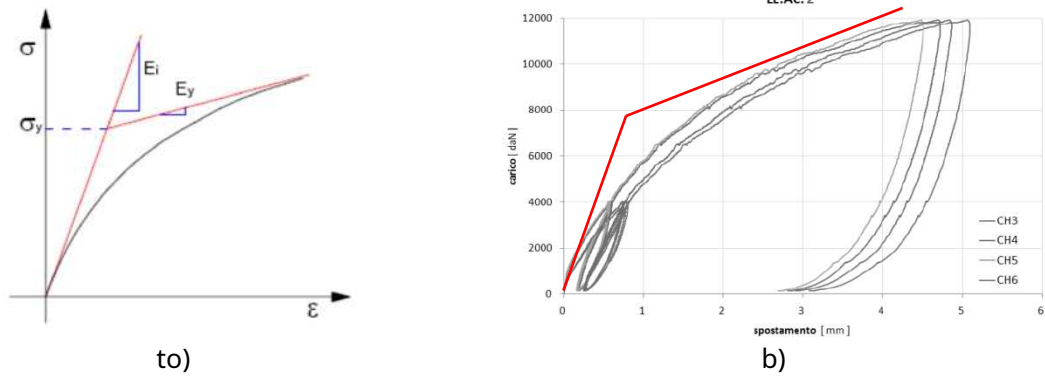


Fig. 13: Constitutive bond

In support of what has been stated, a first interval with an initial tangential elastic modulus can be introduced for the connected system *Heyan* and a second interval with plastic modulus *Heyy*. The tests, however, are able to provide further information especially with reference to the phenomenon of elastic-plasticity. We now want to dwell on this aspect and to do so it will be useful to introduce curves referring to slip values obtained from the average of the 4 displacement transducers. The sample LE.AC.2 was chosen, as this represents the trend of the sliding at the top of the wooden beam where the connectors are subject to greater force and sliding values. Fig. 14 (a), shows the experimental sliding force curve obtained as the average of the 4 transducers for the first loading cycle up to 4000 daN and subsequent unloading up to zero. Once the load has reached a certain level, if this is removed from the specimen, it is observed that only a part of the deformation can be recovered (elastic contribution), while the remaining part remains as residual deformation (plastic contribution). It should be noted that the residual deformation quota represents 30% of the maximum deformation reached with the first cycle and the remaining 70% competes for the completely reversible deformation.

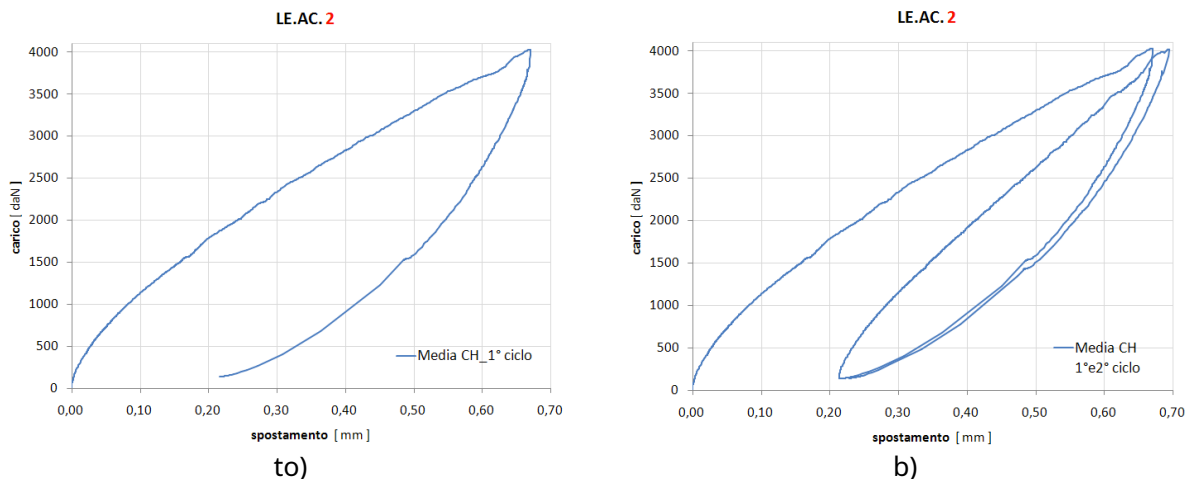


Fig. 14: Fu curve for the 1st and 2nd loading and unloading cycles of test LE.AC.2, mean of the channels.

If the first cycle is followed by a second identical cycle, Fig. 14 (b), it can be seen how the specimen tends progressively to the curve of the first load cycle. Having reached the value of 4000 daN for the second time, the discharge curve faithfully follows that of the first discharge. This aspect denotes a markedly elastic behavior on which the connection can rely. The proof of this last statement can be obtained by observing the trend of the average slip of the entire test schematized in Fig. 15.

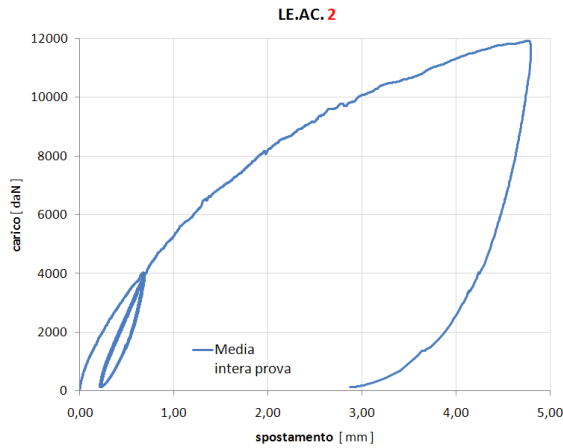


Fig. 15: *Fu curve of the entire test, average values.*

LE.AC. 2				
Campione	prova	fase	carico CH2 daN	scorrimento media mm
LE.AC.2	02_01_acc	1° carico	1999	0,242
			3992	0,659
		2° carico	1999	0,411
			4000	0,689
		3° carico	1999	0,432
			3992	0,698
			11930	4,777

Tab. 4*: *Average numerical values of the entire test.*

the load-slip curve of the third cycle retraces the footsteps of the second load and continues for successive force increments with a non-linear trend until the end of the test. In tab. 4* it is possible to observe the characteristic numerical values for this sample with reference always to the average slip value. Note how the average creep at the end of the second cycle (0.689 mm) differs by only 4% compared to that recorded at the end of the 1st cycle (0.659 mm) and by just 1% compared to the end of the 3rd cycle (0.698mm). These considerations confirm the hypothesis of elastic-plastic behavior assumed initially.

2.4.5 LE.AC.3

For the third and last sample a test similar to that of sample 2 was envisaged, which differs from the latter due to the reduced speed of application of the load with which it was conducted. In fig. 16 (a) shows the load-time curve relating to specimen 3, while in fig. 16 (b) it is possible to observe the comparison between the three specimens. This last image confirms the initial hypothesis of having taken specimen 1 as a test for the following 2 samples. At the discretion of the reader, this last test wants to investigate the effects of a lower loading speed on the system.

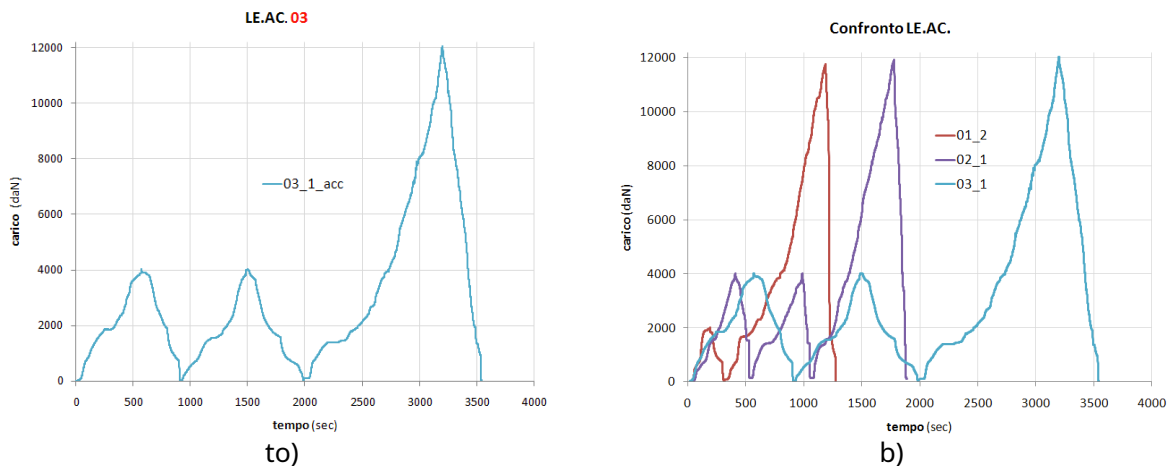


Fig. 16: *on the right, the test mode of the LE.AC.3 sample. On the left, the comparison with the other 2 specimens.*

Also in this test the transducers measure shortening of the rods and therefore 4 curves were obtained with displacement values all positive. As can be seen from the F- u curves (Fig. 17), and from the numerical data in Tab. 5, channel 4 has an unusual trend, not attributable to typical behaviors shown in all the tests presented up to now. The reason for this excessive movement could be attributable to some error during the test, perhaps due to a misalignment which has brought the transducer rod off axis. Although strange, a potential failure of some connectors that could have caused a greater sliding of the system cannot be excluded. However, this fact is implausible by virtue of the slowness with which the test was carried out.

In order to be able to compare the data and make a comparison between similar tests, tab. 5 the characteristic numerical values resulting from the 3rd sample in which the average refers to three channels with the exception of channel 4.

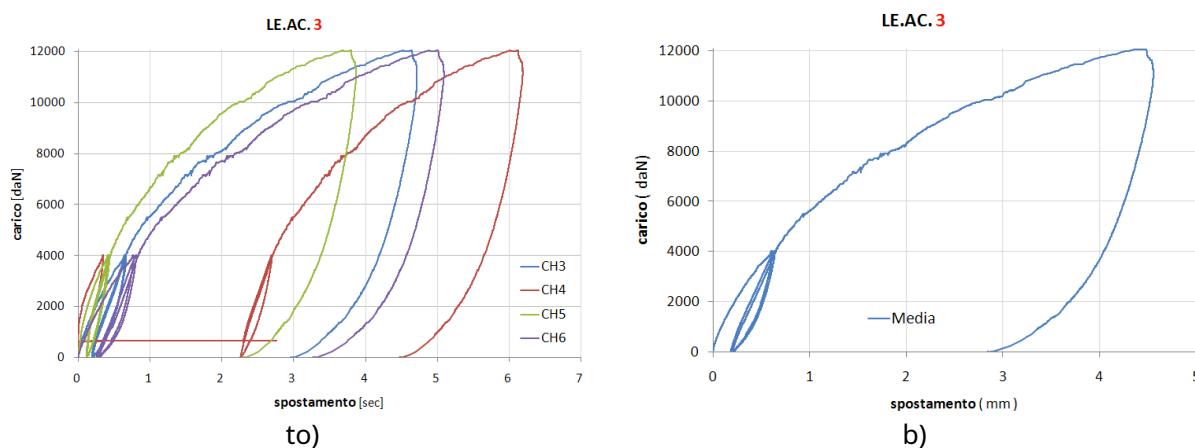


Fig. 17: Fu curve for test LE.AC.3, mean of the channels.

LE.AC. 3								
Campione	prova	fase	carico CH2 daN	scorrimento				
				CH3 mm	CH4 mm	CH5 mm	CH6 mm	media mm
LE.AC.3	03_01_acc	1° carico	1999	0,243	0,051	0,128	0,301	0,224
			4007	0,64	0,34	0,406	0,756	0,601
		2° carico	1999	0,404	2,439	0,219	0,534	0,386
			4000	0,656	2,689	0,429	0,795	0,627
		3° carico	1999	0,426	2,46	0,236	0,584	0,415
			3998	0,666	2,706	0,448	0,835	0,650
		11935	4,384	5,888	3,555	4,743	4,227	

Tab. 5: Numerical values of the test LE.CA.3.

The behavior of specimen 3 does not introduce novelties with regard to the mechanical behavior demonstrated by the connection in all the tests, once it is taken for granted that channel 4 is the result of an anomalous result attributable to reasons of another nature. The behavior is linear elastic within certain force values and then assumes a non-linear elastic character up to the conventional maximum force value reached in the tests.

2.4.6 Conclusions

Three samples subjected to different tests conducted in force control were studied. Each test was used to investigate the main aspects on which the phenomenon depends. It was understood, thanks to the observation of the slip trend as the load varies, that the connection has a non-linear elastic nature and can presumably be schematised by means of a bilinear model with work hardening assuming two different stiffness values.

The tests carried out highlight the critical aspects of the behavior of the materials involved but are of little use when it is desired to investigate further. In fact, much has been said about the response of the specimens to the applied loads and corresponding slips, but the state of stress and deformation has not yet been mentioned. The state of tension that is generated in the materials, for any values of force and sliding, can be quantified by means of the science of constructions by means of ways that contemplate simple equilibrium relationships. Other sources are represented by formulations from regulations which deal with the mixed wood-concrete connection by means of metal connectors through the experiences conducted by various authors such as for example Professor Turrini (University of Padua) and Piazza (University of Trento), Professor Gelfi (University of Brescia) and many others in Italy. First of all, however, was Johansen who in 1949 proposed an approach for the bearing capacity of the connection with cylindrical shank connectors (**European yield model**) obtained from simple considerations on the equilibrium at the limit state, with the hypothesis of a

rigid-plastic behavior for both materials. This approach, which was subsequently perfected by various researchers (Möller, 1950; Aune, 1966; Larsen, 1977), is today the basis of the calculation of the resistance of the connections of various national and international technical standards (DIN 1052:2004, EN 1995: 2004, Nicole document).

Experimental evidence has shown that some of the failure mechanisms, which occur in a wooden connection with connectors with a cylindrical shank, are associated with the bearing phenomena of one of the two connected wooden parts and yielding (bending) of the shank of the metal connector, with the formation of one or more plastic hinges. These concepts will be taken up again in the following with reference to the introduction of finite element numerical models, with which it is possible to investigate the stress and strain aspects of the connection not available from the experimental tests.

3 Connection stiffness

3.1 Introduction

In chapter 2 the push-out tests carried out in the past on the wood-concrete connected system by means of Al-fer dry connectors were described, and the output data from these tests were extensively discussed. With the logic of understanding what happens in the materials with reference above all to the tensions, a finite element model was prepared using the straus 7 program. The introduction of numerical models is an opportunity both as regards the study of local mechanisms not investigated by means of the data available from the experimental tests, both to test different configurations of connections which in reality are onerous in terms of time and economic resources.

The need now arises to refer to certain load-displacement curves of the experimental tests in order to be able to make comparisons with the numerical results.

3.2 Reference specimens

In the context of this chapter it is significant to refer to the average slip values of specimens 2 and 3 since the tests carried out are very similar to each other and the results are sufficiently comparable. The goodness of what is claimed can be seen in Fig. 18 in which the average values of the 4 transducers of the two compared tests, LE.AC. 2/3, I'm all in all in good tune.

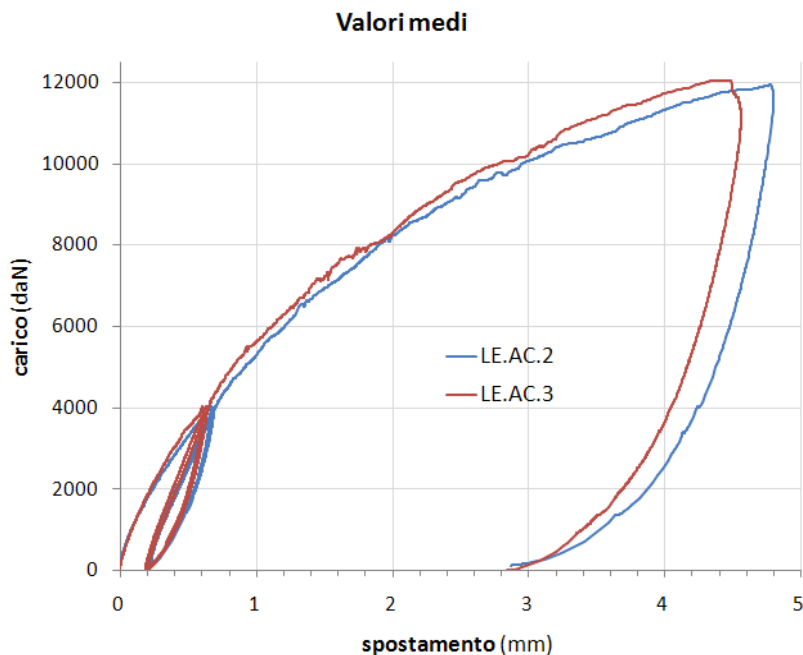


Fig. 18: Average numerical values of tests LE.CA.2/3, (8 connectors).

Before analyzing the numerical models it is necessary to introduce the analytical models available in the literature, already anticipated in the previous paragraphs. This fact becomes indispensable both to be able to correctly set up the FEM modeling and to make comparisons with analogous experiences.

3.3 Analytical models for the calculation of stiffness and bearing capacity

3.3.1 Pin connectors joined to the wood with epoxy resin

This technique is due to the names of professors Turrini G. and Piazza M. and is taken from articles 5,6,7, of the magazine Recuperare (Milan, 1983). The technique essentially consists in making a concrete slab collaborate statically with the existing wooden beams, with the aid of pin connectors joined to the wood with epoxy resin. On the basis of the results of the tests carried out, the authors have proposed behavior laws capable of representing the behavior of the connection itself up to conventional failure states. Below are some sentences taken from the articles considered to be of fundamental importance.

Knowledge of the static behavior of the connection is evidently essential for the purpose of analyzing the global behavior of the mixed wood-concrete structure. In particular, the **stiffness** and the **ultimate resistance** of the connection. The stiffness K is defined as the ratio between the intensity of the mutual force F (parallel to the beam axis) transmitted through the connection and relative displacement u (in the direction of the axis) of the two connected points; by ultimate resistance of the connection we mean the maximum value f_u of conventional failure, attributable to force F itself. The stiffness and strength parameters of the connection are directly related to the behavior of the single steel rod anchored in the wooden beam in its two typical operations, the so-called shear and axial.

With the aim of comparing the behavior of the connection, with Al-fer connectors and that with resin-coated pins, reference will be made to the first operation or to cutting. In the articles, the authors report two main types of operation:

- 1) Shear connector;
- 2) Shear and bending connector.

From the results of the experiments on the resin-coated pins, it was found that the behavior of the pin under shear stress does not practically depend on the diameter of the hole d_f , and as the anchor length L assumes significant importance only for values lower than 8 times the diameter of the peg d_{to} ; about this, being able to be fixed as a minimum practical limit $L \geq 10 d_{to}$, it will be possible to consider the behavior of the stud in shear independent of the anchorage length.

The value has been proposed as the ultimate value of conventional resistance T_u of the Force F - which corresponds to a displacement of about 1 mm (beginning of large displacements) - and as a constant value of the stiffness (in the linear field) the secant value w corresponding to a force value equal to 90÷95% of the value T_u . The following experimental expressions can then be provided for the two quantities considered in which the numerical factors are always to be understood as relating to forces expressed in newtons and lengths in mm:

$$w = 0.08 E d_{to} \quad (1)$$

$$T_u = 0.086 E d_{to} \quad (2)$$

The characteristic parameters of the shear connection, previously defined, coincide with the parameters identified for the stud, it being possible to set:

$$K = F/u = W = 0.08 E d_{to} \quad (3)$$

$$f_u = T_u = 0.086 E d_{to} \quad (4)$$

As far as the behavior of shear and bending connectors is concerned, these can be traced back to those of shear pins, introducing an analytical model that establishes formal equality between expression (3) and the analogous one valid for the end section of a **long beam in the middle elastic**. In this case the beam is made up of the steel peg and the hypothetical elastic means is made up of wood. The proposed adoption of the so-called beam coefficients **long** derives from the observation of the indifference of behavior with respect to the length of the peg. Indicating with E_{to} the linear modulus of elasticity of steel and with J_{to} the moment of inertia of the stud section and expressing the reaction parameter of the hypothetical elastic medium relative to the width d_{to} in the form E/m (m pure number), the stiffness expression is immediately obtained w provided by the analytical model:

$$W = E m^{-1} / \alpha \quad (5)$$

$$\alpha = [E / (4 m E_{to} J_{to})]^{1/4}$$

$$j_{to} = \pi d_{to} / 64$$

Putting now formal equality between the second members of (3) and of (5) we obtain:

$$m = 16.86 (E_{to}/AND)^{1/3}$$

$$\alpha = 0.7513 d^{-1/3} (AND_{to}/AND)^{1/3}$$

thus resulting in the definition of the characteristic parameters of the analytical model introduced.

The final expression of the stiffness is given k of the bending and shear connection:

$$k = qW \tag{6}$$

$$q = 3 [(ah_{or} - 1)^3 + 4]^{-1}$$

where W is the usual shear stiffness of the stud given by (3) or (5) eq represents a reduction factor of expression and h_{or} is the height of the intermediate table.

As regards the value of the ultimate conventional resistance, considering that it is commensurate with a displacement value, the following can still be asked:

$$f_u = q T_u \tag{7}$$

where T_u is given by (2).

From the experiences of professors Piazza M. and Turrini G., analytical models of pegs fixed in wood with resin have been obtained, these can be compared in terms of both stiffness and ultimate resistance with those obtained from tests on the system with dry connectors Al-fer srl. The analytical model just introduced refers however to the behavior of a single steel rod while in the experimental tests carried out on the Al-fer connector the specimens consist of 8 connectors. The comparison is therefore possible as long as it is possible to bring the Al-fer experimental tests back to a single connector. This fact is acceptable if we refer to specimens 2 and 3 in which the displacement transducers, as mentioned in paragraph 2.4.3, detect the sliding of the connectors at the end of the beam.

The force-displacement curves, Fig. 19, of the single Al-fer srl dry connector are presented below. These were obtained by considering specimens 2 and 3 and referring to average slip values and dividing the load applied to the structure by 8 for simplicity and compliance with the equilibrium hypotheses.

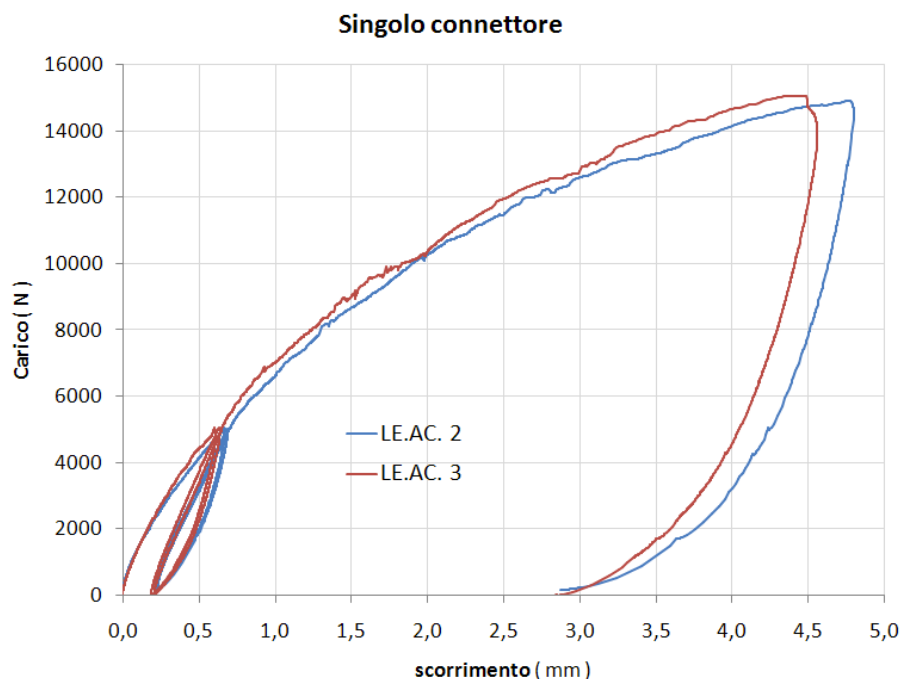


Fig. 19: Average numerical values of tests LE.CA.2/3 on a single connector.

The analytical model of the resin-coated stud requires the definition of parameters that exclusively concern the wood and the stud. These, as already mentioned, consist of steel bars with improved adherence and an elastic modulus value of 200,000 Mpa can be assumed.

For wood, a third category (C18) and a value of the elastic modulus parallel to the fibers equal to 8000 Mpa can be reasonably assumed, a value justified by the presence of evident cracks along the beams, Fig. 10 (c). If the previous hypotheses are assumed, by means of the analytical model introduced, it is possible to make a comparison between a 16 mm diameter resin-coated stud and the behavior shown by the experimental tests on the Al-fer dry connector.

- Assumed assumptions:

Elastic modulus of the wood	AND=	8000	Mpa
Elastic modulus of the stud	AND _{st} =	200000	Mpa
Diameter of the stud	d _{to}	16	mm
Height of the plank	h _{or}	25	mm

- Shear behavior:

Initial stiffness	w	= 10240	Mpa
Ultimate resistance	T _u	= 11008	Mpa

- Shear and bending behavior:

Initial stiffness	k	= 8127	Mpa
Ultimate resistance	f _u	= 8373	Mpa

Fig. 20 shows the comparison between the experimental curves and the analytical model for a 16 mm diameter resin-coated peg.

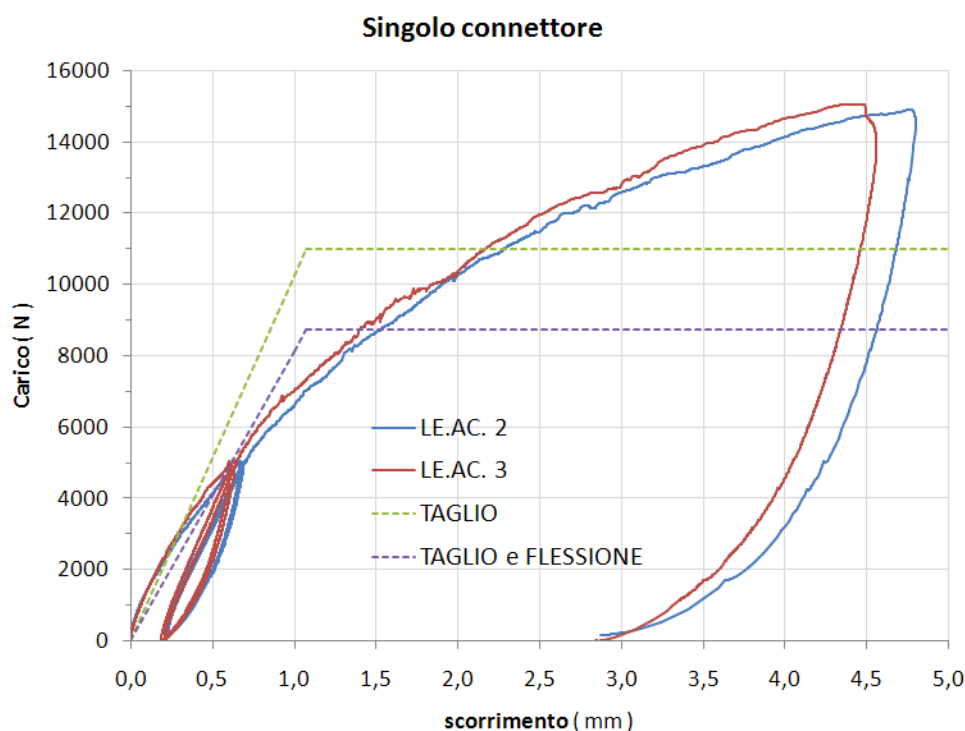


Fig. 20: Comparison between the experimental tests and the analytical model of a domed stud.

The following observations can be made:

- 1) the Al-fer dry connector has a high initial stiffness, and precisely because of this it is close to a 16 mm diameter resin-coated stud with shear behavior. The shear and bending model is too conservative for low load values, while the experimental curve tends to that of the shear and bending pin for force values of about 5000 N;
- 2) both analytical models are too conservative with reference to the ultimate resistance values, resulting in inadequate for a comparison with the Al-fer connector;

We can add a reflection on the causes that lead to a high initial stiffness. This fact is probably attributable to a coercive effect that arises between the wooden beam and the intermediate planking, due to the fact that the Al-fer connector is equipped with a rebate which compresses the

the planking to the beam itself. In Fig. 21 we can appreciate what has been said. The connector, whose central body is reverse conical (it has a diameter of 11.5 mm at the extrados of the beam and 12 mm at the tip), is able to function as a pressure plug. In our opinion, this effect is capable of generating a delay in sliding thus generating a high stiffness tangent to the origin.

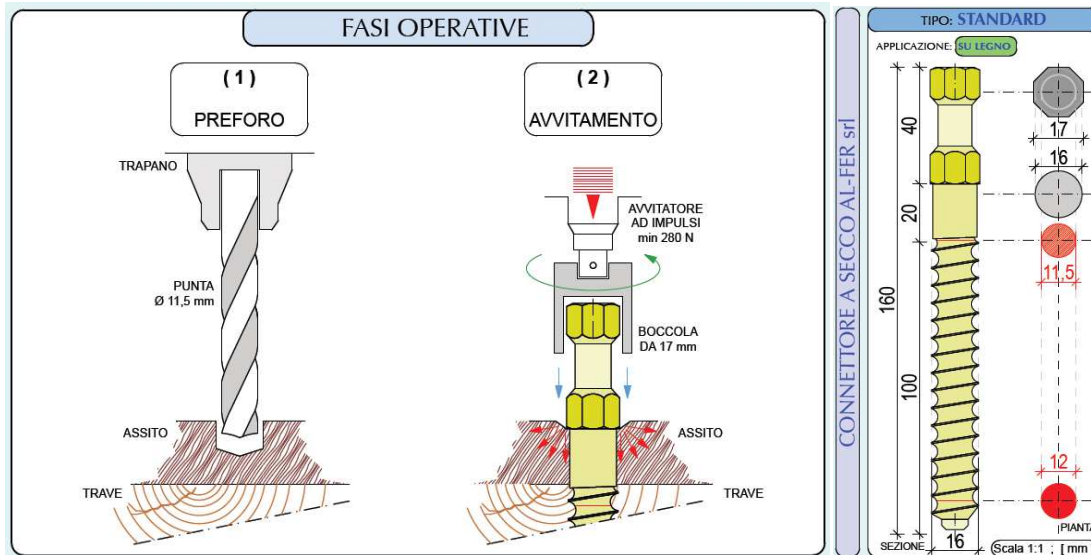


Fig. 21: Fixing the dry connector Al-fer srl

3.3.2 Dry connectors within calibrated holes

This second connection technique has been studied in detail by Professor Piero Gelfi of the University of Brescia. Like the Turrini method, the peg is made with a (now smooth) bar of reinforcing steel, but differs from this in that the resin is removed. The fixing of the peg in the wooden beam is obtained by making a calibrated hole, about one or two mm smaller than the diameter of the connector.

The study conducted by Prof Gelfi and staff concerns the theoretical modeling of the connection between slab and beam made with dry rungs with interposed planking. The approach originates from a theoretical and experimental study for the stud connectors of mixed steel and concrete sections (Gelfi and Giuriani 1987), in which the initially elastic behavior of the connector and the failure behavior with the formation of plastic hinges are modeled in the connector shaft. The results of the theoretical modeling are compared with the experimental results obtained in Gelfi and Giuriani 1995 and Gelfi et al.1995.

THEORETICAL EVALUATION OF THE STIFFNESS OF THE CONNECTION

The behavior of the peg, Fig. 22 (a) is ideally traced back to the classic one of the beam on elastic ground, Fig. 22 (b), both in the section immersed in the concrete and in the section driven into the wood. The section corresponding to the planking interposed between the slab and the beam is considered free, since the planking is not rigidly constrained to the joist and the peg acts in this section within a very yielding medium since it is stresses perpendicular to the fibres.

For the stiffness k_{wf} few experimental results are available for wood. According to the tests carried out by the authors, the stiffness in the elastic range in the direction parallel to the fibres, defined as the ratio between the strength of the stud-wood interface per unit length of the stud and the relative displacement has, for the spruce species, can be assume a value of about 1300 Mpa and does not seem to significantly depend on the diameter of the stud.

The stiffness of the concrete k_c has been studied in detail (in Gelfi and Giuriani 1987), where it is report was proposed $k_c = \text{AND}/b$ with $b = 2.5 \div 3.3$ according to the ratio between the diameter and the center distance of the studs.

The stud is assumed to have unlimited length both in concrete and in wood, Fig. 22 (c), since the depth of the disturbed areas, where the deformations are significant, is modest and comparable with the design length generally adopted for the stud.

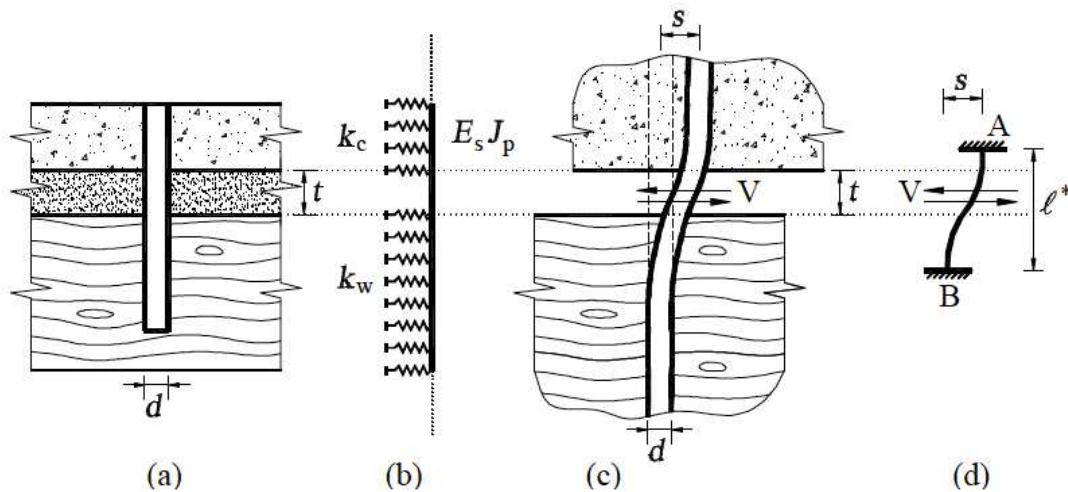


Fig. 22: Model for calculating the stiffness of the connection

Resorting to the classical solutions of the theory of the beam on elastic ground, imposing the continuity of the deformation of the post under the effect of the relative displacement s between the concrete and the wood, Fig. 22 (c), it is possible to obtain the stiffness k_{prof} of the connection as the ratio between the shearing action V and the displacement s :

$$k_{prof} = \frac{12 \cdot E_s J_p}{4 \cdot t \cdot \left(3 + \frac{3 \cdot t \cdot k_w}{E_s J_p} \right)} \quad (8)$$

where t is the thickness of the interposed boarding and $E_s J_p$ the flexural stiffness of the stud.

It is possible to arrive at a simpler formulation, which closely approximates the exact solution, imposing that the stiffness of the connection is equal to that of the doubly wedged stud of ideal length l^* , Fig. 22(d):

$$k_{prof} = \frac{12 \cdot E_s J_p}{l^*} \quad (9)$$

$$l^* = \frac{12 \cdot E_s J_p}{k_{prof}} \quad (9')$$

Function l^* can be expanded in Taylor series around the reference values k_c, k_w, t, d of the four variables:

$$l^* = l^*(k_c, k_w, t, d) = l^*(k_c^0, k_w^0, t^0, d^0) + \frac{\partial l^*}{\partial k_c} (k_c - k_c^0) + \frac{\partial l^*}{\partial k_w} (k_w - k_w^0) + \frac{\partial l^*}{\partial t} (t - t^0) + \frac{\partial l^*}{\partial d} (d - d^0) + \dots$$

It is possible to verify that the dependent terms of derivatives higher than the first order, direct and mixed, are negligible and thus stop the series at the first order terms.

Assuming the most common values for the reference values of the stiffness of the concrete and of the wood, of the thickness of the interposed boarding, and of the diameter of the stud:

- $k_c = 10000 \text{ Mpa}$;
- $k_w = 1300 \text{ N/mm}^2$;
- $t = 25 \text{ mm}$;
- $d = 16 \text{ mm}$

we get:

$$- 17.3 - 0.000572 - 0.00894 \text{ and } \dots \quad 0.880 \quad 4.34 \% \quad (10)$$

with σ expressed in Mpa, t in mm.

It is possible to obtain a further simplification by considering that significant variations of lead to negligible variations of σ . Therefore, placing $\sigma = 10000 \text{ N/mm}^2$, (10) can be rewritten in the following way:

$$- 11.6 - 0.00894 \dots \quad 0.880 \quad 4.34 \% \quad (11)$$

The error made in the evaluation of k_{pc} with (10) and (11) is less than 5% if the parameters vary within the ranges of practical interest:

$$7000 < \sigma < 14000 \text{ N/mm}^2 ; 900 < t < 1300 \text{ N/mm}^2 ; 12 < d < 20 \text{ mm} ; 0 < t < 50 \text{ mm}.$$

This imprecision leads to a maximum error of 14% in the evaluation of the stiffness k_{pc} of the connection.

Note that the expression of k_{pc} cannot be reduced directly to a linearly dependent relationship on the variables, σ , d , t as it is strongly influenced by the terms containing the mixed derivatives and the higher order derivatives of the variables of t .

In the case of connectors with a diameter of $d = 16 \text{ mm}$ with interposed planking, the theoretical straight line practically coincides with the first section of the experimental curves.

THEORETICAL EVALUATION OF THE ULTIMATE STRENGTH OF THE CONNECTION

The length of insertion in the wood and in the concrete adopted in the construction practice is generally such as to allow to reach the maximum resistance of the stud which occurs when a collapse mechanism is formed with two plastic hinges (Gelfi et al.1995 and Gelfi and Giuriani 1987). In the present work, the theoretical evaluation of the resistance of the connection refers to this situation of a post with a sufficient length of insertion in the wood and concrete for the formation of a collapse mechanism with two plastic hinges, also considering the presence of the interposed thickness t , Fig. 23.

The formulation represents an extension of the theory developed for steel-concrete connections (Gelfi and Giuriani 1987) and of the theory proposed by Johansen (1949), called the "European Yield Model", adopted by the EC5, concerning wood-wood and wood- metal plates.

It is considered appropriate to refer to the concept of effective length introduced in (Gelfi and Giuriani 1995). The bearing capacity of the pin is in fact equal to the resultant of the bearing pressure σ_{w1} in the wood acting on the effective length l_{e1} or the bearing pressure σ_{c1} in the concrete acting on the effective length (Fig. 23). The peg must then have a minimum additional length of sinking into the wood and concrete (respectively l_{w1} and l_{c1} in Fig. 23) so that the collapse mechanism can be established with two plastic hinges (Fig. 23 a) which allows to reach the maximum bearing capacity.

Since there is no shear in correspondence with the plastic hinges A and B where the bending moment of the pin is maximum (Fig. 23c), the equilibrium of section AB (Fig. 23d) is expressed by the equation:

$$\sigma_{w1} \frac{l_{e1}}{2} + \sigma_{c1} \frac{l_{e1}}{2} - Q = 0 \quad (12)$$

l_{e1} , l_{e2} concrete side effective lengths; plastic resistance moment of the stud;
 σ_{w1} , σ_{c1} seepage resistance of concrete and wood; ultimate resistance of the connection for each rung.

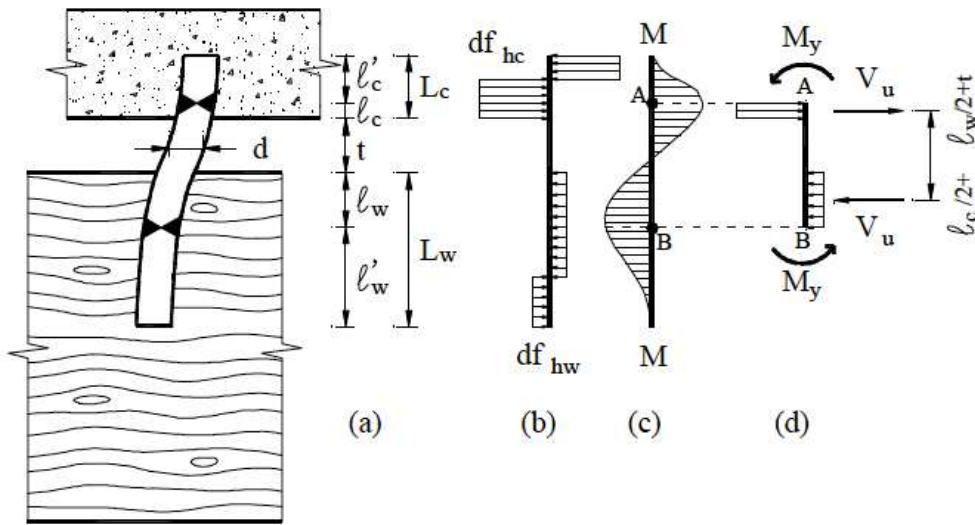


Fig. 23: Collapse mechanism and model for calculating the resistance of the stud

From (12), being the ultimate resistances of the connection for the single rung:

$$R_u = \frac{M_{pl,y}}{l_e} \quad (12')$$

and being:

$$l_e = \frac{1}{\sqrt{1 + \frac{12EI}{l^3}}} \cdot l \quad ; \quad B = \frac{1}{\sqrt{1 + \frac{12EI}{l^3}}} \quad (12'')$$

the effective length of the section fixed in the wood can be obtained:

$$l_e = \frac{1}{\sqrt{1 + \frac{12EI}{l^3}}} \cdot l = \frac{1}{\sqrt{1 + \frac{12EI}{l^3}}} \cdot \frac{1}{\sqrt{1 + \frac{12EI}{l^3}}} \quad (13)$$

Since the plastic resisting moment of the stud is given by the known relation:

$$M_{pl,y} = \frac{\pi}{6} \cdot f_y \cdot I$$

where f_y is the yield strength of the stud, (13) can be written in the more expressive form:

$$l_e = \frac{1}{\sqrt{1 + \frac{12EI}{l^3}}} \cdot l \quad (14)$$

with:

$$I = \frac{\pi}{64} \cdot d^4 \quad (15)$$

The ultimate resistance of the stud is then for (12') and (14):

$$R_u = \frac{\pi}{6} \cdot f_y \cdot d^2 \quad (16)$$

It should be noted that the lengths of insertion in the wood, equal to six diameters, are sufficient for the establishment of the collapse mechanism with two plastic hinges.

Now, by means of the equations presented, it is possible to estimate the behavior of the connection with pegs fixed by means of holes calibrated with the system that we will call Gelfi. A comparison can therefore be made with a Gelfi pin and the Al-fer connector. As usual, the expressions provided are valid for a single stud and therefore the comparison will be made on wood similar to that used for the Al-fer and 16 mm stud tests.

The Al-fer connector is made from a steel with a yield strength twice that of a smooth reinforced concrete bar, but along its axis the section varies from a maximum of 16 mm to a minimum of 11.5 mm. These two aspects, together with the abutment and the previously discussed pulling effect, could, and this is what we want to demonstrate, confer superior strength and stiffness properties to ordinary connection systems with a constant diameter equal to the maximum diameter of the dry connector Al-fer.

COMPARISON OF GELFI SYSTEM AND AL-FER DRY CONNECTOR

The hypotheses are reported below, by means of the analytical model introduced, for a comparison between a 16 mm diameter stud in calibrated holes and the behavior shown by the experimental tests on the Al-fer dry connector.

Assumed assumptions:

1) WOOD:

Fir type (class C18)

Characteristic mass

Bearing resistance

Stiffness

ρ_k	=	320	Kg/mc
f_{hw}	=	35	Mpa
k_w	=	1300	Mpa

2) CONCRETE:

class C25/30

Bearing resistance

Stiffness

$f_{a, extension}$	=	25	Mpa
f_{hc}	=	120	Mpa
k_c	=	10000	Mpa

3) PEG:

Peg diameter

Characteristic yield strength Elastic modulus of the stud

Moment of inertia of the rung

d	=	16	Mpa
f_y	=	350	Mpa
AND_s	=	210000	mm
j_P	=	3217	mm ⁴

4) ASSISTED

height of the table

h_{or}	=	25	mm
----------	---	----	----

Stiffness of the analytical model:

Ideal length of the doubly wedged rung

[equation (10)]

Initial stiffness

[equation (9)]

	=	91	mm
k_P	=	10611	N/mm

Ultimate resistance of the analytical model:

dimensionless parameter.

[equation (15)]

Effective length of the section driven into the wood.

[equation (14)]

Effective length of the section driven into the concrete.

[equation (12'')]

Ultimate resistance

[equation (16)]

THE	=	1.36	
	=	22	mm
	=	6	mm
v_u	=	12223	No

The stiffness and ultimate strength trend of the Gelfi stud can therefore be plotted by superimposing it on the experimental values of the Al-fer dry connector, Fig. 24.

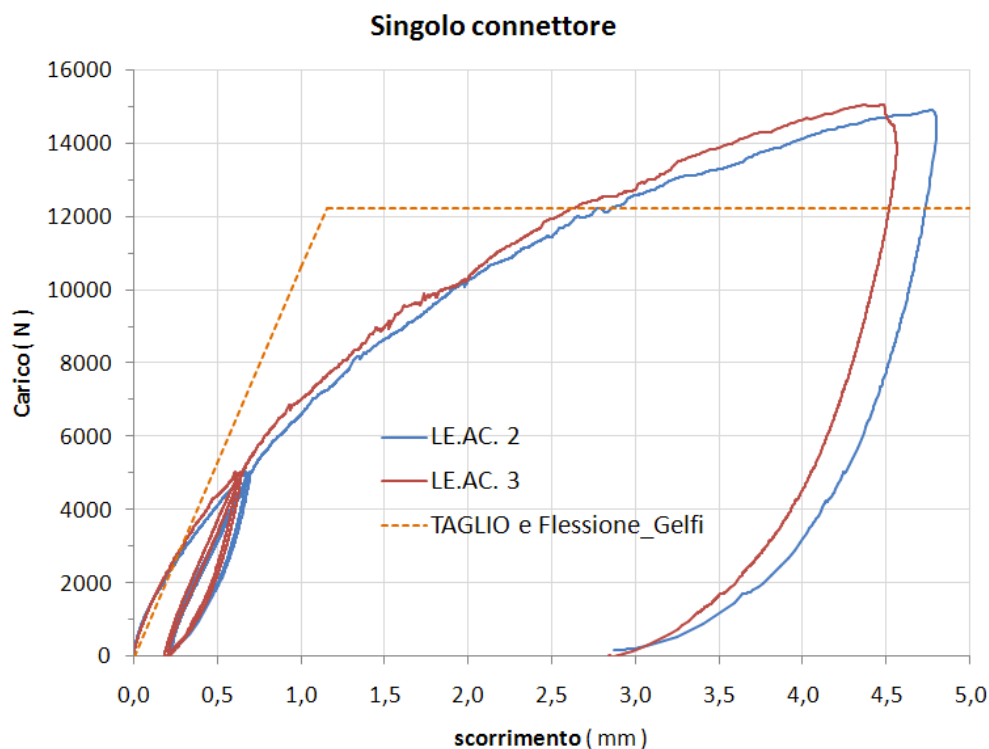


Fig. 24: Experimental curves Al-fer and analytical model prof. Gelfi

The following considerations can be made:

- 1) The analytical model proposed by Professor Gelfi is undoubtedly more complete than the one proposed for the behavior of resin-coated pegs. In the latter the stiffness and resistance parameters are obtained, like that for the studs in calibrated holes, from the theory of the long beam in an elastic medium;
- 2) The analytical model foresees an exact formulation and a simpler one, the latter foresees the use of an ideal length which could be of great help for FEM applications;
- 3) Assuming that the values assumed for the materials are dictated by common sense and are not the result of adequate investigations, we note a good correspondence with the Al-fer experimental data and the stiffness of the studs in calibrated holes with a diameter of 16 mm. The initial stiffness value of the studs is 10611 N/mm and the curve obtained with this slope intersects the experimental curves for values of approximately 3000 N, corresponding approximately to the sliding force to be applied to the connectors in operation;
- 4) The ϕ 16 mm stud connection with planking interposed between the slab and the beam has a behavior very close to that of the Al-fer dry connectors with reference to the initial stiffness. On the other hand, it underestimates the ultimate resistance, in fact V has been obtained $v=12223$ N, incorrect by more than 20% compared to the approximately 15000 N of the Al-fer dry connector;

3.3.3 Regulations

On Italian soil, the mandatory legislation is contained in the text of the DM 14/01/08, also called technical standards for construction "NTC 08". Chapter 4.4 is dedicated to wooden constructions, and in particular paragraph 4.4.9 deals with the connections of the various types of union (wood-wood, steel-wood, etc...). In this sub-chapter the standard explains that the bearing capacity and the deformability of the means of connection can be evaluated with reference to standards of proven validity. These can be found in chapter 12 of the NTC 08, where it is explained that the indications given in the following documents are intended to be consistent with the principles at the basis of the same:

- Structural Eurocodes published by CEN, with the specifications given in the National Appendices or, in the absence of these, in the international form EN;
- UNI EN harmonized standards whose references are published in the Official Journal of the European Union;
- Standards for tests, materials and products published by UNI.

Following a research carried out, the regulations useful for this work are:

- 1) CNR-DT 206/2007_Instructions for the design, execution and control of wooden structures;
- 2) EC5_UNIEN1995-1-1-2009_Design of timber structures.

Examining the regulations, it is clear that the model adopted is of the perfect elastic-plastic type, and the behavior of the joining medium is described by three fundamental parameters:

- k_{LM} instantaneous slip modulus (in N/mm) for each shear resistant section and for each joining means, to be used in the limit state of exercise ;
- k_8 instantaneous slip modulus (in N/mm) for each section resistant to shear and for each means of connection, to be used in the limit state of last ;
- $f_{v,Rk}$ characteristic bearing capacity for nails, bolts, dowels and screws, for single shear plane and for single joining means.

A first observation can be made regarding the difference with which the two standards mentioned determine the parameter k_{LM} :

CNR 206/2007	EC5 2009
$k_{LM} = 2 \cdot \rho \cdot \frac{d_0}{20}$	$k_{LM} = 2 \cdot \rho_{0,R} \cdot \frac{d_0}{23}$

In which ρ and $\rho_{0,R}$ are respectively the density of the wood, average and characteristic. The number 2 is due to the fact that according to the legislation for wood-concrete unions the values of k_{LM} can be doubled.

As for the k_{LM} values and $F_{v,Rk}$, the two regulations are in excellent agreement, the proposed formulations are reported below.

Slip module for ULS:

$$k_8 = \frac{2}{3} \cdot k_{LM} \tag{17}$$

The characteristic value of the load-bearing capacity of wood-concrete joints, with cylindrical shank metal connectors, can be traced back to that of wood-steel joints with a shear plane with plate **thick**. This assumption requires that the connection system is sufficiently embedded in the two materials Fig 25, and that the following minimum conditions are guaranteed:

- $L_w \geq 6d$
- $L_c \geq 2.5d$

Where is it:

- L_w is the plunge length of the dowel into the wooden element (Fig 25)
- L_c is the plunged length of the dowel into the concrete;
- D is the diameter of the connector.

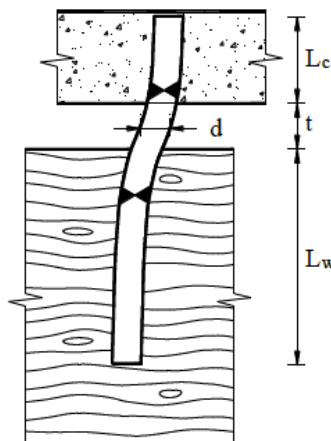
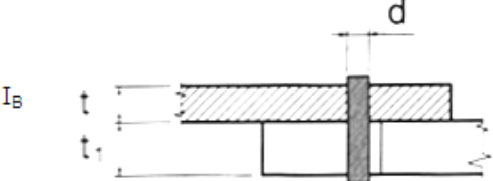
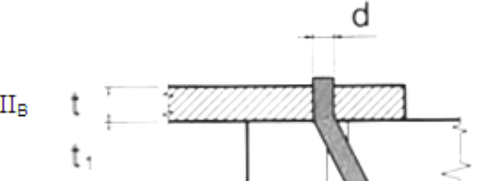
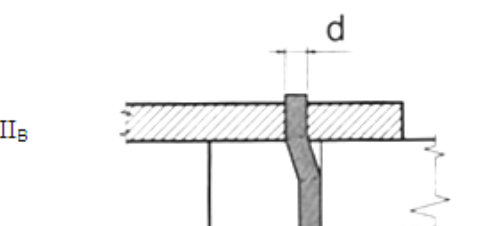


Fig. 25: Connection made with pins with cylindrical shank

The characteristic value of bearing capacity, for each joining means and shear plane with steel plate *thick*, will be assumed as the smallest of the values obtainable from the following formulas:

Piastre spesse $t \geq d$	
Modi di rottura	Valori caratteristici di resistenza a taglio
 <p>I_B</p>	$R_k = f_{h,k} t_1 d$
 <p>II_B</p>	$R_k = f_{h,k} t_1 d \cdot \left[\sqrt{2 + \frac{4M_{y,k}}{f_{h,k} t_1^2 d}} - 1 \right]$
 <p>II_B</p>	$R_k = 2,3 \cdot \sqrt{M_{y,k} f_{h,k} d}$

Tab. 6: Modes of failure and characteristic values of steel-wood joints

In which the terms contained in table 6 have the following meaning:

- R_k is the characteristic bearing capacity, by shear plane and by means of joining as a function of the failure mode;
- $f_{h,k}$ is the characteristic resistance to boiling over in the wooden element;
- t_1 is the smallest of the element thicknesses on the wood side, or the penetration depth;
- d is the diameter of the joining medium;
- $M_{y,Rk}$ is the characteristic yield moment, for the means of union;

Ultimately, the bearing capacity can be determined as the minimum value:

$$F_{V,Rk} = \min (R_{k,I_B}, R_{k,II_B}, R_{k,III_B}) \quad (18)$$

This approach, contained in the standards, was proposed for the first time by Johansen in 1949. The equations of the bearing capacity of the connection with cylindrical shank connectors are obtained from simple considerations of equilibrium at the limit state, with the assumption of a rigid behavior -plastic for both materials. The ways of breaking that can take place in a connection are substantially the following:

- **Way I** Replenishment of the wooden part;
- **Way II** Burdening of the wooden part and simultaneous yielding of the metal connector, with the formation of a plastic hinge;
- **Way III** Burdening of the wooden part and simultaneous yielding of the metal connector, with the formation of a plastic hinge;

The formulation proposed by Johansen has two fundamental limitations. The former is of relatively little interest to the connections of wooden beam and collaborative slab while the latter is of undoubted interest. With reference to the former, the model does not take into account some collapse modes, in particular of the wooden part, associated with the occurrence of stresses orthogonal to the grain in the wood, and which can determine fragile failure mechanisms. These mechanisms are therefore responsible for structural collapses to values lower than those predicted by the Johansen model. While as regards the other limit, this is inherent in the analysis model itself: the model is therefore able to predict, in the hypotheses made, the limit load at failure but cannot provide any indication on the deformability of the connection nor, consequently, on the stiffness and ductility properties of the connection. In fact, the CNR and EC 5 regulations are used for the formulation of the stiffness of the link to the NICOLE document, using the formulas already mentioned above.

We now have all the tools to be able to characterize the behavior of a cylindrical shank connector according to the models proposed by the standards. It is therefore easy to compare a hypothetical pin fixed in a wooden medium, with (assumed) characteristics comparable to those used for the experiments, and the dry connector Al-fer srl

An equivalent pin having a diameter of 16 mm is first analysed. For the value of the wood's bearing resistance, the expression contained in the standards can be used, for $\alpha=0$ (direction parallel to the fibres):

$$f_{h,0,k} = 0.082 \cdot \rho_k \cdot \frac{1}{\gamma_M} \quad (19)$$

While for the yield characteristics of the connector

$$f_{y,k} = 0.08 \cdot \rho_k \cdot \frac{1}{\gamma_M} \quad (20)$$

Similarly to the previous chapters, the following hypotheses have been assumed:

1) WOOD:

Fir type (class C18)

Characteristic density $\rho_k = 320$ Kg/mc

Average characteristic mass $\rho_m = 380$ Kg/mc

Boiling resistance $f_{h,0,k} = 22$ Mpa
[equation 19]

2) PLUG:

Reinforcement bars with improved adhesion (B450 C)

Diameter of the cylindrical shank connector $d = 16$ mm

Length of insertion in the wood $t_1 = 100$ mm

Characteristic yield strength $f_{y,k} = 450$ Mpa

Characteristic breaking strength Plastic $f_{u,k} = 540$ Mpa

moment $<= \cdot = 176947$ Nmm
[equation 20]

In which the length of insertion in the wood, was adopted in line with that of connector a t_1 , dry Al-fer, or 100 mm

From which it is possible to obtain the mechanical stiffness parameters:

CNR 206/2007

EC5 2009

- KLM extension- 9159Q/SS

- KLM extension- 10306 Q/SS

- 8- 6106 Q/SS

- 8- 6870 Q/SS

For the values of ultimate bearing capacity, it turns out:

CNR206/2007/EC5 2009

$T^*_{,UV}$ - 35267 Q/SS

$T^*_{,UUUV}$ - 17050 Q/SS

$T^*_{,UUUV}$ - 18169 Q/SS

w_{X,Y^*} - 17050 Q/SS

It should be noted that the value of K_{ser} , determined by one or the other regulation differs by 12.5%. Much has already been said about the high initial stiffness of the Al-fer dry connector, therefore the EC5 version 2009 model is used for comparison purposes. The numerical values are shown below:

EC5-2009

- $K_{LM\ extension}$ - 10306 Q/SS

- δ - 6870 Q/SS

w_{X,Y^*} - 17050 Q/SS

By reporting the parameters in the usual graph, the trend in Fig. 26 is obtained.

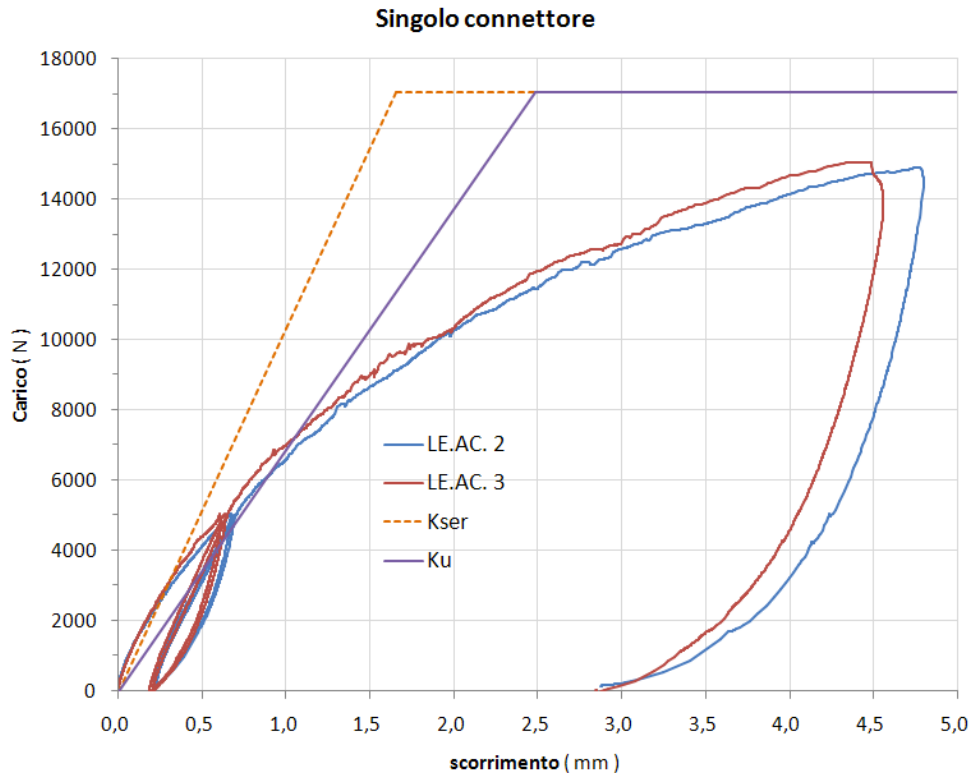


Fig. 26: Connection made with EC5 2009 cylindrical shank plugs

The hypothesis of comparing the connector with a 16 mm diameter pin turns out to be a valid idea if we stop at the observation of the curves up to low values of the applied load, around 4000 N. For higher loads, however, it is a bad solution especially with reference to the ultimate carrying capacity. In fact, according to the analytical model proposed by the standard, the gudgeon pin should theoretically yield with a failure mode of the II type, which provides for the wood to boil over and the consequent formation of a plastic hinge for loads of around 17,000 N. This value is well in addition to the approximately 15,000 N obtained experimentally. It should be remembered that these results are strongly influenced by the uncertainty on the wooden medium, as arbitrary mechanical characteristics have been estimated.

It is important to observe what is reported in Professor Gelfi's discussions regarding the analytical model proposed by the legislation. In fact, unlike what happened for analytical models

proposed by Gelfi and Turrini, the regulations propose a sliding module, K_{ser} , which does not take into account the detachment due to the planking. In this circumstance, however frequent, the Eurocode supplies stiffness values that are not always in favor of safety Fig 27.

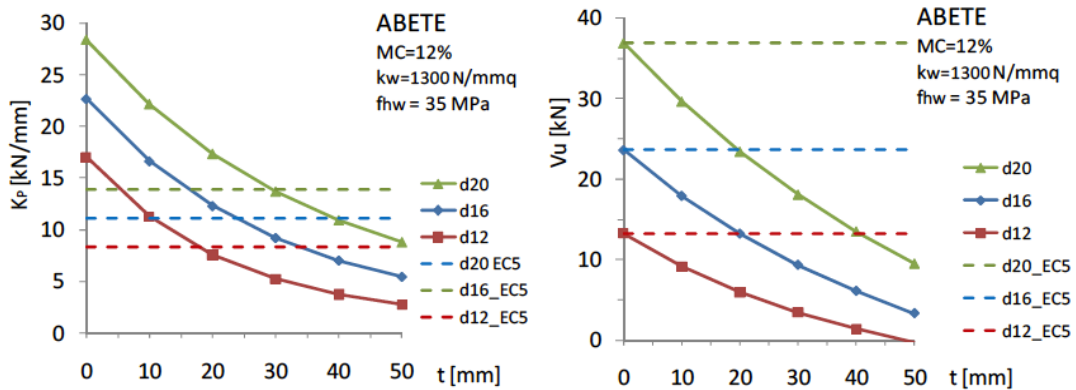


Fig. 27: Variation of the stiffness and bearing capacity of the connection as a function of the planking. Gelfi.

The image is taken from a publication by prof. Gelfi and clearly shows how stiffness and bearing capacity of the connection depend on the thickness of the planking. It is logical to expect that for high values of detachment between the slab and the wooden beam there is a penalization of the mixed system. As the image shows, for plank values of about 25 mm, the stiffness with the Gelfi model and the EC5 are in good agreement with the Al-fer experiments, i.e. there is an initial stiffness k_{of} of about 10,000 N. While there is no harmony with the analytical and experimental Al-fer models with reference to the ultimate capacity. According to the values of the tests, the ultimate strength is 15,000 N, a value that is right in the middle of the values obtainable from the analytical models (Gelfi around 12,000 N and EC5 around 17,000 N).

It is worth mentioning a second shortcoming which, in the opinion of the writer, is inherent in the regulations, and which concerns concrete. It was possible to treat the wood-concrete joint as a steel-wood joint assuming that the slab behaves like a thick steel plate that is infinitely stiff. This fact is not so obvious, since, although much more rigid, concrete is also subject to seepage phenomena. This aspect, which only Professor Gelfi's analytical model considers and which therefore, for the reasons mentioned above, is believed to be the most valid to represent the phenomenon even if it must be modified in order to be applied to the mixed system with Al-fer dry connectors.

3.3.4 Comparison of the proposed analytical models

In the previous chapters various analytical models have been studied, each of which is able to describe the mechanical behavior of metal connectors fixed in the wood suitable for the creation of wood-concrete joints. The different systems do not differ much in terms of construction technology, but each author has proposed his own formulation. The various models were compared with the experimental data of the Al-fer connectors, with the aim of measuring the stiffness and resistance of the latter. Below is a table summarizing the experiences conducted in this regard for an equivalent connector with a diameter of 16 mm.

Means of union	Author	Analytical model	
		k [N/mm]	v [N]
Resin-coated peg	Turrini	10240	11008
Dry peg	Gelfi	10611	12223
Plug	Regulations (Johansen, Nicole)	10306	17050

Tab. 7: Comparison of analytical models using a 16 mm diameter steel union

It can be observed that there is a good agreement between the stiffness values, while the variation of values regarding the breaking strength is significantly evident.

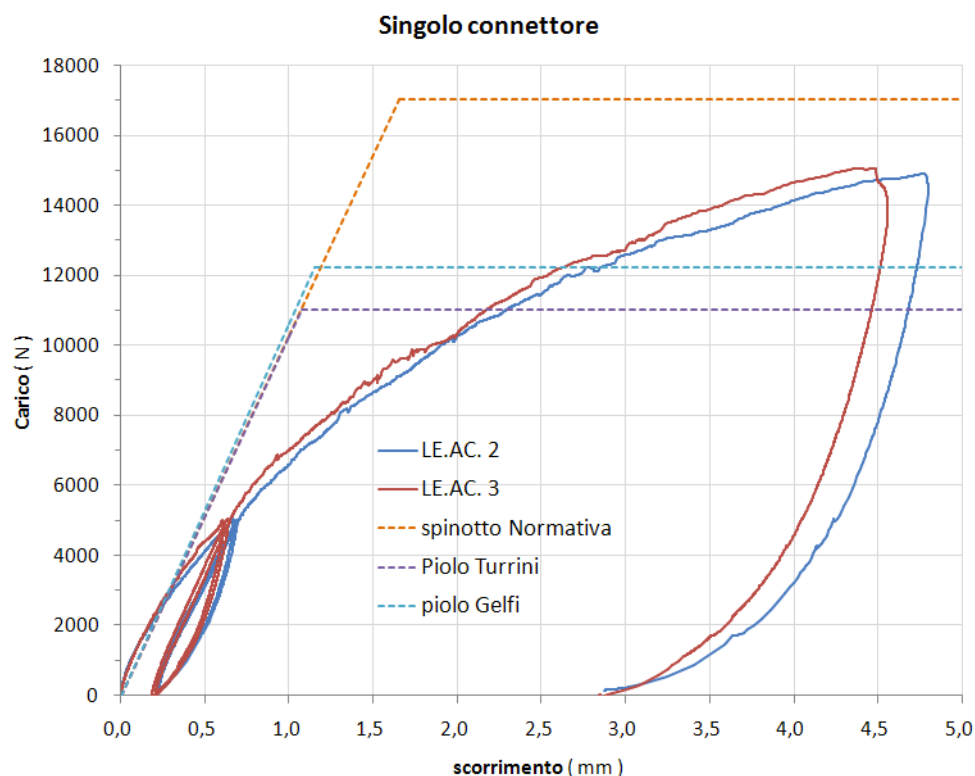


Fig. 28: Comparison between experimental tests and analytical models for a 16 mm diameter joining medium.

From all the experiments carried out, it is concluded that it is not possible to describe the behavior of the Al-fer dry connector using the models known in the literature.

One could think of using the analytical model of Professor Gelfi, as regards the estimate of the initial stiffness. This model, as already mentioned, is the most complete as it takes into account the stiffness of each material constituting the mixed system and also considers the presence of the through planking. As far as the ultimate bearing capacity of the connector is concerned, it could be thought of adopting an elastic-plastic model which is hardening which is able to approximately reflect the capacity curve shown by the experimental tests.

3.3.5 Linearization of the capacity curve

Pushover analysis or thrust analysis (literally pushover means "to push further") is a non-linear static procedure used to determine the behavior of a structure in the face of a given action (force or displacement) applied.

It consists in "pushing" the structure until it collapses or a deformation control parameter reaches a pre-set limit value; the "thrust" is obtained by applying a pre-established profile of forces or displacements in a monotonous way.

This technique is used to obtain an accurate and realistic forecast of the seismic response of a structure, and requires the use of analysis tools that allow us to understand its non-linear behavior and its evolution over time.

The capacity of a structure depends on the resistance and deformation capacities of its individual components.

The capacity curve defines the capacity of the structure independently of any specific seismic demand (in fact no reference is made to the seismic action) and therefore describes the intrinsic characteristics of the resistant system; in other words it is a sort of simplified constitutive bond of the structure.

But this is exactly what was done for the Al-fer dry connector. In fact, in the previous chapters, extensive use was made of the capacity curve exhibited by the system and we then returned to curves representing the behavior of the single connector.

When we intend to analyze the response of real structures, we can further simplify the problem

piecewise linearizing the response of the system, and therefore its capacity curve, adopting bilinear or trilinear approximations as shown by way of example in Fig. 29.

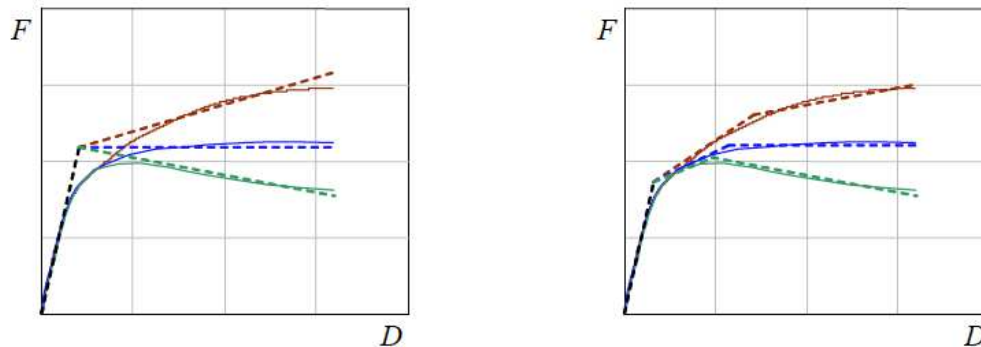


Fig. 29: Bilinear (right) and trilinear (left) linearizations of the capacity curve of a real system.

This is just a chosen way of presenting some possible linearizations and not a condition necessarily to be met. In fact, there is no single criterion to linearize the capacity curve. For example, different methods of nonlinear static analysis employ different criteria. In principle, the approximation is all the more accurate the more the linear segment "closely follows" the real curvilinear trend around the point which represents the expected response.

By way of example, Figure 30 shows some different linearizations of the same capacity curve.

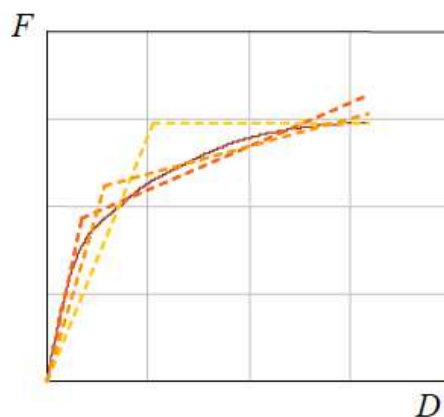


Fig. 30: Different linearizations of the capacity curve of a real system.

The behavior of the system can therefore be ideally schematized with a linear elastic branch up to the yield point and with a strain-hardening post-elastic branch (*the*), perfect (*p*) or degrading (*d*). The curves shown in Fig. 31 represent the relative force-displacement relationships, i.e. the respective capacity curves.

This representation allows to identify the nominal global resistance and displacement of the structure: in particular the yield strength f_y , the effective elastic stiffness k_{and} and the post-elastic stiffness $k_p = p k_e$ (the hardening ratio p is positive, negative or null respectively in the cruelty-free, degrading or perfect case).

As mentioned, a number of criteria are available to linearize the capacity curve. In the Capacity Spectrum Method (CSM) the bilinear representation is related to a point of presumed functioning PP of the system and is based on an energy equivalence criterion (principle of equal energy): the first segment of the bilinear is a line passing through the origin with slope defined by the initial stiffness of the system and the second is a line passing through PP and slope such that the area subtended by the bilinear is equivalent to that subtended by the capacity curve ($A_1 = A_2$ in Figure 32).

The capacity curve is bilinear, for a certain displacement d , is completely defined by three parameters:

- the initial elastic stiffness k_{and} which is proportional to the tangent at the origin of the capacity curve;
- the yield strength f_y ;
- the hardening factor p equal to the ratio between the post-elastic stiffness and the elastic one; through the following relationship:

$$f = \begin{cases} -LZ & d \leq d_y \\ W = [-LZ - Z] & d > d_y \end{cases}$$

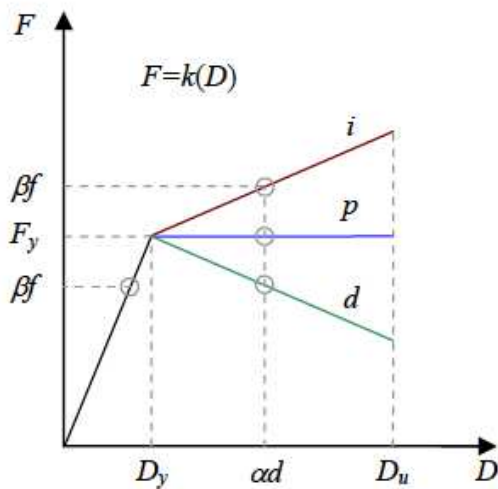


Fig. 31

Hardening (i), degrading (d) and perfect (p) plastic elastic behavior.

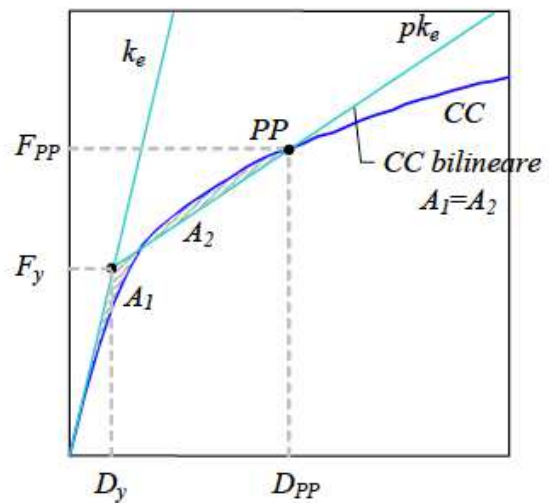


Fig. 32

Bilinear representation of the capacity curve (used in the CSM)

3.3.6 Al-fer bilinear model

In analogy with what is explained in the previous subparagraph, it is possible to think of linearizing the capacity curve of the Al-fer dry connector with an elastic-plastic hardening behavior. The initial stiffness can be given by Professor Gelfi's model, for rungs with a diameter of 16 mm, as it has been seen that this model correctly approximates the initial stiffness of the system and provides an ideal length of a doubly wedged rung. Conventionally, 6000 N can be assumed as the value of the yield strength and therefore the value of displacement in the elastic range equal to 0.565 mm. As far as the plastic branch is concerned, the conventional value of 4 mm can be assumed, which corresponds to a force value equal to 14900 N. Fig. 33 shows the comparison between the results Al-fer,

The numerical parameters used for the bilinear representation are:

	Elastic branch		Plastic branch	
Stiffness	$k_{AND} =$	10611 N/mm	$k_P =$	2591 N/mm
Power	$f_y =$	6000 No	$f_{it\ was} =$	14900 No
scroll	$d_y =$	0.565 mm	$d_u =$	4 mm

The bilinear model introduced, despite being a considerable simplification of the phenomenon in question, is able to accommodate the system capacity with adequate precision.

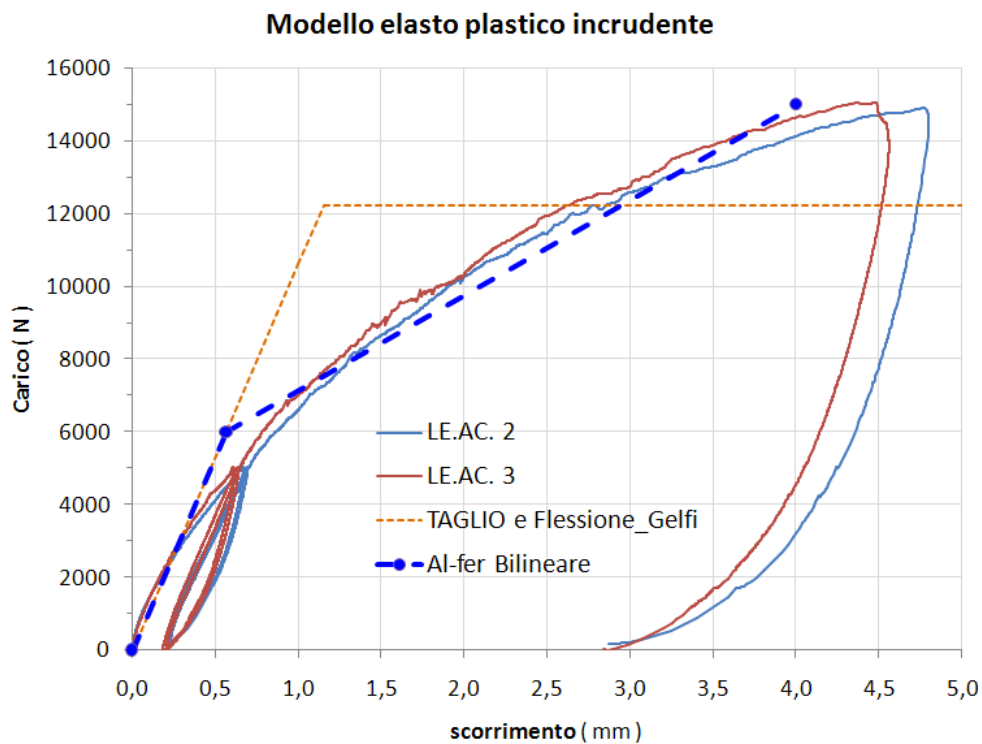


Fig. 33: Bilinear representation of the Al-fer connector capacity curve.

3.4 Considerations

First, some analytical models were studied, from which the complexity of the phenomenon and the main aspects were understood. A simplified formulation was then proposed through the use of a cruelty-free bilinear model.

Numerical applications now follow, with which it is possible to further investigate the resistance capacity of the Al-fer connection, and where it is possible to make considerations on the stress field of the entire analyzed system. In fact, numerical simulations, through the use of the finite element method, represent a fundamental aid in understanding the complex mechanical processes activated during the loading phase of the mixed system.

4 Numerical models

With the aim of deepening the mechanical behavior of the mixed system with Alfer dry connectors, a numerical finite element analysis was carried out, with the STRAUS7 program of G+D Computing, the results of which are presented in the following paragraphs.

The first application to finite elements, which we will refer to below with the acronym FEM (Finite Element Analysis), concerns the discretization of the entire specimen subjected to the push-over test.

4.1 Entire specimen

This model was created respecting as much as possible the geometrical dimensions of the real samples. We now describe this model and the hypotheses assumed for it.

To perform this analysis, we will refer to a standard sequence of steps commonly used in finite element modeling:

- 1) Definition of geometry and type of elements
- 2) Definition of the constraint conditions
- 3) Definition of load conditions
- 4) Definition of material properties
- 5) Resolution of the model
- 6) Post-processing of the model, for visualization and interpretation of the results.

4.1.1 Definition of the geometry and type of elements

The real specimen was discretized using the following finite elements:

<i>Actual audition</i>	<i>Finished item type</i>
Wooden beam	Brick Hex 8
Planked concrete slab	Brick Hex 8
	truss
Al-fer dry connector	beam

Figure 34 shows a series of images able to intuitively convey the geometry used in the FEM analyses. The numerical model reproduces the real model rather faithfully, in fact it can be seen that there is a good similarity between figures 34 b) and c). Through a visualization **wireframe** it is also possible to see the modeling of the eight connectors inside the beam.

As for the units of measurement used:

- Length	mm
- Power	No
- Mass	T
- Elastic/tension modules	Mpa

Hexa 8 brick elements were used for the wood and the slab and one was chosen **mesh** with cubic parallelepipeds of side 10 mm. The creation of the model took place starting from elements **plate** suitably extruded and mirrored until a quarter of the entire model is obtained, the length of which represents, not by chance, the positioning distance between the connectors. By organizing each quarter into 4 groups, it was possible to insert each connector at the correct level. There **mesh** of 10 mm for the wood and the slab was an apt choice with particular reference to the possibility of introducing for the connector the section variation along its own axis, fig 35, through the use of 4 **beam** different:

- beam1	17 mm hex 14 mm	Part embedded in the concrete. Part
- beam2	diameter barrel 16 mm	anchored in the concrete. Part in
- beam3	diameter barrel 13 mm	contact with the boarding. Part
- beam4	diameter barrel	inserted in the wood

A diameter of 13 mm was used to take into account the presence of the thread which tapers the section from 16 mm to 12 mm.

Finally, a truss element was chosen for the wooden plank, used for the slab and for the wood, i.e. $10 \times 10 \text{ mm}^2$.

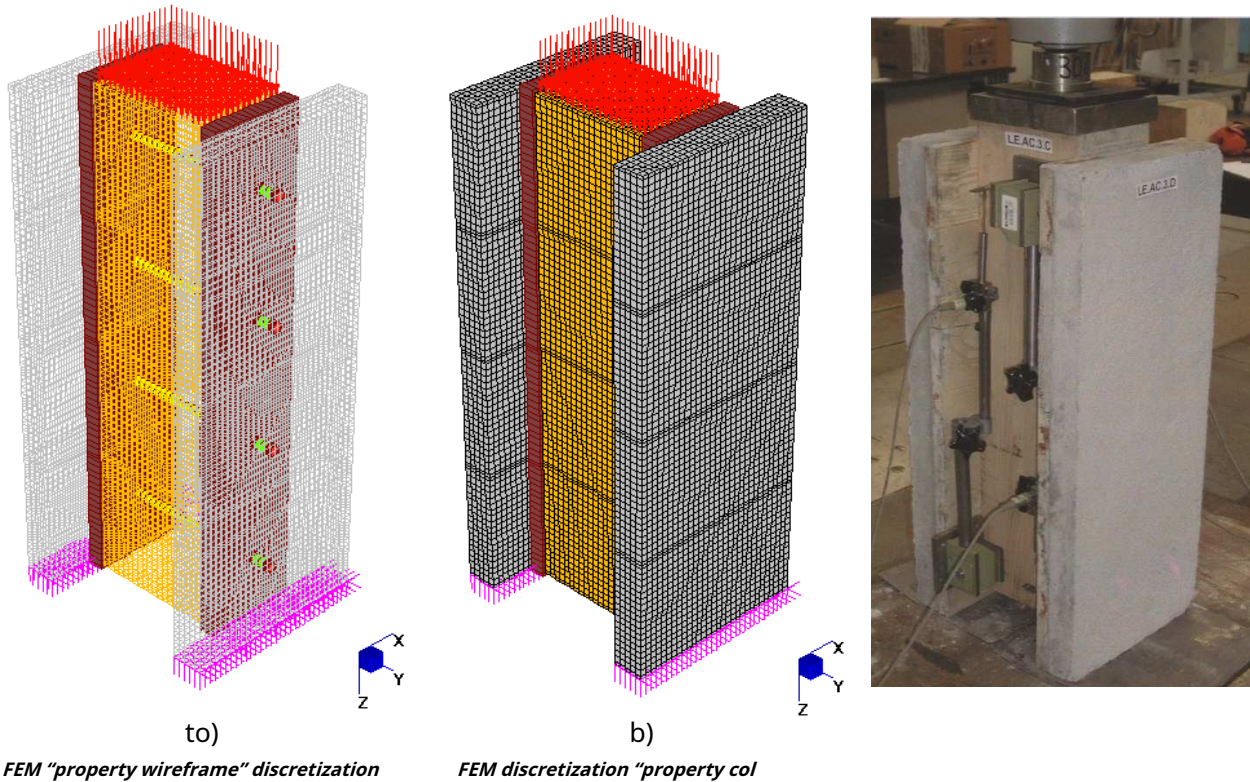


Fig. 34

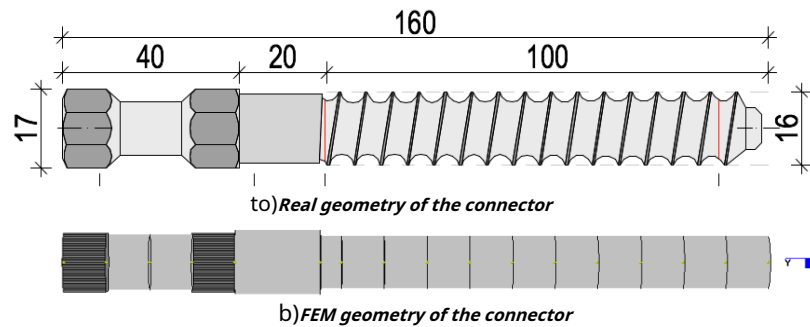


Fig. 35

4.1.2 Definition of constraint conditions

Once the geometry of the structure has been created, it is necessary to assign appropriate constraint conditions, because in the absence of these, the structure is free to move in space. To provide the necessary constraints, attention must be paid to the physical situation being simulated. Each node has six degrees of freedom (dof, degrees of freedom) and therefore six possibilities of movement: three translations according to X, Y, Z and three rotations around the same axes.

As shown in fig. 34 a) and b), the real vertical axis has been made to coincide with the Z axis. The only constraint conditions have been assigned preventing the three displacement components of the nodes belonging to the lower face of the concrete slabs, fig 34 a) and b). Physically only the lower bench on which the specimen rests is able to prevent the movement along Z, but it is necessary to prevent the other two translations to avoid rigid motions of the FEM specimen.

The wooden beam is thus able to move vertically, while it is connected to the slabs by means of the connectors and the planking. It should be noted that the planking was inserted as an element capable of absorbing the lateral contractions of the wooden beam, but in shear, being a **truss**, offers no scrolling impediments.

Figure 36 shows the FEM model, in which a cross-section was made to better grasp some details of the modeling.

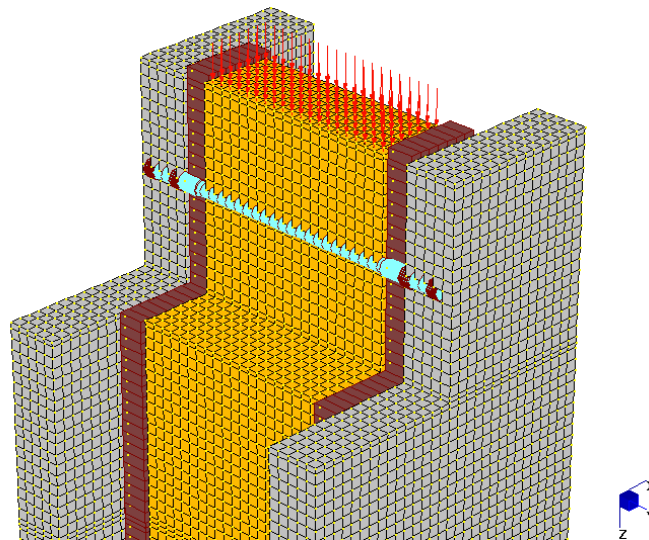


Fig. 36: Cross-section of the FEM model.

4.1.3 Definition of load conditions

The jack actually applies the load to the wooden beam via a thick steel plate, fig 34 c). It is therefore possible, with a good approximation, to apply the external force to the model **FEM** using the tool **Face pressure(global)**, fig. 37, to the elements **brick** of the wooden beam.

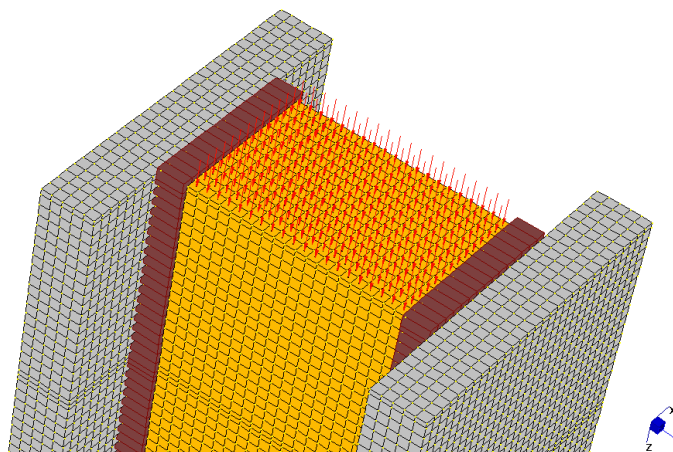


Fig. 37 Load application via the Face pressure attribute (Global).

As was done for chapter 3, it is believed that the simulation can be significant with reference to the average results of the LE.AC 2 and 3 specimens. Of these, the first load cycle can be considered by suitably choosing some values of the force impressed on the entire audition.

The force was assigned by dividing the transformed load value in Newtons by the area of the wooden beam, by means of 13 **Load cases**, in accordance with the data available from the tests, see table 8 for the numerical values. Figure 38 shows the curve obtained from the discretization of the experimental values.

Finally, it should be noted that major points near the origin have been considered in order to precisely investigate the initial stiffness of the system.

As we will see in the post-processing phase the various load conditions will be compared with the experimental data.

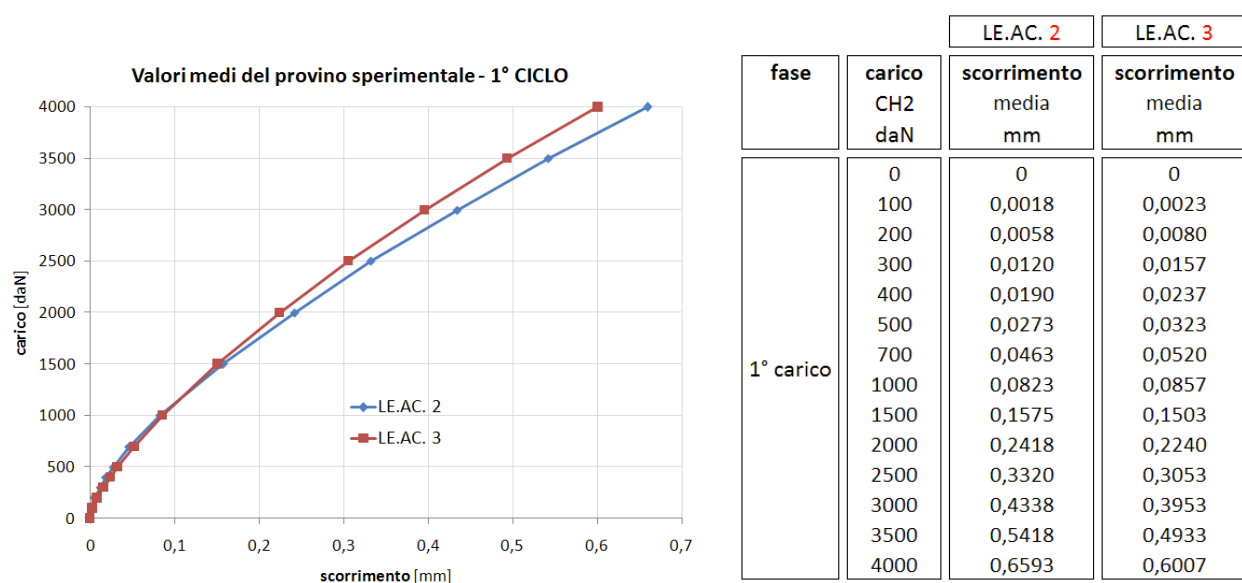


Fig. 38
Load displacement curve considered for FEM comparison.

Table 8
Experimental values of Load and Displacement

Each load combination has been named with the value of the sum of the loads in the Z direction, i.e. equal to the force applied to the experimental specimen, thus obtaining the following correspondence:

primary Load Cases	global Face Pressur [MPa]
1) F=100 daN	0.0357
2) F=200 daN	0.0714
3) F=300 daN	0.1071
4) F=400 daN	0.1429
5) F=500 daN	0.1786
6) F=700 daN	0.25
7) F=1000 daN	0.3571
8) F=1500 daN	0.5357
9) F=2000 daN	0.7143
10) F=2500 daN	0.8929
11) F=3000 daN	1.0714
12) F=3500 daN	1.25
13) F=4000 daN	1.4286

Table 9: Load combinations and corresponding pressures applied to the beam in the FEM analysis.

4.1.4 Definition of material properties

For the definition of the properties of the various finite elements, the values of table 10 were assumed:

ELEMENT :	Wooden beam	Concrete slab	Al-fer connector	Boarded up
Guy =	Brick (Hexa8)	Brick (Hexa8)	Beam-shear area	trusses
material =	Isotropic	isotropic	Steel	Wood
AND[MPa] =	8000	27460	200000	7000
ν =	0.3	0.25	0.25	-
Density[T/mm ³] =	5.50x10 ⁻¹⁰	2.50x10 ⁻⁹	7.85x10 ⁻⁹	5.50x10 ⁻¹⁰

Table 10: Material properties for FEM analysis.

The reasons that led to the choice of these values have already been extensively discussed in the previous chapters, to which reference should be made for further information.

4.1.5 Model resolution

A three-dimensional model made in this way lends itself purely to a linear static analysis since the high number of degrees of freedom of the system strongly constrains the choice. Indeed, the system **FEMs** made up of 55655 **nodes**, 2558 **beams** and 46400 **bricks** and takes about 10 minutes to fix.

A linear static analysis has been launched in which the solver has been asked to calculate:

- Node Reactions;
- Beam Force/Stress;
- Beam Strain/curvature;
- Brick Stress;
- Brick Strains;

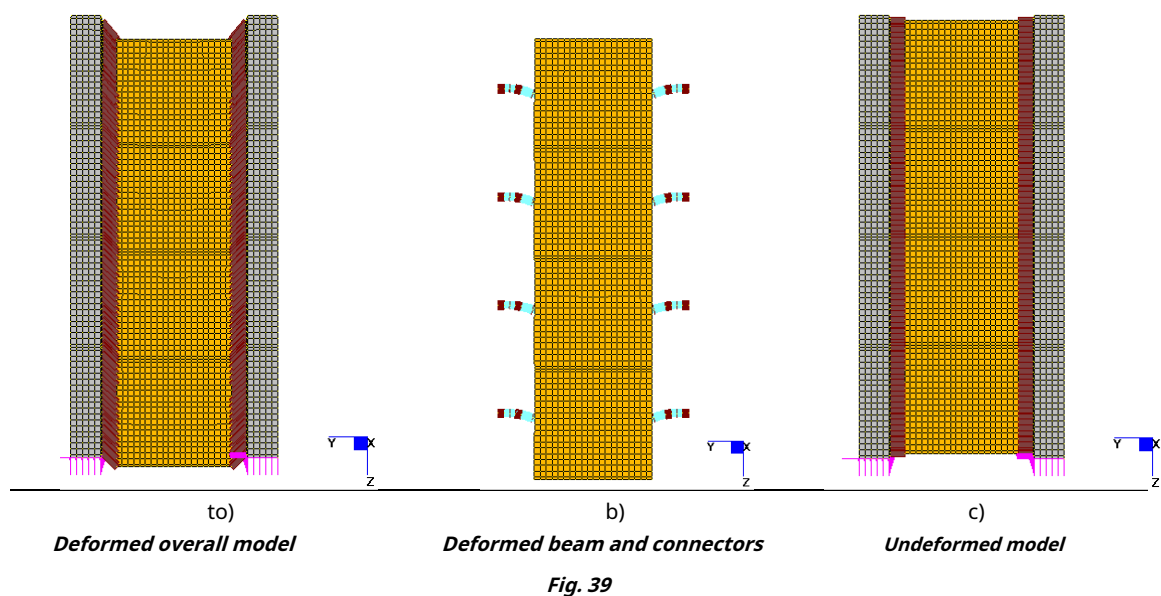
These quantities were calculated for each of the 13 load combinations.

4.1.6 Post-processing of the model

Post-processing is the name given to the phase of evaluation and interpretation of the results of a finite element analysis. In Straus7, the post processor allows you to view the results in various ways, through color "contours" that with color maps represent quantities of interest (such as tensions, strains, displacements, etc.), through graphs, animations, deformed configurations, data lists etc.

It is good practice to check the Log file, which contains the list of all messages generated by the solver during the solution procedure. First, it was ensured that the desired loads were applied to the structure itself. Then, you searched for any messages or errors but the search failed.

It is important to be able to evaluate the deformed configuration of the structure to ensure that it exhibits the expected behavior with respect to the forces and constraints that have been applied. Using the "Displacement Scale" function it is possible to investigate this deformation, figure 39 shows the trend of the deformation.



From figure 39 a) it can be understood how the entire specimen undergoes, following the application of pressure at the end of the wooden beam, an expected deformation or rather a sliding of the whole beam is generated in the positive Z direction. From figure 39 b), however, it can be seen how the transfer of force from the beam passes to the slabs by means of the sliding of the connector, which becomes the only element able to offer resistance to the shearing action. Figure 39 c) shows for comparison the case of unloaded specimen, wooden beam and slabs are aligned.

We dwell on this aspect of fundamental importance for one last consideration. In figure 40 a) the deformation of the FEM model of a connector is shown, and for comparison in figure 40 b) the deformation obtained experimentally. A good correspondence is noted despite the fact that the real deformation represents a connector at the end of the push-over test and therefore it is logical to expect plasticization of the materials. Finally, figure 40 c) shows the image taken from CNR-DT 206/2007 for connection made with pins with cylindrical shank of constant section.

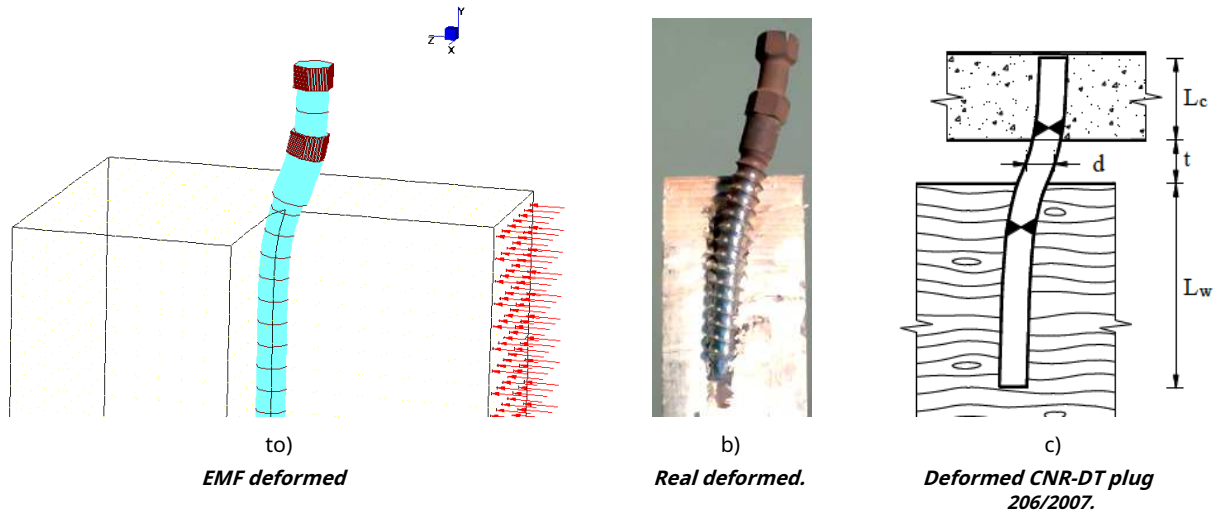


Fig. 40: Various deformed

From the images above it is evident that in this first model, which we will indicate with FEM 1.00, the free inflection length of the connector is less than that which is created by subjecting the specimen to an experimental test. In fact, this model sees the connector connected to the extrados of the wooden beam and to the intrados of the concrete slab. In this situation, the connector has a free length of inflection equal to the plank (25 mm). Therefore a higher stiffness than that exhibited during the tests is expected.

The FEM forecasts of this first model are reported below, together with the average values introduced in the previous paragraphs for comparison.

TRAVELS

With the logic of making an optimal comparison with the experimental data, it is necessary to choose which displacement is the most significant. The answer can be found by observing figure 41, which shows the displacement of the brick elements for a load value of 100 daN applied to the entire sample.

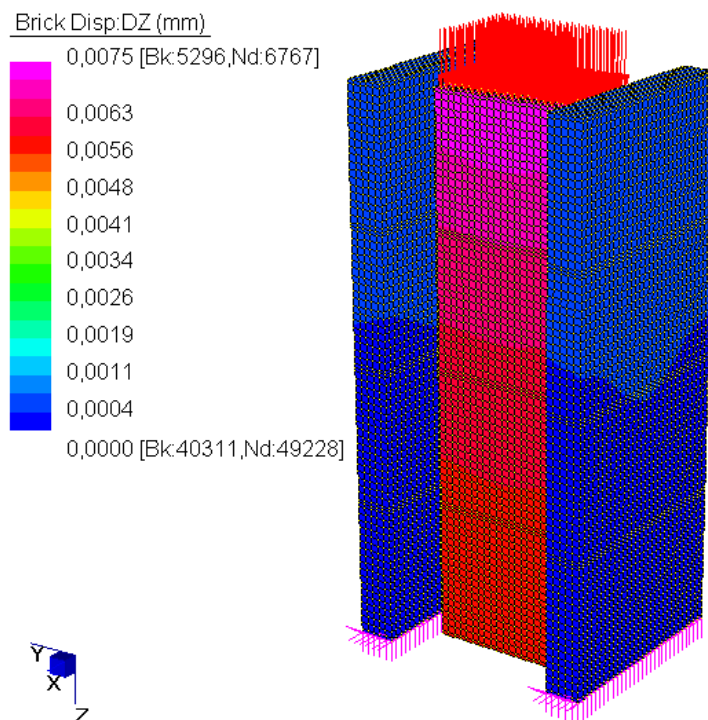


Fig. 41: Displacement range of the bricks elements for a load of 100 daN

Further enlarging the previous image, figure 42, it can be seen that the displacement of the elements *bricksit* is maximum near the first two connectors. The transducer was mounted on this ideal line, formed by the longitudinal axis of the connectors. It therefore appears legitimate to compare the maximum displacement of the beam with the average values of the LE.AC 2 and 3 specimens.

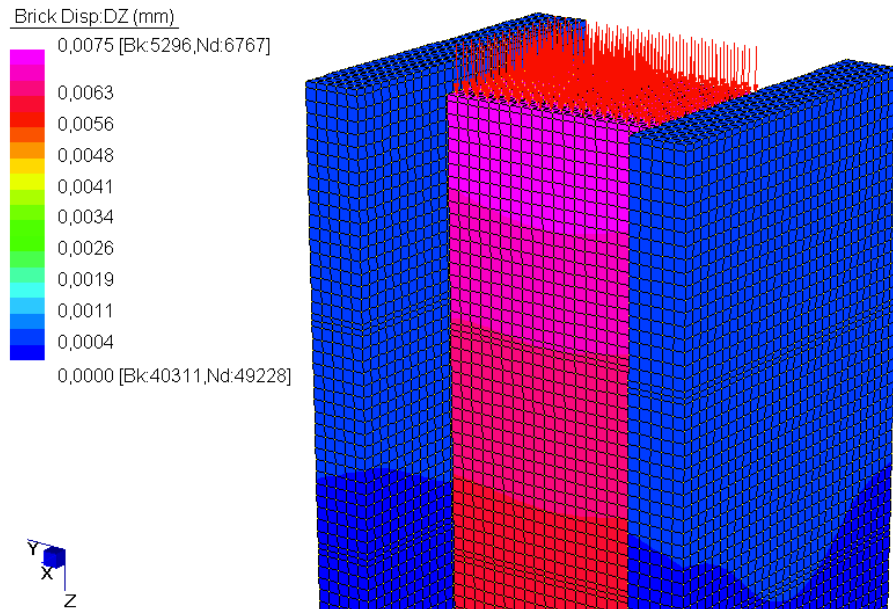
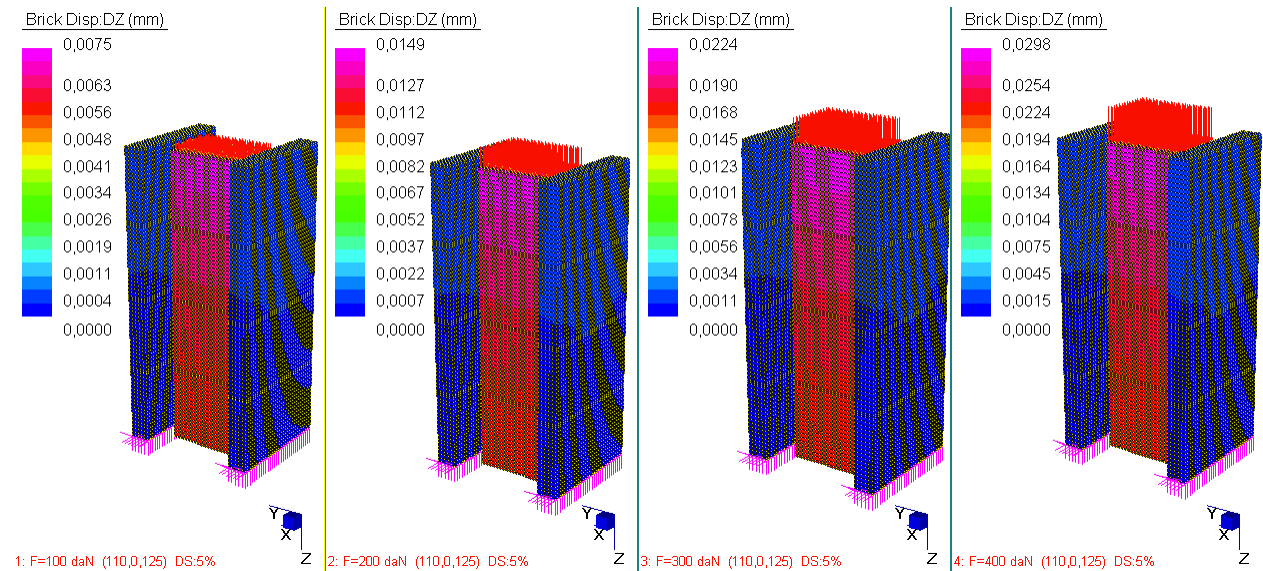


Fig. 42: Enlargement of a portion of the FEM model 1.00

After these introductory considerations, the results of the FEM analysis are reported below with reference to the displacement field DZ for each load combination.



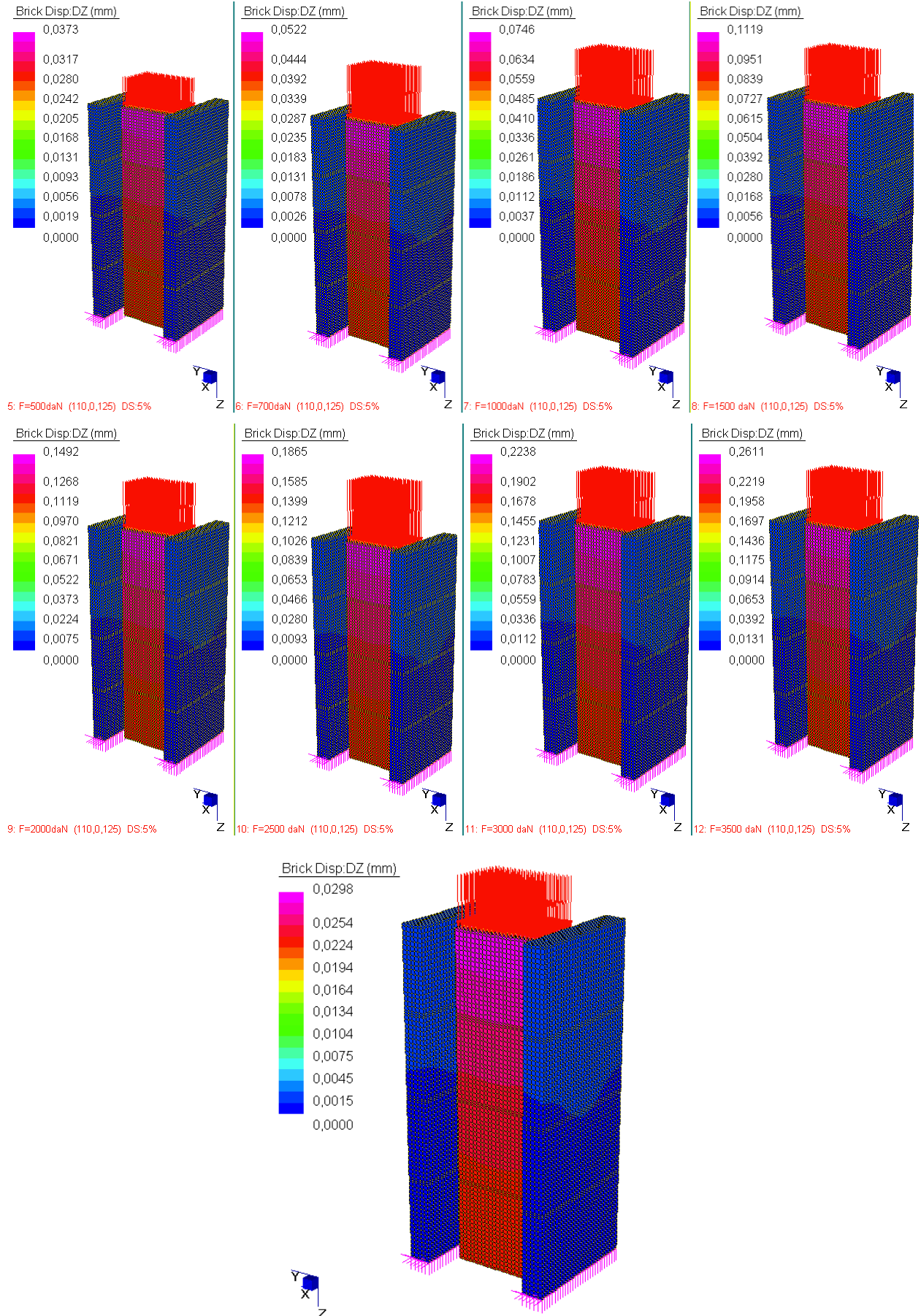


Fig. 43: DZ offset for combination 13: F=4000 daN, model FEM 1.00

To summarize and make some useful considerations, the numerical values are reported in tab. 10 and the respective trends in the sliding force graph in figure 44.

fase	carico CH2 daN	LE.AC. 2	LE.AC. 3	FEM 1.00
		scorrimento media mm	scorrimento media mm	scorrimento DZ_bricks mm
1° carico	0	0	0	0
	100	0,0018	0,0023	0,0075
	200	0,0058	0,0080	0,0149
	300	0,0120	0,0157	0,0224
	400	0,0190	0,0237	0,0298
	500	0,0273	0,0323	0,0373
	700	0,0463	0,0520	0,0522
	1000	0,0823	0,0857	0,0746
	1500	0,1575	0,1503	0,1119
	2000	0,2418	0,2240	0,1492
	2500	0,3320	0,3053	0,1865
	3000	0,4338	0,3953	0,2238
	3500	0,5418	0,4933	0,2611
	4000	0,6593	0,6007	0,2984

Tab. 10: Numerical values DZ displacement force

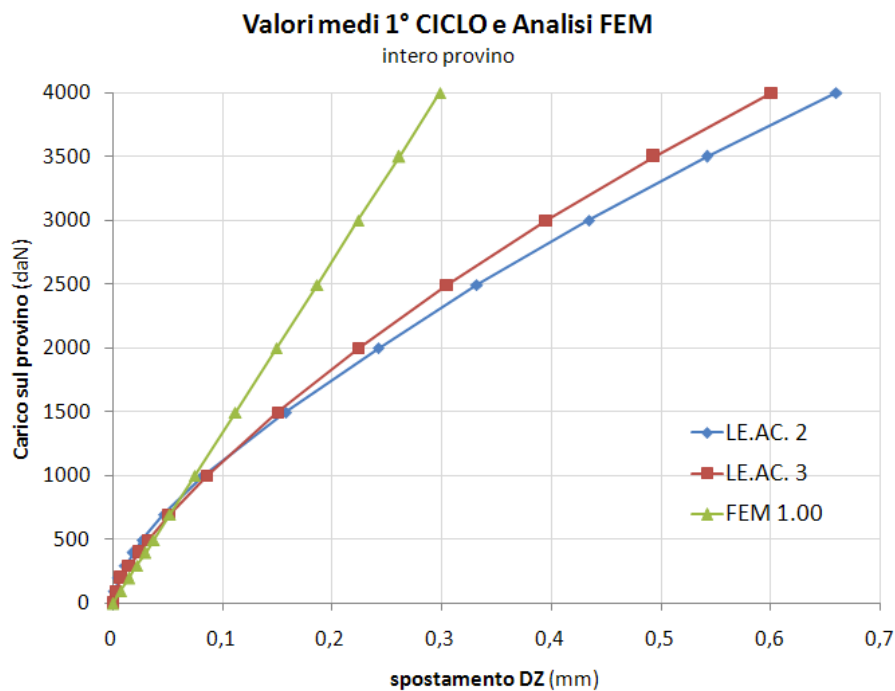
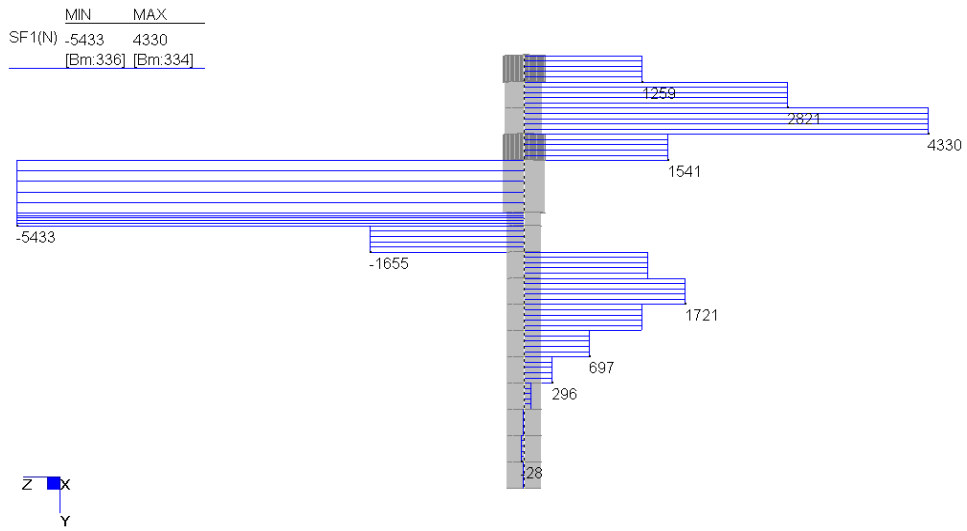


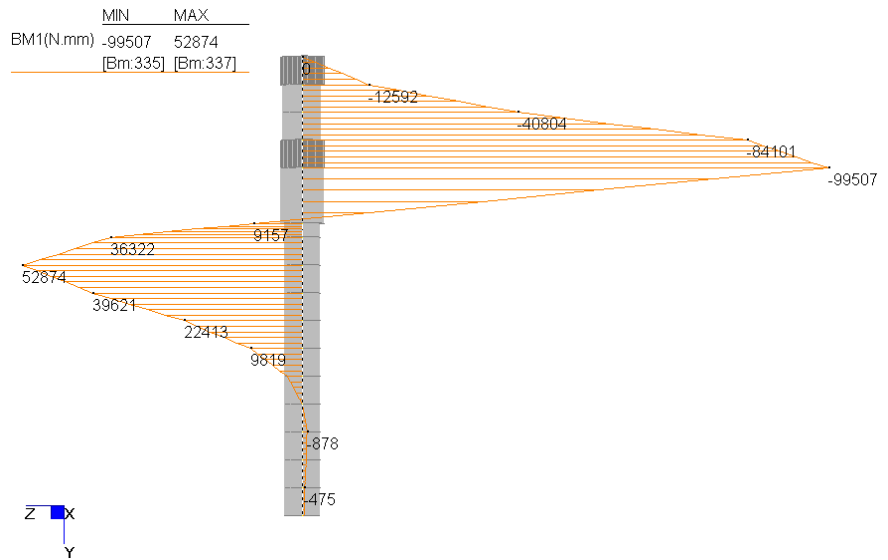
Fig. 44: Comparison of experimental analyzes and FEM 1.00 model

With this model, always with reference to the load-displacement curve, it is possible to investigate and confirm what was stated in the previous chapters regarding the shear force absorbed by each connector, as well as the sliding suffered by the latter.

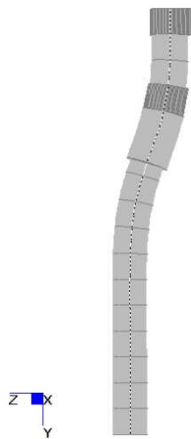
Take the load combination 13 as an example, which corresponds to a load impressed on the wooden beam of 4000 daN. By diagramming the trend of the shear, figure 45 a), and of the moment in figure 45 b), it is possible to find the formulation proposed by gelfi, figure 45 d).



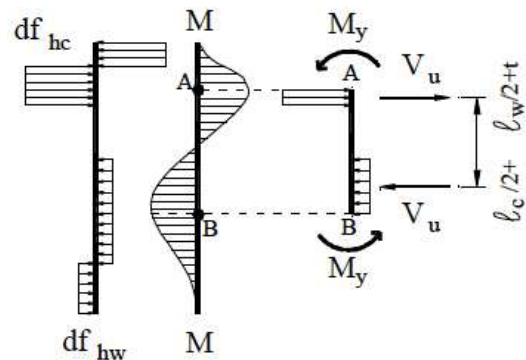
a) trend of the shear on the connector, model FEM 1.00



b) trend of the moment on the connector, model FEM 1.00



c) deformed connector



d) Professor Gelfi's model of resistance capacity

Fig. 45

Table 11.1 shows the numerical values and figure 46 shows the qualitative trend of the latter.

fase	carico provino intero sperimentale (daN)	Forza carico/8 stimato (N)	Forza taglio sul connettore FEM 1.00 (N)	scorrimento media LE.AC. 2 (mm)	scorrimento media LE.AC. 3 (mm)	scorrimento DZ_bricks FEM 1.00 (mm)
1° carico	0	0	0	0	0	0
	100	125	136	0,0018	0,0023	0,0075
	200	250	272	0,0058	0,0080	0,0149
	300	375	407	0,0120	0,0157	0,0224
	400	500	543	0,0190	0,0237	0,0298
	500	625	679	0,0273	0,0323	0,0373
	700	875	950	0,0463	0,0520	0,0522
	1000	1250	1358	0,0823	0,0857	0,0746
	1500	1875	2037	0,1575	0,1503	0,1119
	2000	2500	2717	0,2418	0,2240	0,1492
	2500	3125	3396	0,3320	0,3053	0,1865
	3000	3750	4075	0,4338	0,3953	0,2238
	3500	4375	4754	0,5418	0,4933	0,2611
	4000	5000	5433	0,6593	0,6007	0,2984

Table 11.1: Comparison between experimental and numerical data on a single connector

Valori medi 1° CICLO e Analisi FEM

singolo connettore

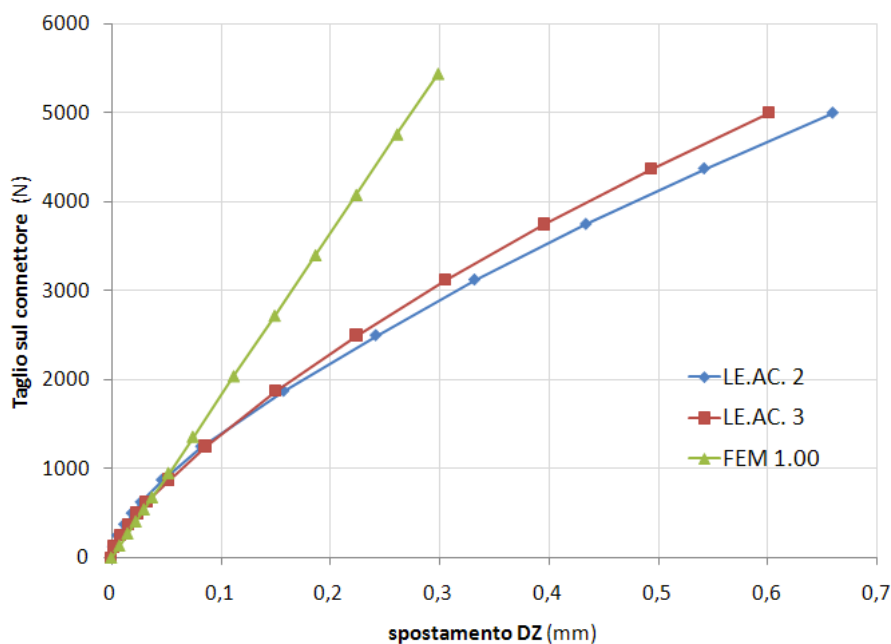
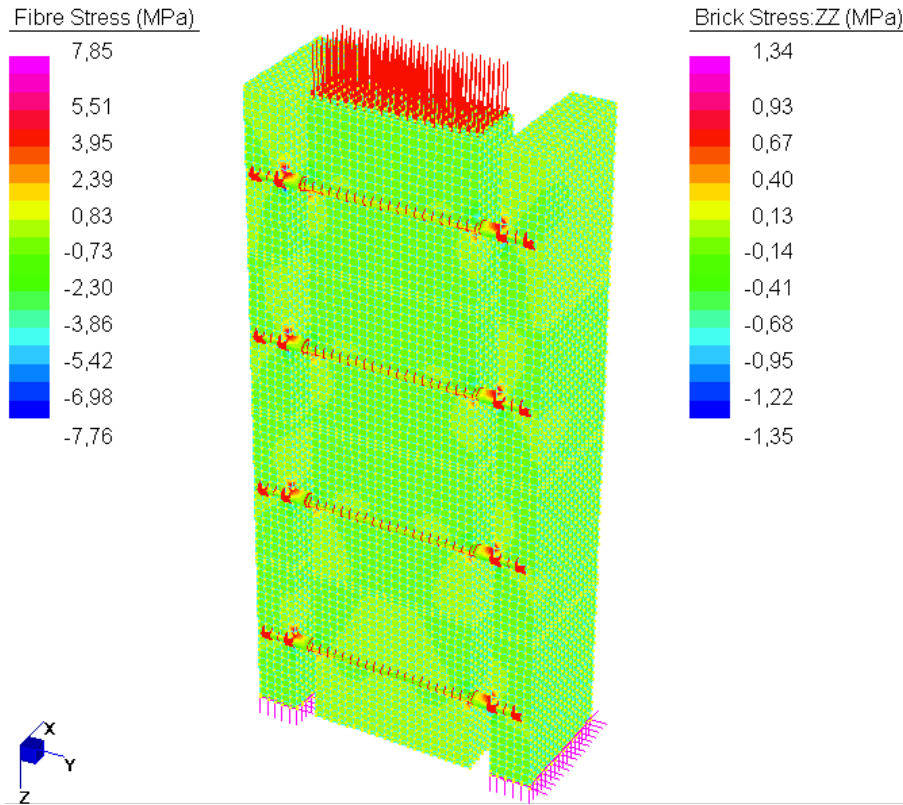


Fig. 46: Load-displacement curve for the single connector

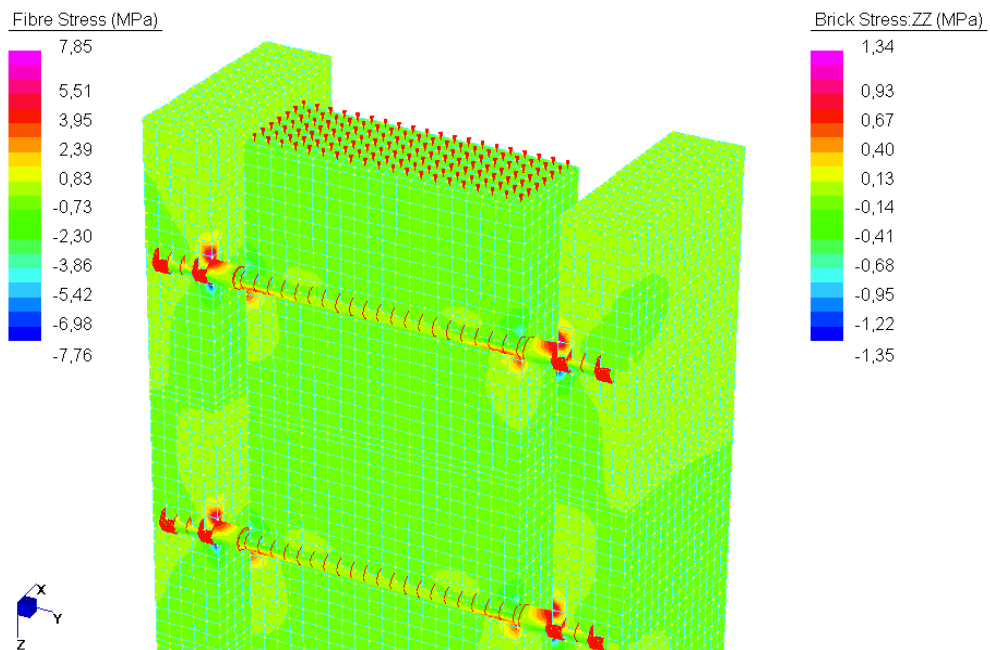
As already anticipated, the stiffness of this first model is much higher than that shown in the experimental tests, in fact we are dealing with a stiffness *FEM* initial value of 18200 N against the 10600 N estimated in chapter 3. This fact, once again, is attributable to the small free length of inflection adopted in this model. It is therefore useful to unhook a few knots between the wooden beam-connectors and the concrete slab-connectors with the aim of increasing the free span of inflection due to probable plasticization due to the materials in contact with the connector. This will be addressed in the following, immediately after having investigated the stress field in solid elements.

TENSIONS

The FEM model allows to study the stresses that are generated in the various materials for each load condition implemented. As an example, figure 47 shows the load condition equal to 100 daN.



a) ZZ and total fiber stresses for load combination 1



b) Magnification. ZZ tensions and total fibers for load combination 1

Fig.47

Table 11.2 instead shows the numerical values of the maximum stresses in the materials. It should be noted that the maximum values are recorded at the interface between the concrete slab and the planking, or between the latter and the wooden beam, with the formation of plastic hinges.

Load Cases	BEAM Brick stress ZZ [MPa]		INSOLE Brick stress ZZ [MPa]		CONNECTOR Total Fibers [MPa]	
	Trac.	Comp.	Trac.	Comp.	Trac.	Comp.
1) F=100 daN	+ 0.71	- 0.77	+ 1.34	- 1.35	+ 7.85	- 7.76
2) F=200 daN	+ 1.42	- 1.54	+ 2.68	- 2.71	+ 15.70	- 15.52
3) F=300 daN	+ 2.13	- 2.31	+ 4.02	- 4.06	+ 23.55	- 11.28 pm
4) F=400 daN	+ 2.84	- 3.08	+ 5.35	- 5.42	+ 31.40	- 31.04
5) F=500 daN	+ 3.55	- 3.84	+ 6.69	- 6.77	+ 39.25	- 38.79
6) F=700 daN	+ 4.97	- 5.38	+ 9.37	- 9.48	+ 54.95	- 54.31
7) F=1000 daN	+ 7.10	- 7.69	+ 13.39	- 1.55 pm	+ 78.51	- 77.59
8) F=1500 daN	+ 10.65	- 11.54	+ 20.08	- 20.32	+ 117.76	- 116.38
9) F=2000 daN	+ 14.20	- 15.38	+ 26.77	- 27.10	+ 157.01	- 155.18
10) F=2500 daN	+ 17.74	- 19.23	+ 33.46	- 33.87	+ 196.26	- 193.97
11) F=3000 daN	+ 21.29	- 23.08	+ 40.16	- 40.64	+ 235.52	- 232.77
12) F=3500 daN	+ 24.84	- 26.92	+ 46.85	- 47.42	+ 274.77	- 271.56
13) F=4000 daN	+ 28.39	- 30.77	+ 53.54	- 54.19	+ 314.02	- 310.35

Table 11.2: Stresses in the various materials of the FEM 1.00 model

Considerations:

- 1) For load values lower than 2500 daN on the entire specimen, which corresponds to a shear of 3396 N on each connector, the materials have not yet plasticized, if we consider about 20 Mpa as the limit value for the return of wood;
- 2) This model, as can be seen from the numerical values, provides positive and negative stresses for the wood and for the concrete. This aspect is inherent in the nature of the model itself, but represents a very restrictive limit for the use of data since the connector shares some nodes with the solid elements, generating implausible tractions in these;
- 3) In the light of this defect, it can be seen that the concrete, for each load condition, remains within the assumed overflow value and equal to about 120 Mpa;
- 4) The characteristic of the connector is a high yield strength which is equal to approximately 850 Mpa, a value which is never reached in the first load cycle.

4.1.7 Free buckling length

From the previous study it has been seen that the numerical stiffness of the connection is overestimated, due to plasticization of the materials that this modeling is not able to capture. In real experiments around the connector, and at the interface with the wood and the concrete, voltage peaks are produced, and therefore the materials return. Once the bearing value has been reached, the material is no longer able to offer resistance and the connector undergoes sliding increases for constant values of applied force.

The FEM model must therefore be modified in order to better capture this aspect. One proposed technique is to increase the free span of bending of the stud, detaching some nodes in such a way as to make them less rigid and thus simulate the effect of the lack of compressive reacting material. To this end, two other models were studied, identical to the first, where the free lengths of deflection of the stud were modified as follows:

TEMPLATE	Free length of buckling [mm]
FEM1.00	25
FEM1.01	45
FEM1.02	55

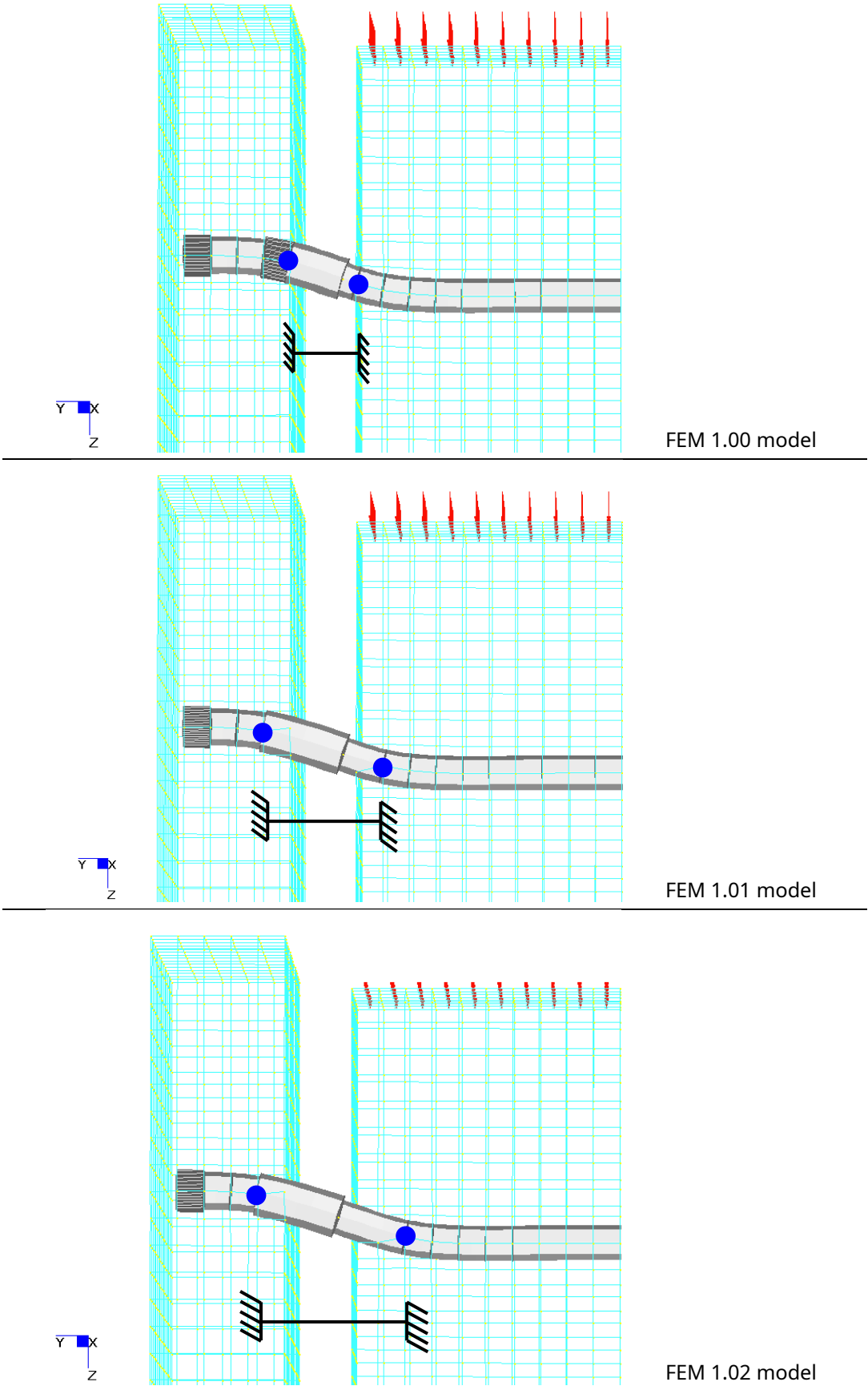


Fig. 48: Free buckling length for each FEM model

The numerical values obtained from the analysis are shown below, tab. 12, while in figure 49 the qualitative trend of the curves of each model compared with the experimental data.

fase	carico CH2 daN	LE.AC. 2	LE.AC. 3	FEM 1.00	FEM 1.01	FEM 1.02
		scorrimento media mm	scorrimento media mm	scorrimento DZ_bricks mm	scorrimento DZ_bricks mm	scorrimento DZ_bricks mm
		Lunghezza libera di inflessione			25 mm	45 mm
1° carico	0	0	0	0	0	0
	100	0,0018	0,0023	0,0075	0,0129	0,0177
	200	0,0058	0,0080	0,0149	0,0258	0,0355
	300	0,0120	0,0157	0,0224	0,0387	0,0532
	400	0,0190	0,0237	0,0298	0,0516	0,0709
	500	0,0273	0,0323	0,0373	0,0645	0,0887
	700	0,0463	0,0520	0,0522	0,0904	0,1241
	1000	0,0823	0,0857	0,0746	0,1291	0,1773
	1500	0,1575	0,1503	0,1119	0,1936	0,2660
	2000	0,2418	0,2240	0,1492	0,2581	0,3547
	2500	0,3320	0,3053	0,1865	0,3227	0,4433
3000	0,4338	0,3953	0,2238	0,3872	0,5320	
3500	0,5418	0,4933	0,2611	0,4518	0,6207	
4000	0,6593	0,6007	0,2984	0,5163	0,7093	
3° carico	6000	1,2080	1,1187	0,4476	0,7744	1,0640
	8000	1,9020	1,8457	0,5968	1,0326	1,4187
	10000	2,9490	2,7873	0,7460	1,2907	1,7734
	12000	4,7770	4,3017	0,8952	1,5489	2,1280
				Rigidezza [N/mm]	Rigidezza [N/mm]	Rigidezza [N/mm]
			16756	9684	7049	

Table 12: Comparison of numerical values

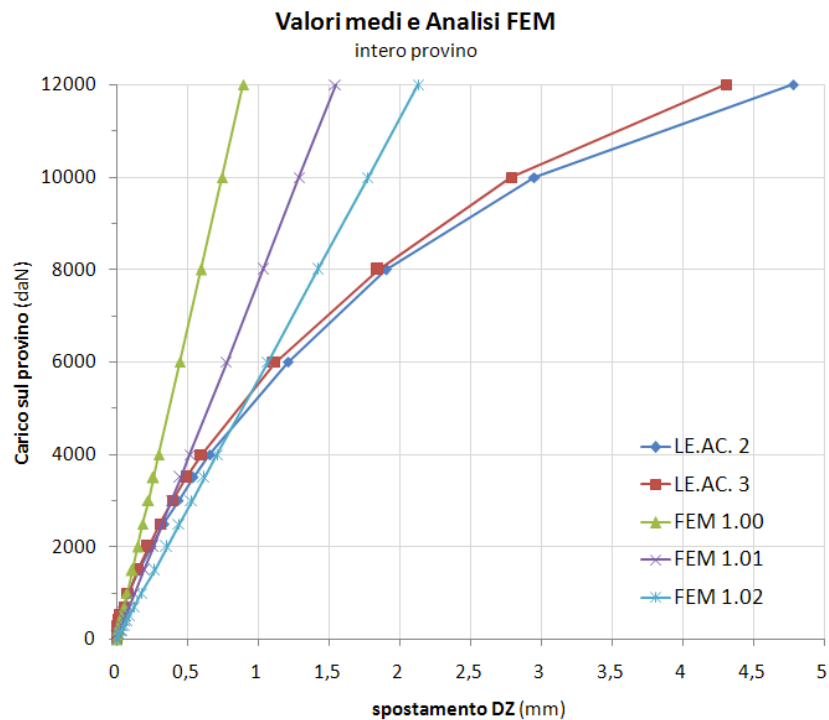


Fig. 49: Comparison between the stiffnesses of the FEM analysis and the experimental data for the whole specimen

For low load values applied to the model, it is logical to expect that the materials retain the linearity characteristics, and it is therefore plausible that the connector can slide as if it were doubly wedged between the extrados of the beam and the intrados of the slab. This behavior is shown in fig. 48, model **FEM1.00**, in which the connector shares the two nodes (in blue) of the bricks elements of beam and slab at a distance of 25 mm.

Observing table 12 and figure 49, we note how the stiffness of the model **FEM1.00**, represents a good approximation of the experimental curves up to load values on the entire specimen of 1000 daN, which corresponds to a stiffness of the single connector equal to 16756 N/mm.

For load values higher than 1000 daN, the FEM 1.00 model becomes inadequate. One can then think of referring to the model **FEM1.01** in which the effect of plasticization is represented by having increased the free length of the connector by 10 mm for a total of 45 mm, figure 48. The FEM curve of this second model is close to the experimental data for load values equal to 2500 daN, where the numerical and experimental slips differ by 3% (table 12 blue boxes) and the numerical stiffness is equal to 9684 N/mm. A decrease in stiffness equal to 42% was recorded due to the effect of the plasticizations.

As repeated several times, concrete has a resistance to hammering about 6 times greater than wood. In the light of this consideration, the FEM 1.02 model provides for an increase in the free inflection length of the connector equal to 10 mm in the wooden beam alone, for a total of 55 mm. Comparable values can be obtained for loads of approximately 6000 daN, which corresponds to a stiffness value of each rung equal to 7049 N/mm. The decrease in stiffness is of the order of 58%.

4.1.8 Conclusions

In this paragraph, a numerical analysis has been described which has allowed us to better understand the local phenomena that arise in contact between materials with different stiffnesses. In fact, around the connector due to increasing loads, the materials undergo crushing, thus reducing their ability to offer resistance.

The local plasticization of the slab and of the wood can be taken into account by assuming the absence of material where the return value is reached, and operationally in the field **FEM** detaching some node of the connector. Therefore, numerical models with different deflection lengths of the connector were studied. From these it was therefore possible to understand to what extent the stiffness reduction occurs for the phenomena in question. The results obtained with reference to the stiffness of the single connector as the free length of inflection varies are shown below:

TEMPLATE	Free length of buckling [mm]	Initial stiffness [N/mm]
FEM1.00	25	16756
FEM1.01	45	9684
FEM1.02	55	7049

The rifollamento of the materials, studied through the increase of free length of inflection from 25 to 45 mm, involves a reduction of the stiffness of the system equal to about 40%. A further 10 mm free length increase in wood, since it is the softest material, reduces the initial stiffness value to 60%.

By adding the results of the previously analyzed models, it is possible to partially grasp the non-linearity of the connection due to the materials used, while they are inadequate if taken individually.

As regards the single connector, figure 50 shows the deformation suffered at the end of the experimentation and the numerical one using the numerical **FEM1.03**. The latter model considers a free bending length of 55 mm, while in reality it is observed that the non-reactive material is much more at failure. Therefore, to grasp the ultimate behavior it would be necessary to detach at least one other knot in the slab and in the wood, qualitatively obtaining a free length of 75 mm.

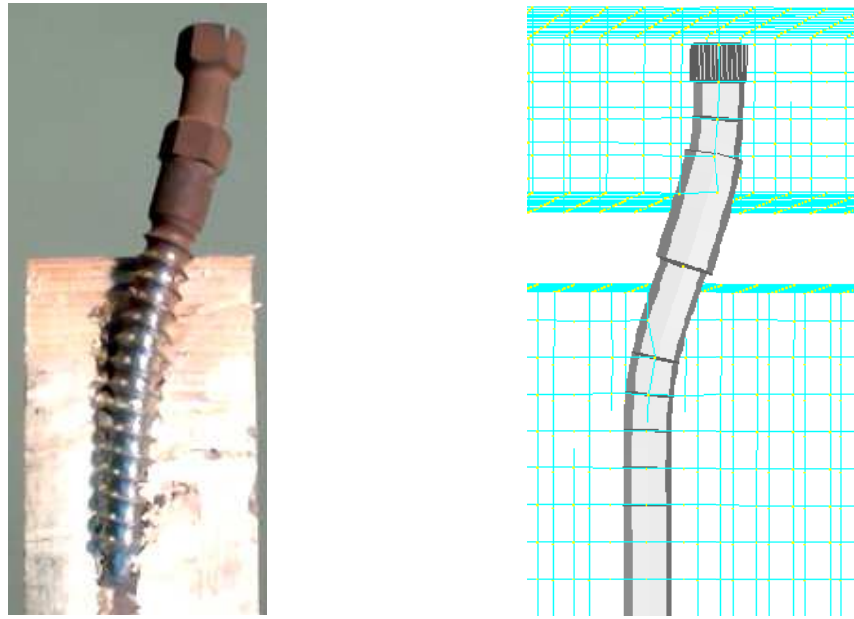


Fig. 50: Real (right) and analytical (left) deformation of the connector.

It has been seen that it was possible to determine a point for each of the three FEM models where the numerical curves correspond to the experimental curves. In these points the stress state of the connector can be evaluated and therefore the effect of the free buckling length on the connector can be evaluated, figure 51 a, b, c.

These data can be interpreted as follows. Up to 1000 daN applied to the specimen, the free length of the connector is equal to 25 mm and the stress state of the materials is certainly within the elastic values.

From 1000 to 2500 daN, the experimental trend can be followed by imagining increasing the free length of inflection from 25 to 45 mm; the connector has not yielded yet since maximum tensions of 350 MPa are observed (equal to approximately one third of the yield point).

From 2500 to 6000 daN, the free flexion length goes from 45 to 55 mm, maximum stresses of 998 Mpa are recorded which are higher than the connector yield strength (850 Mpa).

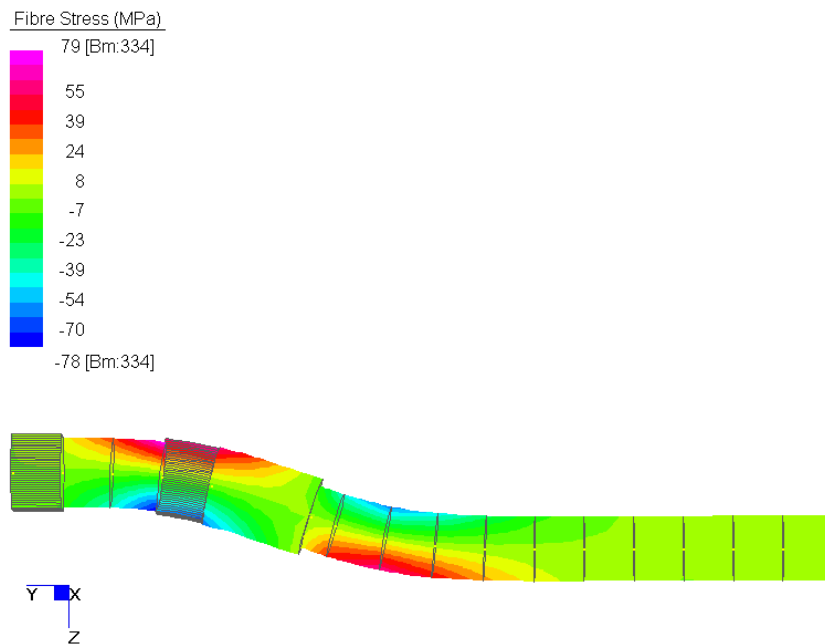


Fig. 51 a: Stress state of the connector model FEM 1.00 and applied load of 1000 daN.

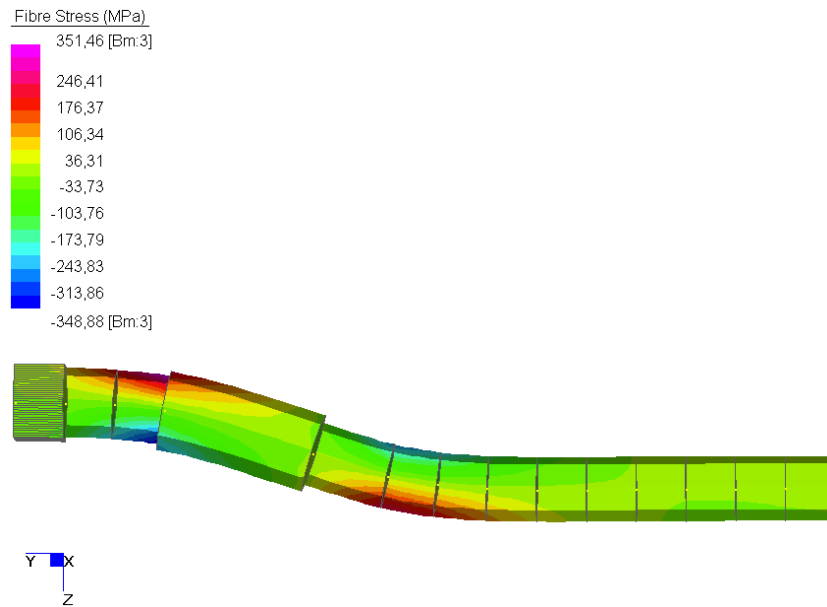


Fig. 51b: Stress state of the connector model FEM 1.01 and applied load of 2500 daN.

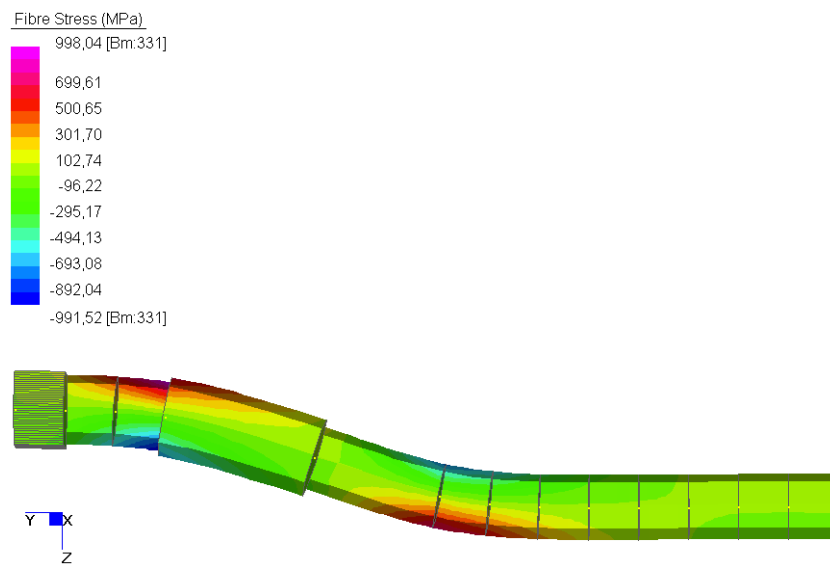
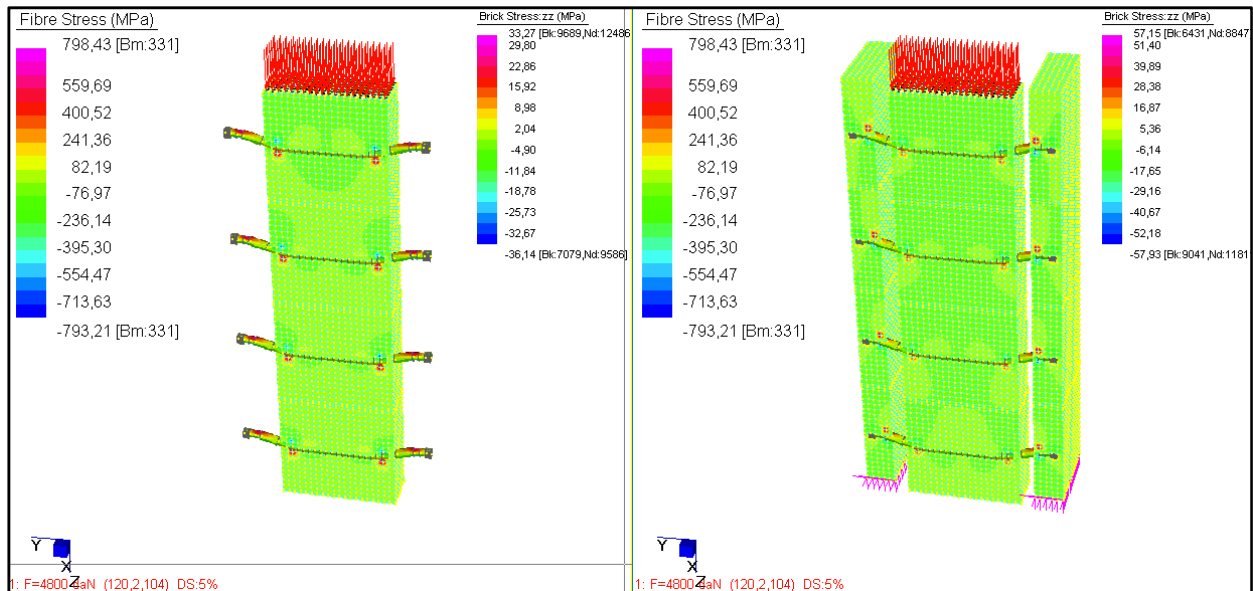


Fig. 51 c: Stress state of the connector model FEM 1.02 and applied load of 6000 daN.

Finally, these FEM models allow us to confirm the hypotheses assumed for the bilinear model. In the latter a theoretical linear behavior was arbitrarily established for force values on the single connector up to 6000 N, which correspond to 4800 daN applied to the entire specimen. Considering the FEM 1.02 model and figure 49, a good correspondence can be seen in correspondence with a force value of 4800 daN. Therefore, if an analysis is launched with this load value applied to the FEM 1.02 model, the voltage values shown below can be investigated.

	Load Cases	BEAM Brick stress ZZ [MPa]		INSOLE Brick stress ZZ [MPa]		CONNECTOR Total Fibers [MPa]	
		Trac.	Comp.	Trac.	Comp.	Trac.	Comp.
FEM 1.02	F=4800 daN	+ 33.27	- 36.14	+ 57.15	- 57.93	+ 798.43	- 793.21



From the results it can be seen that only the wood exceeds the overflow limit (assumed to be 20 Mpa) and therefore it is concluded that the bilinear model represents a sufficient approximation of the experimental results if we consider, once again, the already mentioned defects of the numerical model which lead to questionable voltage spikes. Beyond the conventional limit of 6000 N plasticization of the connector is reached with the formation of a plastic hinge capable of changing the static pattern of the connection and allowing rotations of the connector itself which translate into greater shear slip (hardening of the connection and corresponding lowering of stiffness, plastic branch).

4.2 Composite beams

4.2.1 Introduction

In the previous chapters an analysis was carried out aimed at defining the stiffness characteristics of the mixed wood-concrete system through the use of Al-fer srl dry connectors. An elastic-plastic model was introduced, through the force-displacement curve, valid for solid wood beams of approximately class C18 and concrete slab type C25/30.

We now want to discuss an application to a practical case of dimensioning a real mixed wood-concrete beam connected by means of the connectors in question. To do this it will be necessary to introduce the analytical method, available in the literature, from which the stresses on the single components are obtained. For comparison, a finite element numerical model of easy and immediate use will be proposed.

4.2.2 Composite beam theory

The coupling of two or more structural elements working in bending, through the use of semi-rigid connection systems, allows the creation of composite-type structures. The efficiency of the composite structural element is all the higher the more the connection systems are rigid (ie the more they prevent the relative displacements between the surfaces in contact of the component elements). The real static behavior of the composite structure in bending will therefore be intermediate between the extreme cases:

- 1) zero stiffness (ineffective connection for the purposes of sliding, $k = 0$);
- 2) infinite stiffness (rigid connection with impeded sliding, $k = \infty$).

The parameter k defines the specific stiffness (per unit of length) of the connection system, assuming that its effect can still be thought of as distributed along the axis of the beam even when the connection itself is of the punctual type (as occurs in most cases).

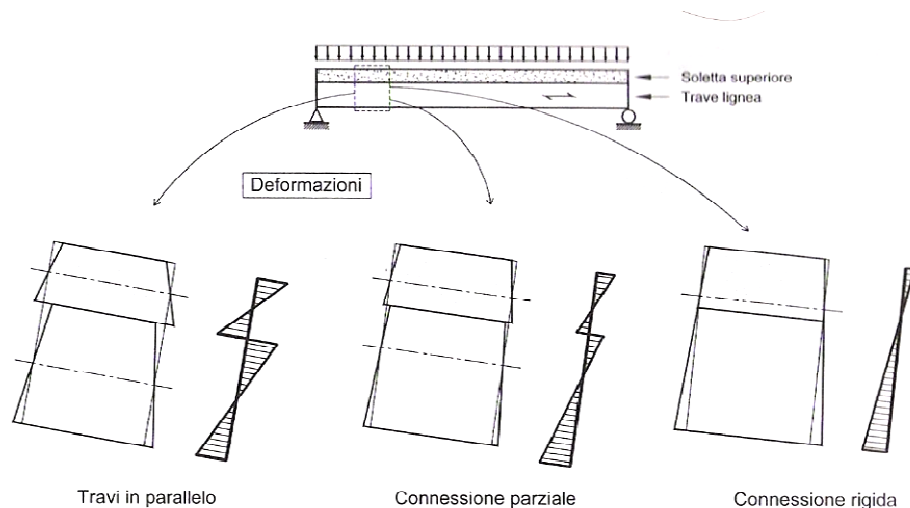


Fig. 52: Distribution of bending strains in a composite beam as a function of the connection stiffness

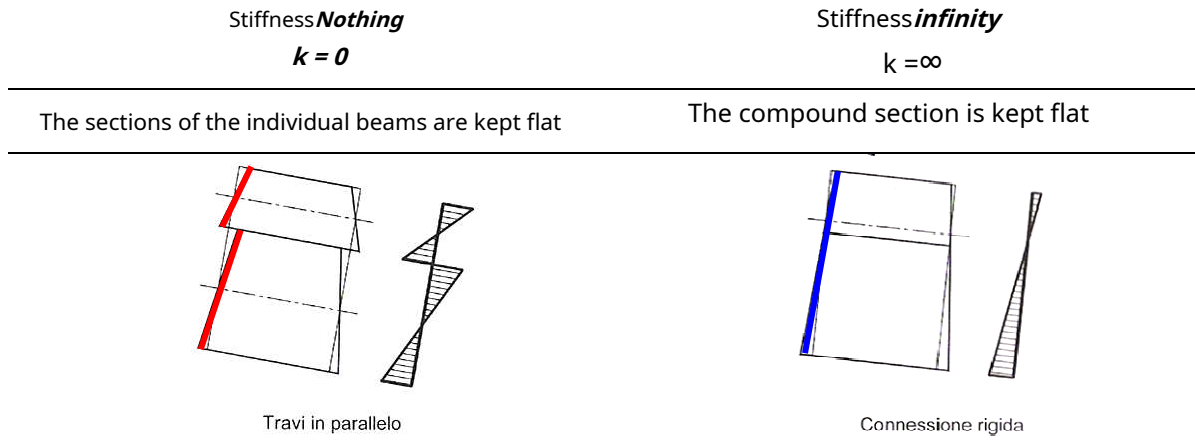
(Ballerini et al., 2002)

As can be seen in figure 52, an increase in the stiffness of the connection corresponds to a rise in the neutral axis, with a corresponding increase in the tensile area in the lower wooden beam (which corresponds to a decrease in the maximum deformation). This is accompanied by a decrease in curvature of the composite structure.

In the limit cases of zero stiffness and infinite stiffness, the stress and strain states can be determined on the basis of the classical theory of bending elements, i.e. I consider Bernulli's hypothesis valid on the conservation of flat sections from which the well-known relationship between the stressing moment and beam curvature:

$$\chi = -\frac{M}{EJ}$$

We can therefore distinguish for each case:



4.2.2.1 Stiffness Nothing

In this situation the generic global section of the beam is not kept flat, the state of stress and deformation of the mixed structure will be that shown in figure 53a.

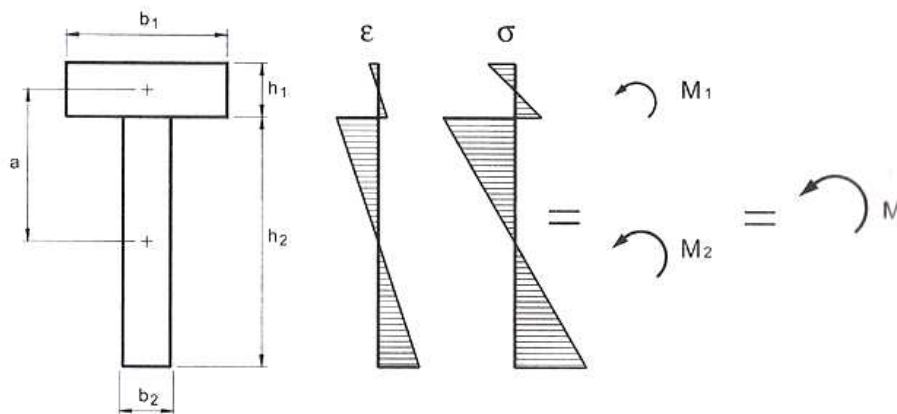


Fig. 53a: Deformations and bending stresses in a composite beam with zero stiffness connection

For the congruence on the transversal displacement, the two beams will still present the same curvature in sections initially of the same abscissa x , measured starting from one end of the beam (figure 53b).

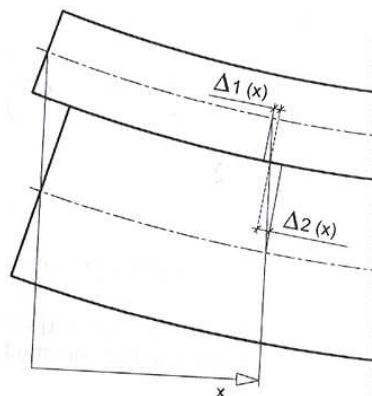


Fig. 53b: scrolling at the interface

The system can be viewed as consisting of two beams operating "in parallel", and thus the flexural stiffness of the composite beam can be calculated as follows:

$$EI_{total} = \frac{1}{12} \sum (d_i^3 b_i E_i)$$

The stressing moment $M(x)$ is distributed on the beams proportionally to the respective stiffnesses. In fact, given the congruence hypothesis and considering the maintenance hypothesis of the flat sections valid for the single elements subjected to bending, we obtain:

$$C_{d_i} = C_{d_i} = C_{d_i} = \frac{I_{d_i}}{I_{total}} M$$

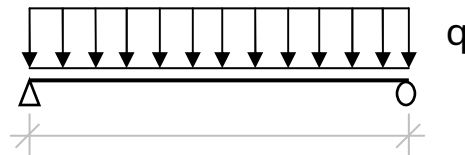
It is therefore possible to know the moments stressing the two sections as a function of the external stressing moment:

$$M_{d_i} = \frac{I_{d_i}}{I_{total}} M$$

Finally, it is possible to evaluate the flow at the interface between the two sections:

$$e_b = \Delta d_b \Delta b = g \frac{I_{d_i}}{I_{total}} \frac{M}{h} < \frac{I_{d_i}}{I_{total}} \frac{M}{h} < b \frac{I_{d_i}}{I_{total}} \frac{M}{h} < b \frac{I_{d_i}}{I_{total}} \frac{M}{h} < b \frac{I_{d_i}}{I_{total}} \frac{M}{h}$$

In the case of a simply supported beam with a uniformly distributed load over the entire span, we obtain:



$$M_{max} = \frac{q l^2}{24} = 6b \quad 4b$$

Slip is null in the center and maximum at the supports, where the following value is found:

$$M_{pkh} = \frac{q l^2}{24}$$

4.2.2.2 Infinite stiffness

The generic global section of the composite beam remains flat, with no sliding at the beam-slab interface. With respect to the previous limiting case, the stressing moment M appears to be balanced not only by the moments M_1 and M_2 , but also by the torque offered by the axial forces N_1 and N_2 . The state of stress and deformation of the composite section will therefore be similar to that illustrated in figure 54.

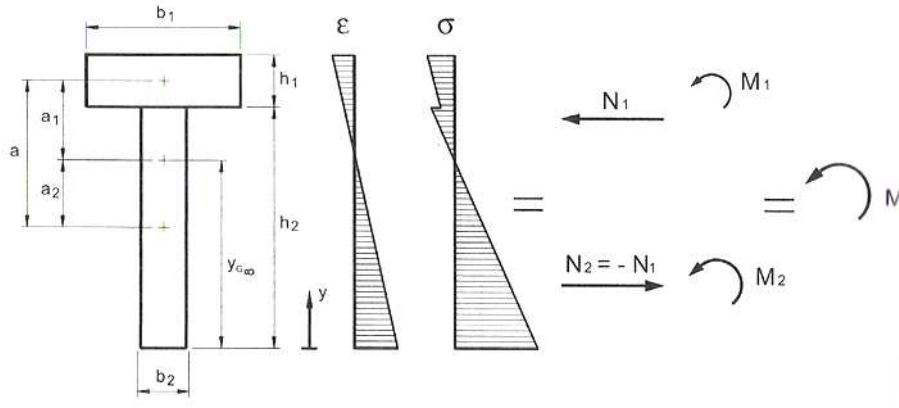


Fig. 54: Deformations and bending stresses in a composite beam with rigid connection

The position of the center of gravity of the global section, weighted with the relevant material moduli of elasticity, can be calculated starting from the lower edge, as follows:

$$L_{mn} = \frac{\sum_{i=1}^n \frac{E_i b_i h_i}{2} y_{i,cg}}{\sum_{i=1}^n E_i b_i h_i} - \frac{a}{2} \frac{\sum_{i=1}^n E_i b_i h_i}{\sum_{i=1}^n E_i b_i h_i}$$

The distances of the centers of gravity of the individual elements from that of the entire section are:

$$y_{i,cg} - L_{mn} = \frac{a}{2} - \frac{y_{i,cg}}{\sum_{i=1}^n E_i b_i h_i} \sum_{i=1}^n E_i b_i h_i$$

$$y_{mn} - \frac{a}{2} = \frac{y_{i,cg}}{\sum_{i=1}^n E_i b_i h_i} \sum_{i=1}^n E_i b_i h_i$$

$$y_{i,cg} - \frac{a}{2} = \frac{1}{\sum_{i=1}^n E_i b_i h_i} \sum_{i=1}^n E_i b_i h_i \left(\frac{a}{2} - y_{i,cg} \right)$$

The flexural stiffness of the composite section can then be calculated via the transposition theorem, being I_{mn} the bending stiffness of the system with zero connection stiffness:

$$I_{mn} = \sum_{i=1}^n E_i b_i h_i \left(\frac{a}{2} - y_{i,cg} \right)^2 + \sum_{i=1}^n E_i b_i h_i \frac{h_i^3}{12}$$

With the usual congruence assumptions, $\epsilon_{c,d} = \epsilon_{d,c} = \epsilon_{d,c} = \epsilon_{d,c}$, the stresses in the two component elements:

$$\sigma_{c,d} = E_c \epsilon_{c,d} = E_c \frac{M}{I_{mn}} \left(\frac{a}{2} - y_{i,cg} \right)$$

$$\sigma_{d,c} = E_d \epsilon_{d,c} = E_d \frac{M}{I_{mn}} \left(\frac{a}{2} - y_{i,cg} \right)$$

Through the equilibrium relation, $Q_b - Q_{nob} - \frac{\sigma_i}{\rho} < b$, we get the following expression for the normal urging action Q_b or Q_{nob} , except for the sign:

$$Q_b - Q_{nob} = \frac{\sigma_i}{\rho} < b$$

The sliding stress at the beam-slab interface is calculated by derivation of the axial action:

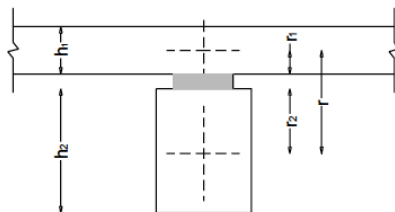
$$\sigma_b = \frac{dQ_b}{dx} = \frac{d}{dx} \left(Q_{nob} + \frac{\sigma_i}{\rho} x \right) = \frac{\sigma_i}{\rho}$$

4.2.2.3 Semi-rigid connection

In intermediate situations with semi-rigid connection, due to the relative sliding between beam and slab, the real static behavior of the composite structures in question can be traced back to the scheme of two beams in parallel, connected by means of a deformable connection. The elastic general treatment of this problem was provided by Newmark et al. (1951), with the following assumptions:

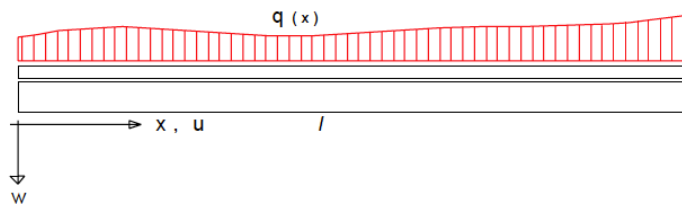
- Elastic-linear behavior of the material and of the connection;
- Small displacements and deformations (1st order theory);
- Identical curvatures for beam and slab elements;
- Conservation of the flat sections for each element constituting the section;
- Connection uniformly distributed along the beam and beams with constant section along the longitudinal axis.

TRAVE COMPOSTA A CONNESSIONE DEFORMABILE



IPOTESI:

- Comportamento elastico lineare
 - Analisi del 1° ordine
 - Curvature identiche per gli elementi
 - Connessione "uniforme"
- $k = K/s = \text{cost}$



EQUIVALENT STEP

In the general discussion, the connection is considered "uniform": in the case of punctual connectors of stiffness k , hypothesized identical and equally spaced with pitch s , this is equivalent to considering a specific stiffness of the system equal to k . However it is quite common, for beams in simple support with uniformly distributed load, vary the pitch of the connectors between a maximum value $L_c = 0.75 \cdot P_y$ in the center line, and a minimum value $L_c = 0.25 \cdot P_{kh}$ at the ends.

TENSION STATE OF THE COMPOSED STRUCTURE

According to the general treatment for a mixed system with two elements (Newmark, 1951), with reference to figure 55, it is possible to impose:

- **equilibrium equations** for the stretch % of composite beam, for elements 1 and 2;
- **congruence conditions**;
- **elasticity relationships** in the hypothesis of maintaining the flat sections.

For simplicity of exposition, without going too far into mathematical elaborations, it is possible to obtain a solving differential equation of the second order of the following type:

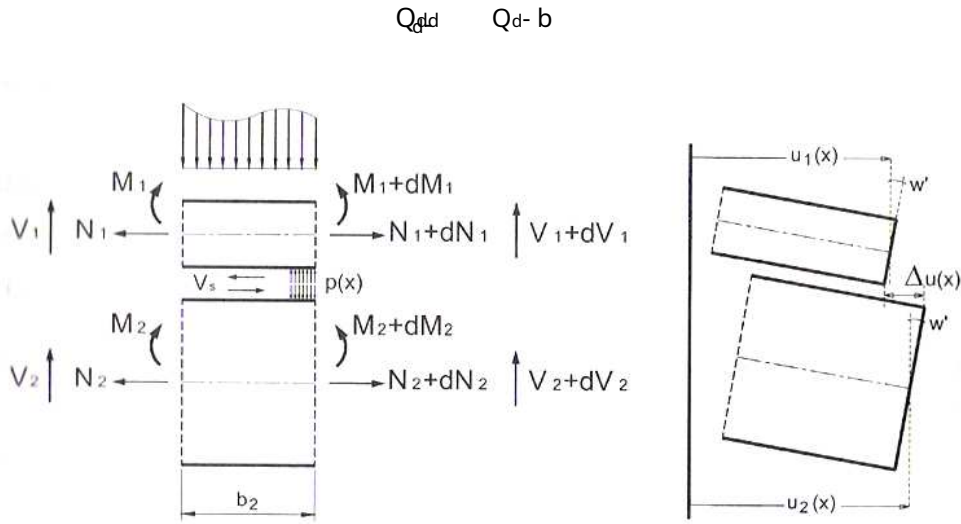


Fig. 55: Composite beam with deformable connection

The following assumptions can be made:

- $j \ll b$;
- $\frac{b}{j} < \frac{b}{8}$.

it is therefore possible to obtain the expression of Q_d :

$$Q_d = \frac{b}{j} \left(\frac{b}{8} - \frac{u}{b} \right)$$

Knowing the expression above, it is possible to obtain the other quantities and, consequently, the stress state of the composite structure.

TREATMENT SIMPLIFIED BY REGULATIONS

The current regulations, DIN 1052, Eurocode 5, propose for the verification of composite beams with deformable connection, some formulas deriving from a simplified treatment of the problem, in the case of beam in simple support and distributed load j variable with sinusoidal law with maximum value j in the middle of the beam:

$$j = j_0 \cos \frac{\pi x}{b}$$

The composite section has a vertical symmetry plane and is constant along the rectilinear axis of the beam: in the present case, element 1 represents the slab, element 2 the beam. The writing of the equilibrium equations for the horizontal translation of the elements, as well as the rewriting of the equilibrium equations for the stretch ϵ , allows to arrive at the solving system of 3 differential equations in the unknowns s_d , and c :

$$\begin{aligned} d_{or} d_{dd} &= -d \quad \text{cathe} = 0 \\ \text{or } d_{dd} &= -d \quad \text{the}^d = 0 \quad \dagger \\ \wedge_{Cd} &= d - it - td \quad \text{cdthe} = -j \end{aligned}$$

Assuming the load with sinusoidal distribution allows us to express the unknown axial displacements d_x , and d_y in the following forms:

$$d_x = D \sin UV \quad \epsilon b /$$

$$d_y = -U \sin UV \quad \epsilon b /$$

$$c = c_x \sin UV \quad \epsilon b /$$

Under these hypotheses the solving system is reduced to a system of equations in the unknowns D, U, c, c_x .

Leaving aside the complete discussion for the sake of brevity, the expressions relating to mixed structures are given below as reported in the various regulatory documents (see DIN 1052, EN 1995):

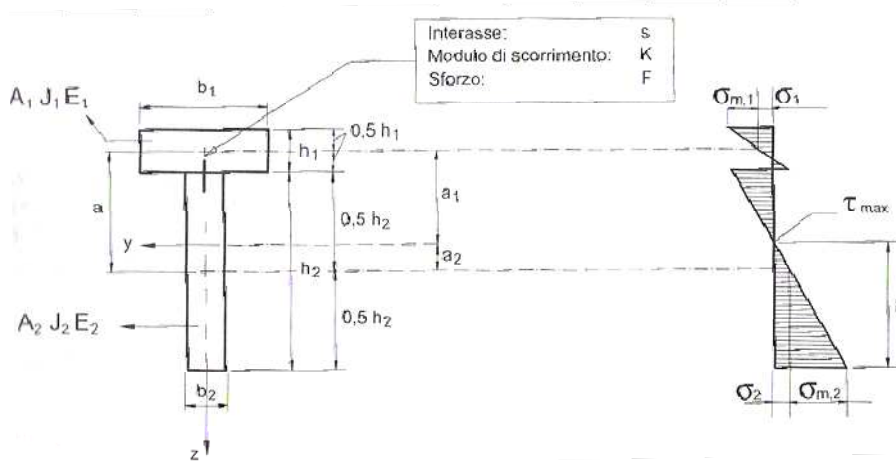


Fig. 56: Composite beam with deformable connection. regulatory scheme

The effective stiffness of the mixed system is determined by the following expression:

$$L_j \wedge_D \quad \ddagger oi \quad \ddagger d \cdot d \text{ or } \text{the}^d$$

where is it:

<i>element 1</i> <i>INSOLE</i>	<i>element 2</i> <i>BEAM</i>
$\ddagger d \wedge \frac{\epsilon 1 d_{or} d}{L_j \wedge_D^{SD}}$	$\ddagger - 1$
$i = \frac{t_{od}}{2} \frac{t_o}{2}$	
$\text{the}^d - i - i$	$\text{the} \frac{\ddagger d \text{ or } \text{the}^d}{\ddagger D \text{ or } d}$

Where is the effective calculated span of the composite beam for a simple supported system.

In fact it is as if element 1 were "weighted" by a coefficient $\alpha_d < 1$.

You have identified the variable e such as the distance between the geometric section barycentres of elements 1 and 2, plus the possible presence of a detachment due to the presence of a continuous planking.

In the calculations, for the value of the slip modulus s , relating to the type of connector considered, the following value will be assumed:

- $s = s_{ser}$ for checking the serviceability limit states (deformability);
- $s = s_{ult}$ for checking the ultimate limit states (stresses).

Once the effective stiffness of the member has been determined, it will be possible to determine, by means of the following expressions, the normal and flexural stresses acting on the i -th element, as well as the tensions at the edges (see figure 56):

<i>element 1</i>		<i>element 2</i>	
<i>INSOLE</i>		<i>BEAM</i>	
STRESSES			
$Q_{D,0}$	$\frac{\alpha_d \cdot e}{L} \cdot < 0$	Q_{0}	$\frac{o_i}{L} \cdot < 0$
$<_{D,0}$	$\frac{d}{L} \cdot < 0$	$<_{,0}$	$\frac{\quad}{L} \cdot < 0$
TENSIONS			
$P_{D,-}$	$\frac{Q_d}{O r d} \cdot \frac{0.5 y_d}{d} \cdot <_{D,0}$	$P_{,-}$	$\frac{Q}{o r} \cdot \frac{0.5 y}{\quad} \cdot <_{,0}$
$P_{D,-}$	$\frac{Q_d}{O r d} \cdot \frac{0,5 a d}{d} \cdot <_{D,0}$	$P_{,-}$	$\frac{Q}{o r} \cdot \frac{0.5 y}{\quad} \cdot <_{,0}$

Being the barycentric stress of the i -th element, p_i the flexural component of tension to be added or subtracted from the barycentric tension to obtain the tensions at the edges of the constituent elements.

It will also be possible to calculate the maximum shear stress acting in the web element (element 2, wooden beam) and the force to which each connector is subjected, using the following expressions:

$$P_{kh} = \frac{0.5 \cdot \quad \cdot t_o}{L} \cdot 0$$

$$W_{yy} = \frac{\alpha_d \cdot d \cdot o r d \cdot \quad}{L} \cdot 0$$

Since the behavior of the mixed structure, in addition to being a function of the mechanical characteristics of the component elements, is heavily influenced by the behavior of the connection, it is interesting, in this regard, to introduce a parameter capable of synthetically indicating the capacity of the connection to limit the sliding between the components of the composite beam. This dimensionless parameter, indicated with η , can be assumed to quantify the efficiency of the connection and can be expressed by means of the following formula:

$$\eta = \frac{M_{k@L} \cdot \quad}{n_o \cdot \quad}$$

The values of the above parameter are in the range (0 and 1):

- With deformable connections η gets close to 0;
- With very rigid connections η gets close to 1;

Usually the values of η found in the design of the usual wooden composite floors, with concrete slab, are between 0.4 and 0.7.

The efficiency parameter can be of some help in the design phase. Indeed, during the design phase, it is possible to set a limit value for the flexural deformation (for example w_{lim}) induced, in exercise, from the sum of the variable and permanent loads, thus obtaining a minimum value required for L :

$$w_{lim} = \frac{5j''}{384EI} L^4 \leq \frac{2500}{500} j$$

Through this value, having checked that $0 \leq \eta \leq 1$, it turns out it is possible to set up a nonlinear system of four equations in the unknowns $\eta, \epsilon_d, \delta_d, \eta_d$, which once solved allows to obtain the minimum value for the specific stiffness of the connection system, necessary in order to obtain the desired value of L :

$$\eta = \frac{\epsilon_d \text{ or } \delta_d}{1 - \eta_d}$$

from which it is finally possible to determine the equivalent spacing of the connectors, known that the specific stiffness is equal to the ratio between the stiffness of the single connector and the equivalent spacing $k_{eq} = k/L_c$:

$$L_c = \frac{k}{k_{eq}}$$

4.2.3 FEM application: wood-lime composite floor with Al-fer srl connectors

The previous chapters introduced the analytical method, described by the current regulatory documents, with which it is possible to size a composite floor with a deformable connection. The Al-fer dry connector, as far as learned in the course of this discussion, is configured precisely as a semi-rigid connection system.

The intention that arises now is to devise a numerical finite element model, with the ambition, that this tool is able to describe with sufficient approximation, the behavior of a real beam mixed in wood and concrete with dry connectors Al-fer srl. The validation of this model may take place by comparison with the previously introduced analytical model. This study may also be of help in correctly setting up future experiments on real beams already carried out at the Alfer srl company in Verona and waiting to be tested.

The case of a wood-concrete floor slab is considered, made with 100 x 200 mm solid wood beams, class C18, 16 mm diameter Al-fer dry connectors embedded in the 50 mm concrete slab (figure 57). Only the verification in the single operating phase of the structure with matured concrete is described below, assuming that the wooden beams are propped up in the casting phase.

Project data

• **Geometric features**

Insole thickness	th = 50mm
Wooden table	t = 25mm
Beam section base	b = 100mm
Beam section height	h = 200mm
Spacing between beams	• = 600mm
Theoretical span of the beams	= 4000mm
Dry connectors Al-fer Pigging	d _{max} = 16mm
length of the pegs	
in the wood	- 100mm
in the concrete	- 40mm

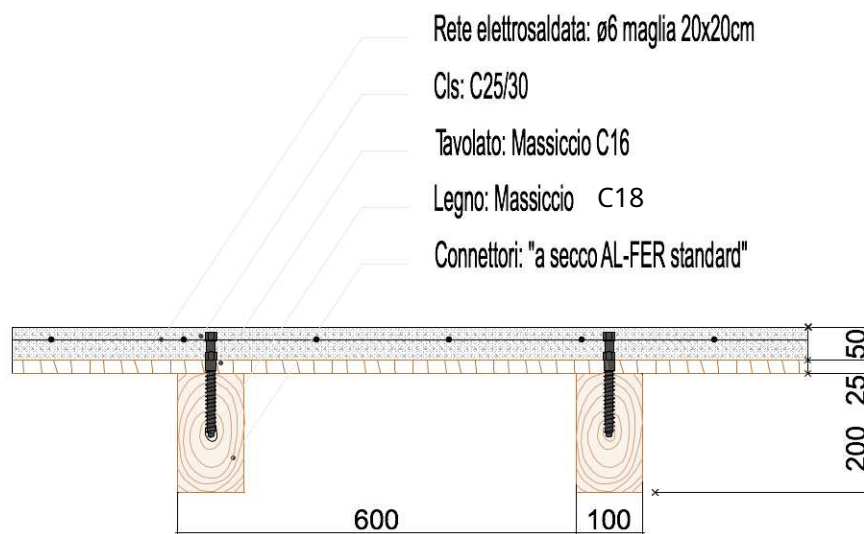


Fig. 57: Cross section of the floor

• **Material characteristics**

Concrete

Class C25/30	No*- 25KN/mc
Density considered Average	d- 31476N/mm ²
secant modulus of elasticity	

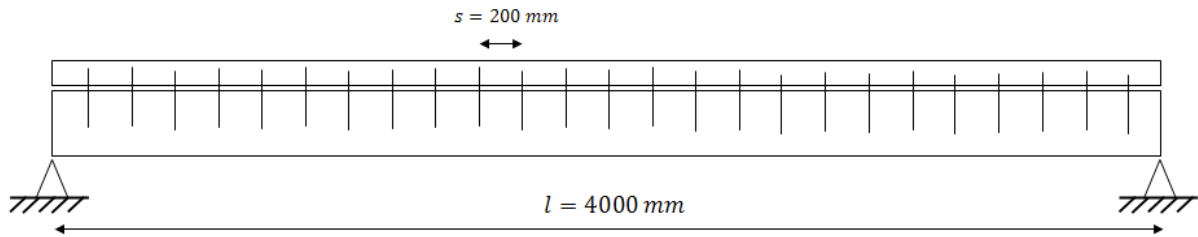
Solid wood

Class C18	No*- 6KN/mc
Density considered Elastic	- 9000N/mm ²
modulus	

Al-fer dry connectors

Lead steel type 9SMnPb36 Elastic	- 210000N/mm ²
modulus	- r _y - 10610N/mm
Elastic phase stiffness	
(Al-fer bilinear model)	

- **Connection system with dry connectors Al-fer srl**



Arrangement of connectors inside the beam

For the sake of simplicity, a uniform arrangement of the connectors has been chosen, therefore, in determining the effective quantities of the system, reference is made to the pitch $s = 200$ mm.

- **Loads and internal actions**

The floor is designed for a total operating load of 5.6 KN/m², which corresponds to a load on the joist of 3.36 KN/m. The usual loads which are generally the basis for the calculation of a mixed floor to be used as a residential building were considered:

Structural permanents	Beam and slab	-D,*- 1.45KN/sqm
Permanent brought	Substrate, planking, screed, floor, partitions	-,*- 2.15KN/sqm
Variables	Civil residence	—*- 2.00KN/sqm
		TOTAL = 5.60 KN/m ²

Midpoint moment

$$M = \frac{j}{8} \cdot \frac{3.36 \cdot 4}{8} = 6.72 \cdot 10^{-3} \text{ QS}$$

Support cut

$$V = \frac{j}{2} \cdot \frac{3.36 \cdot 4}{2} = 6720 \text{ Q}$$

ANALYTICAL MODEL

The stress characteristics in the materials constituting the composite section are determined below, with reference to the simplified theoretical model introduced in the previous paragraphs.

Flexural stiffness of the two elements in parallel

$$E_{eff} = \frac{1}{12} \cdot \frac{E_c \cdot I_c + E_s \cdot I_s}{1 + \mu} \quad \text{to }] = 7.97 \cdot 10^{10} \text{ DQSS}$$

Flexural stiffness of the compound section:

$$L_{mn} = \frac{d_{ord} \cdot t_o \cdot \frac{7P}{2} \quad \text{or } \frac{7H}{2}}{\sum \dots} = \frac{t_o}{2} \cdot \frac{d_{ord}}{\sum \dots} = 226 \text{ SS}$$

$$i - \frac{t_o}{2} \frac{t_{od}}{2} - 150 \text{ SS}$$

$$\text{the}, n - L_{mn} - \frac{t_o}{2} - 126 \text{ Sts}$$

$$\text{the}, n, o - t_o - \frac{t_{od}}{2} - L_{mn} - 24 \text{ SS}$$

$$n - \wedge - \wedge \text{ or the } - \& \text{ or } i - 4.20 \cdot 10^4 \text{ QSS}$$

Flexural stiffness for system with deformable connection:

$$L_f - uv - 200 \text{ SS}$$

$$-- k_{SER,AL-FER} = 10610 \text{ N/mm}$$

$$\#_d \wedge \frac{1}{-} \frac{\epsilon_{dORDL} \% 0}{-}^{SD} - 0.083$$

$$\# - 1$$

$$i - d \frac{t_o}{2} \frac{t_o}{2} - 150 \text{ SS}$$

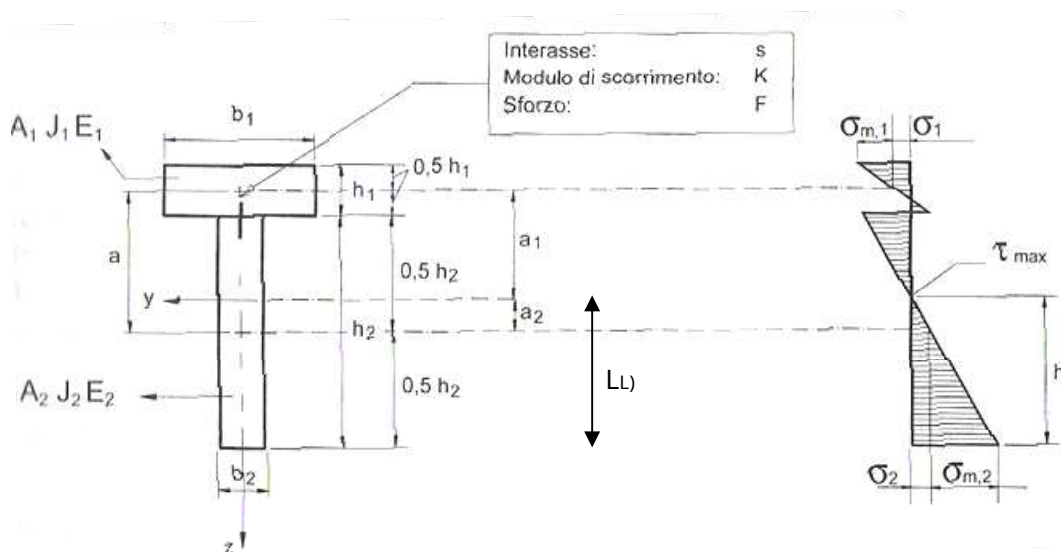
$$i - \frac{\#_{dORd} \text{ the}_d}{\#_d \text{ dORd} \text{ or}} - 46 \text{ SS}$$

$$\text{the}_d - i - i - 104 \text{ Sts}$$

$$L_f - \wedge_D \quad \# \text{ oi} \quad \#_d \text{ dORd the}_d - 2.03 \cdot 10^4 \text{ QSS}$$

$$LL_f - \frac{t_o}{2} \text{ the } 146 \text{ Sts}$$

The neutral axis cuts the wooden beam as in the following image



connection efficiency

$$\eta = \frac{L}{n_0} = 0.36$$

Value in accordance with the assumption previously made, $0.4 \leq \eta \leq 0.7$.

It is therefore possible to determine the maximum stresses acting on the various elements:

$$\sigma < \frac{j}{8} = 6.72 \cdot 10^{-5} Q$$

INSOLE

$$Q_d = \frac{Q}{L} = 27218 \text{ Q}$$

$$\sigma_d = \frac{d}{L} = 6.51 \cdot 10^{-5} Q$$

$$\sigma_{D, K8Z} = \frac{Q_d}{\sigma_d} = \frac{0.5 y_d}{d} < 1 < 3.5 \text{ } \tau_{ij}$$

$$\sigma_{D, y} = \frac{Q_d}{\sigma_d} = \frac{0.5 y_d}{d} < 1.70 < \tau_{ij}$$

BEAM

$$Q = \frac{oi}{L} = 27218 \text{ Q}$$

$$\sigma = \frac{Q}{L} = 2 \cdot 10^{-5} Q$$

$$\sigma_{K8Z} = \frac{Q}{\sigma} = \frac{0.5 y}{or} < 1.62 < \tau_{ij}$$

$$\sigma_{y} = \frac{Q}{\sigma} = \frac{0.5 y}{or} < 4.34 < \tau_{ij}$$

shear force acting in the web element:

$$\tau = \frac{j}{2} = 6720 \text{ Q}$$

$$\tau_{Ph} = \frac{0.5 \cdot \tau}{L} = 0.43 < \tau_{ij}$$

force to which the most stressed connector is subjected:

$$W_{yy-d} = \frac{Q}{L} = 5444 \text{ Q}$$

maximum deflection in the center line:

$$\tau_{Ph} = \frac{5j}{384 L} = 5.52 \text{ SS}$$

The analytical model is simple and can be applied immediately, but the most restrictive limit is the one that provides stress and tension values in well-defined points of the beam.

This fact can be solved by introducing a finite element numerical model capable of correctly answering the problem and simultaneously supplying discrete values along all the sections of the elements constituting the mixed system.

NUMERICAL MODEL

For the numerical model, the beam was divided into 18 ashlar of 200mm length and 4 ashlar of 100mm length, adopting a static scheme of beam in simple support of the hinge type at the right support and trolley at the left support.

In the finite element analysis, using the straus 7 Release 2.3.3 program, the beam and the slab were modeled with beam elements, as shown in figure 58.

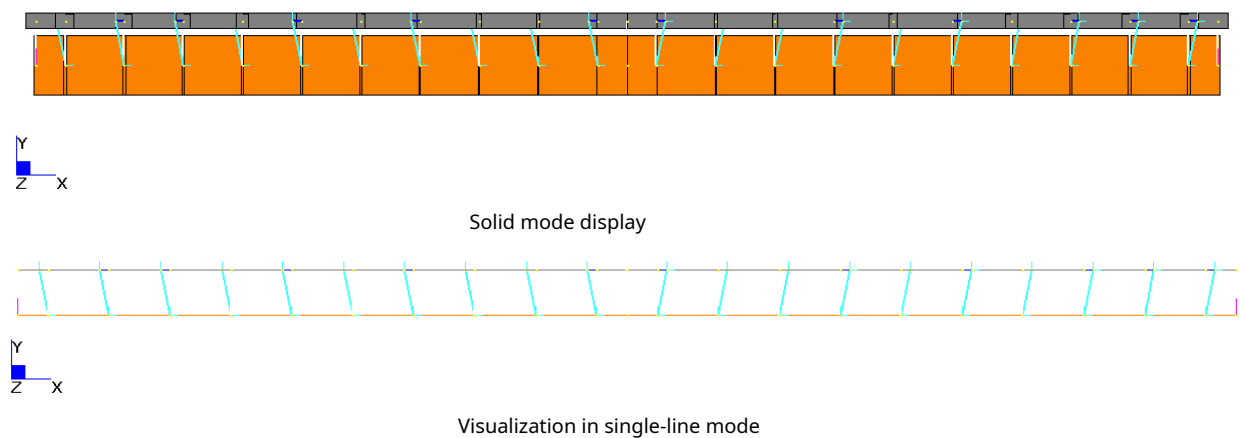


Fig. 58: Longitudinal section adopted for the FEM model

With the hypotheses assumed, both the beam and the slab are schematized with beams capable of describing well both the mechanical and geometric parameters, for the latter aspect see the cross section in figure 59. As regards the presence of the continuous planking, this was modeled with the presence of a gap proportional to the height t , as suggested by the regulatory documents.

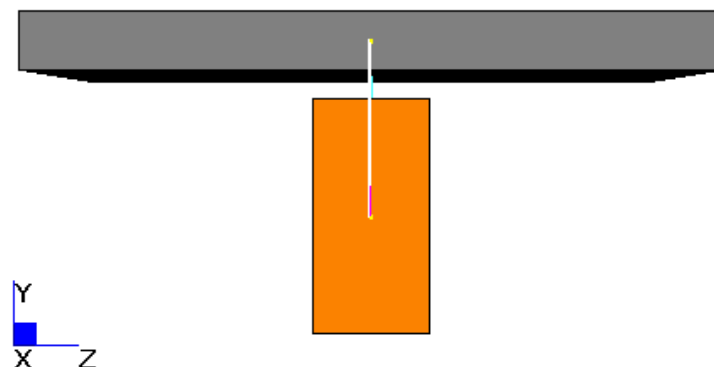


Fig. 59: Element geometry in a cross section of the FEM model

Al-fer dry connector

The Al-fer dry connector was modeled with springs inserted between the nodes of the slab and rigid links connected to the nodes of the wooden joist (figure 60a). The joist and slab nodes are also connected with connecting rod links to prevent relative vertical displacements.

This approach is justified by the fact that in chapter 3 a bilinear model for the behavior of the Al-fer dry connector was proposed, and a force-displacement curve derived from laboratory experiments is now available (figure 60b). In addition to what has been stated, the logic of exploiting this model is reasonable due to the fact that the mixed system in question has analogous mechanical and geometric characteristics of the specimens tested experimentally.

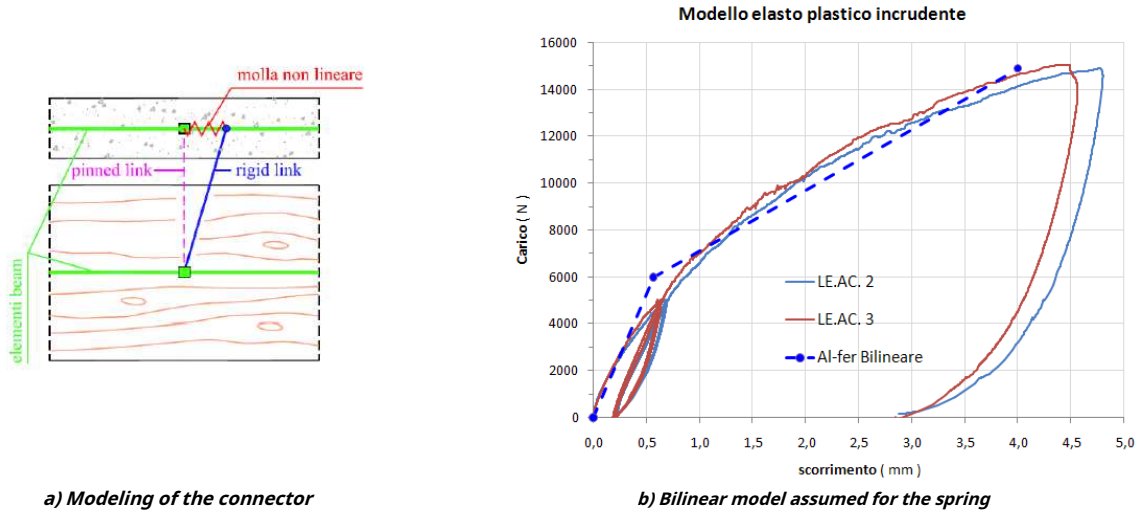


Fig. 60: Element geometry in a cross section of the FEM model

	Elastic branch		Plastic branch	
Stiffness	$k_{AND} = 10611$	N/mm	$k_P = 2591$	N/mm
Power	$f_y = 6000$	No	$f_{t was} = 14900$	No
scroll	$d_y = 0.565$	mm	$du = 4$	mm

The above bilinear model has been applied to the spring-Damper element through the assignment of a table **Force vs Displacement**.

In order to validate the numerical model through the analytical one, an analysis was carried out considering a linear elastic behavior of each element of the system. The assignment of the loads was done by creating 3 load cases:

- 1_Structural permanent (assigning gravity to beam and slab $g_y = - 9810 \text{ mm/s}^2$)
- 2_Perm worn (assigning a distributed load on the wooden beam beam)
 $\xi, * - -, * \bullet - 1,29 \text{ KN/m}$
- 3_Variables (assigning a distributed load on the wooden beam beam)
 $j, * - —, * \bullet - 1,20 \text{ KN/m}$

2 load combinations were then created:

	SLE extension	ULS
1_Structural permanents	1	1.3
2_Perm worn	1	1.5
3_Variables	1	1.5

It should be noted that such an approach lends itself well to structural verifications (SLU), however this would imply the adoption of a specific regulation and the use of the relative safety coefficients, introducing elements that could complicate the comparison with the analytical model.

The results obtained from the FEM analysis are reported below.

SLIDING FORCE

	MIN	MAX
Force(N)	-27609	27609
	[Bm:26]	[Bm:27]

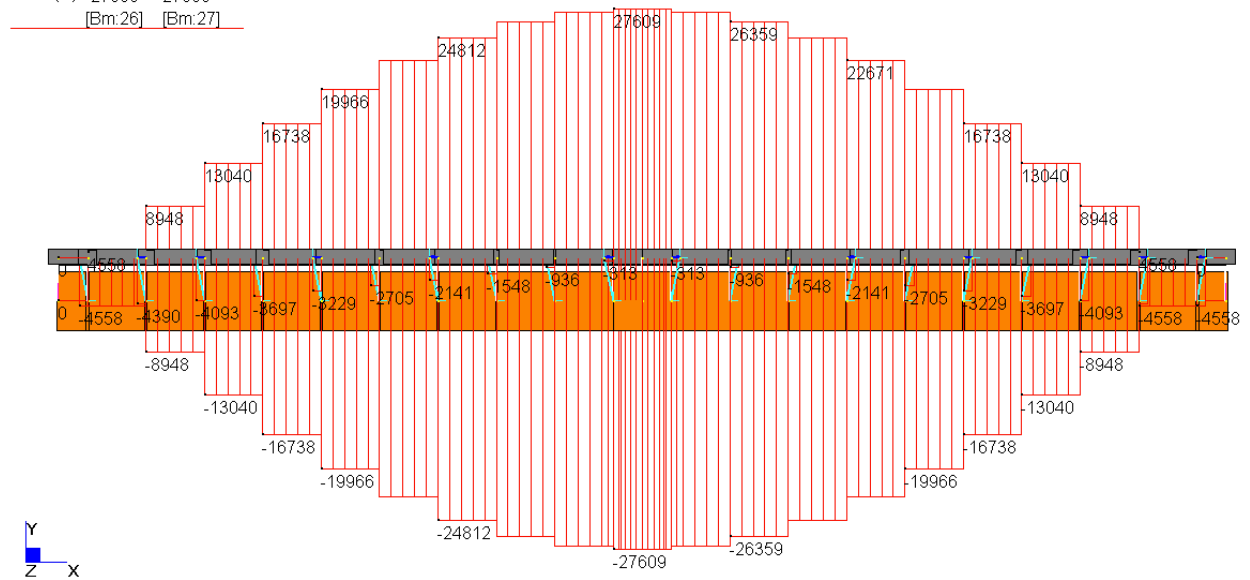


Fig. 61: Sliding force on the slab (bottom diagram, No negative) and on the beam (upper diagram N positive)

	MIN	MAX
Force(N)	-4558	-313
	[Bm:59]	[Bm:64]

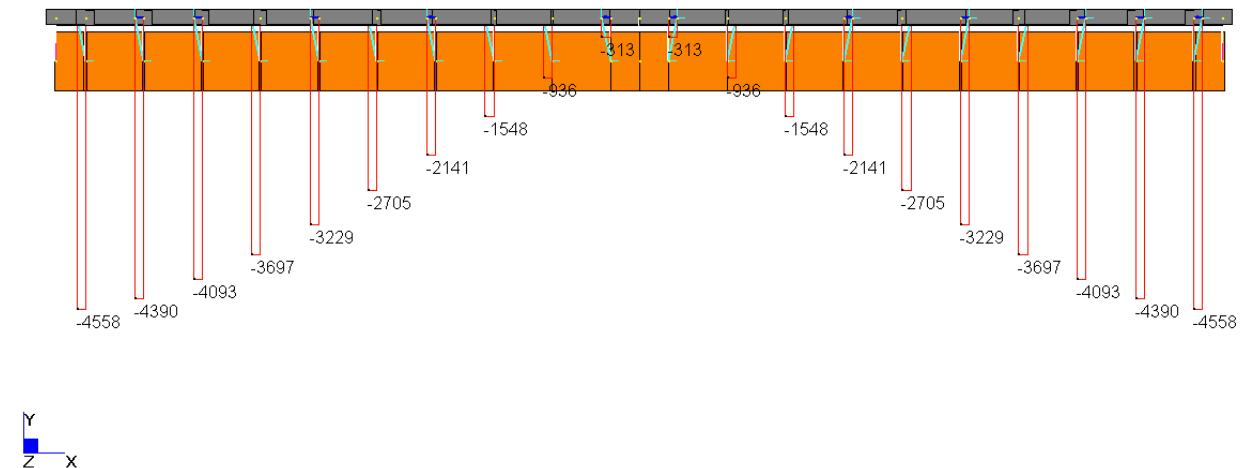
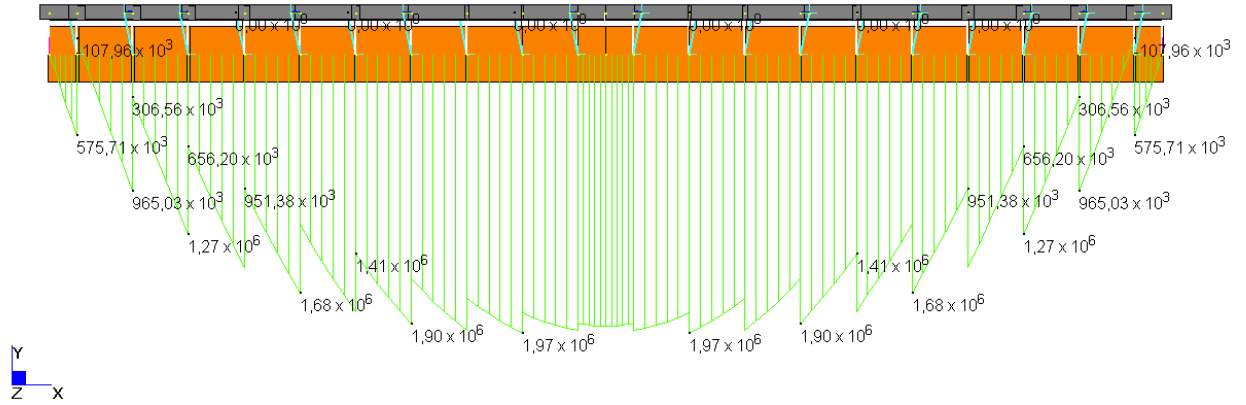


Fig. 62: Sliding force on the connectors

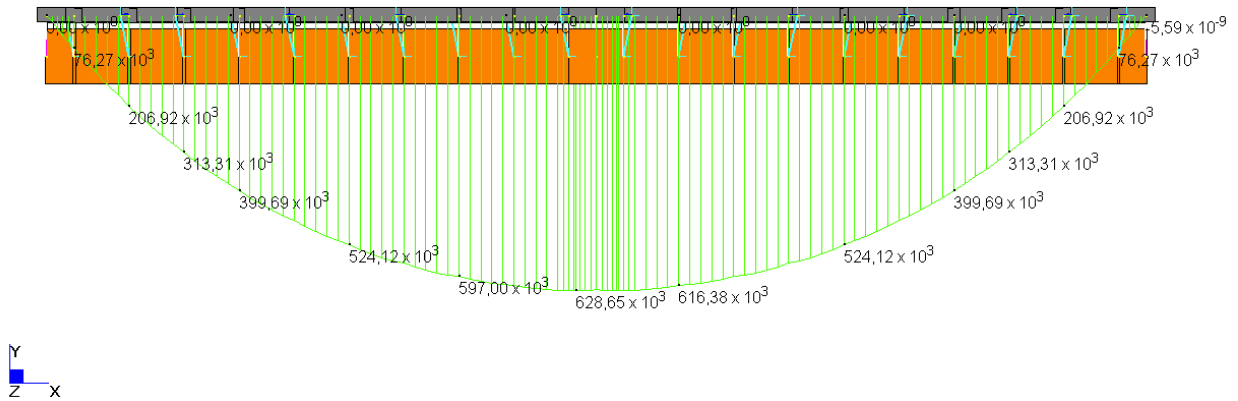
BENDING MOMENTS

	MIN	MAX
BM2(N.mm)	$-107,96 \times 10^3$	$1,97 \times 10^6$
	[Bm:10]	[Bm:3]



m: Bending moment on the beam

	MIN	MAX
BM2(N.mm)	$-5,59 \times 10^9$	$628,65 \times 10^3$
	[Bm:51]	[Bm:26]



m: Bending moment at the slab

Fig. 63: Bending moments on the elements

Fibre Stress (MPa)

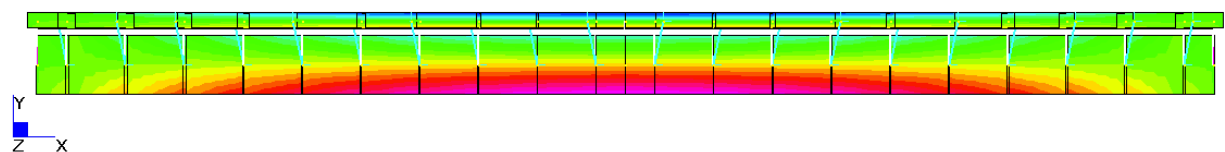
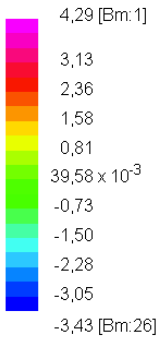
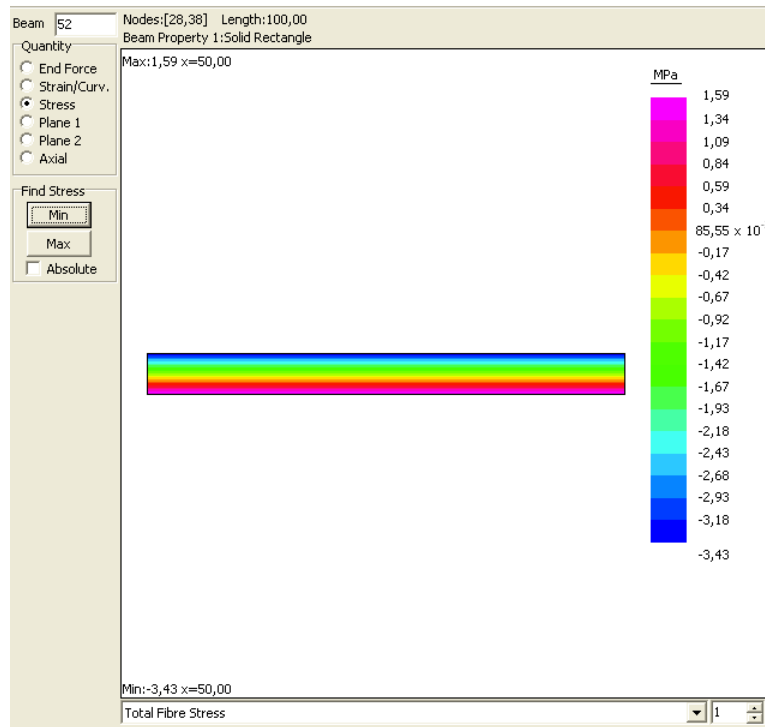
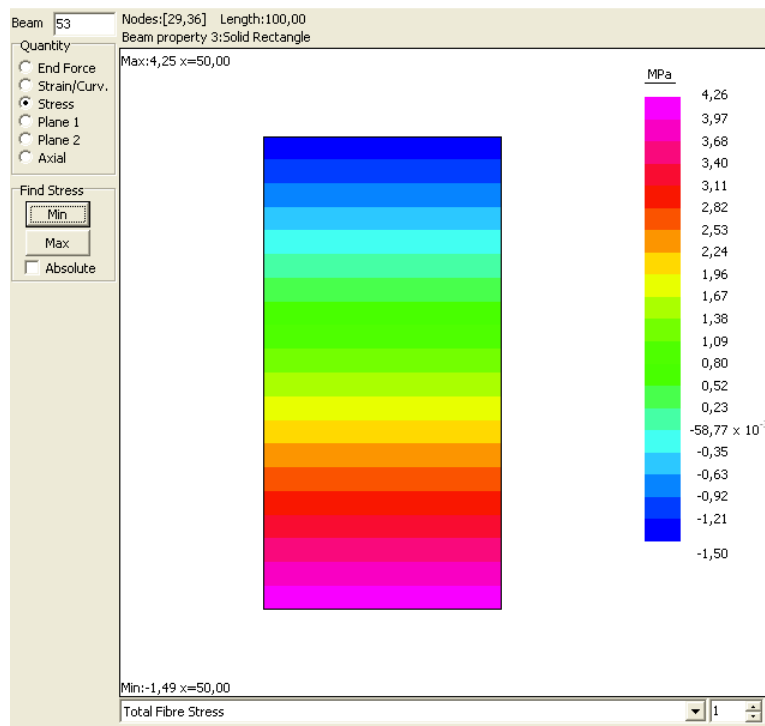


Fig. 64: Total stresses on the mixed system



Total stresses on the slab,K8Ž and_y)



Total stresses on the beam,K8Ž and_y)

Fig. 65: Stresses on materials

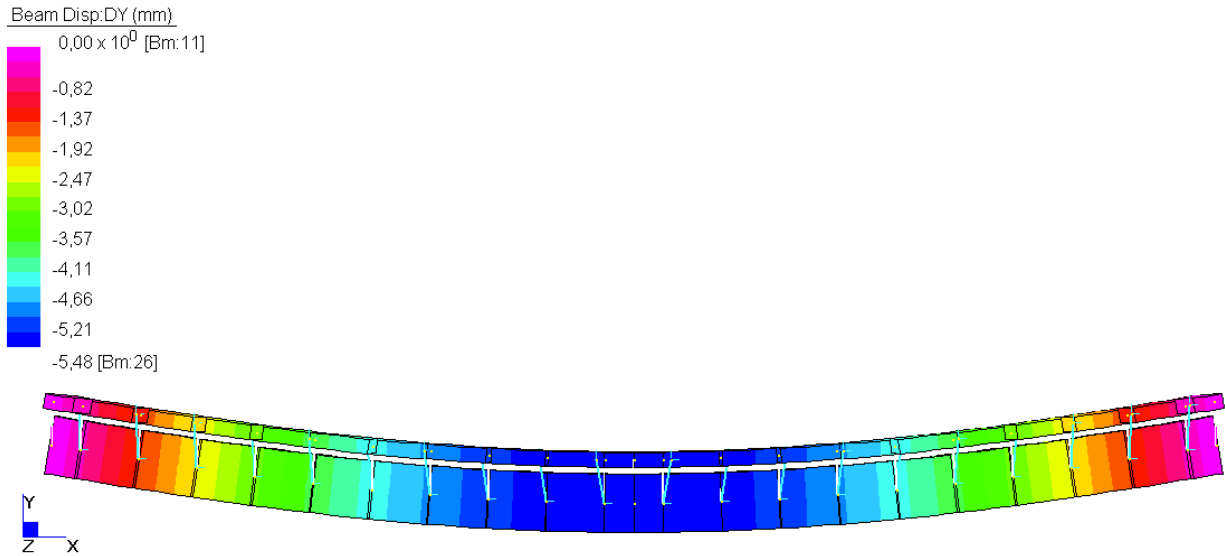


Fig. 67: displacements along y of the mixed system. Max arrow in the middle

The presented numerical model can now be compared with the results obtained from the analytical model.

	Analytical	female	Offset
Arrow	5.52mm	5.48mm	0.7%
Scroll force	27218 No	27609 No	1.4%
Concrete moment	$6.51 \cdot 10^5$ N mm	$6.29 \cdot 10^5$ N mm	3.5%
Wood moment	$1.99 \cdot 10^6$ N mm	$1.97 \cdot 10^6$ N mm	1 %
F connector	5444 No	4558 No	20 %

From the evaluation of the variance between the results, it can be seen that the numerical model introduced is in good agreement with the analytical model. The errors committed by the use of the two models are less than approximately 3% if the data relating to the last row of the above table are excluded. In fact, the maximum force on the connector of the numerical model deviates from the analytical one by 20%; presumably due to the fact that the analytical model provides values excessively in favor of safety since it does not take into account the deformability of the connection, which redistributes the sliding force.

Bibliography

- [1] TURRINI G. and PIAZZA M., ***A static recovery technique for wooden floors***, To retrieve **5**, 1983.
- [2] TURRINI G. and PIAZZA M., ***The static behavior of the mixed wood-concrete structure***, To retrieve **6**, 1983.
- [2] TURRINI G. and PIAZZA M., ***Application aspects of techniques for the construction of mixed wood-concrete structures***, Proceedings of the 1st Congress: Wood in restoration, wood restoration, Florence, 1983 (c).
- [4] Piazza M., Tomasi R., Modena R., ***wooden structures***, Hoepli, 2005.
- [5] Scibilla N., ***Mixed steel-concrete wood-concrete structures***, Dario Flacovio Editore srl, 2002.
- [6] Giuriani E., Frangipane A., ***Wood-to-Concrete composite section for stiffening of ancient wooden beam floors***, University of Trento, Proceedings of the "1st Italian Workshop on Composite Structures", Trento, 17-18 June 1993.
- [7] Capretti S., Ceccotti A., ***Wood-concrete composite floors: calculation method according to EC5***, L'Edilizia, n.12, p.747-752, 1992.
- [8] Modena C., Tempesta P., Tempesta F., ***A dry technique***, The Building n.11-12 p.22-32, 1997.
- [9] GELFI P., MARINI A., ***Mixed floors in wood and concrete. Verification methods***, building no. 153-154, 2008.
- [10] GELFI P., GIURIANI E., ***Influence of slab-beam slip on the deflection of composite beams***, International Journal for the Restoration of Buildings and Monuments no. 9, pp. 475-490, 2003.
- [11] GELFI P. – GIURIANI E. – CATTANEO E. – NICHETTI E., ***Mixed beams in wood and concrete with pin connectors***, Department of Civil Engineering of the University of Brescia, Italy, Technical Report no. 2, 1995

Normative requirements

- (1) Ministerial Decree 14/01/2008 "Technical Standards for Construction - NTC2008"
- (2) CNR-DT 206/2007 – "Instructions for the Design, Execution and Control of Wooden Structures"
- (3) Eurocode 5, ***Design of wooden structures***. UNI ENV 1995-1-1.